An elastoplastic model for saturated freezing soils based on thermo-poromechanics

Enlong Liu, Yuanming Lai, Henry Wong, Jili Feng

An elastoplastic model for saturated freezing soils based on thermo-poromechanics

Enlong Liu[1,2], Yuanming Lai[1,*], Henry Wong[3], Jili Feng[4]

1 State Key Laboratory of Frozen Soil Engineering, Northwest Institute of Eco-Environment and Resources, Chinese Academy of Sciences, Lanzhou 730000, China; 2 State Key Laboratory of Hydraulics and Natural River Engineering, College of Water Resource and Hydropower, Sichuan University, Chengdu 610065, China; 3. LTDS (UMR CNRS 5513), ENTPE, Vaulix-en-Velin 69120, France; 4. School of Mechanics and Civil Engineering, China University of Mining and Technology (Beijing), Beijing 100083, P. R. China. Corresponding author: Yuanming Lai. Contact Tel: +86 931 4967024 and Email: ymlai@lzb.ac.cn.

Abstract:

An elastoplastic theory for saturated freezing soils is presented on the basis of thermoporomechanics. A saturated freezing soil considered as an open system and both Eulerian and Lagrangian formulations considering the phase transition between ice crystals and unfrozen water are given for mass conservation, momentum balance, kinetic energy theorem, first and second thermodynamics, the Clausius-Duhem inequality and conduction laws for fluid mass and heat. Using the Lagrangian saturation and considering solid-fluid interface interactions, a constitutive model for poro-elastoplastic saturated freezing soils is formulated based on the irreversible process. For isotropic linear thermo-poro-elasticity and ideal plasticity, the stress strain relationship for saturated freezing soils considering the influence of temperature and interface energy is proposed. In addition, for hardening plasticity, the general stress strain relationship is formulated under the conditions that the associated or non-associated flow rule is assumed, and a corresponding constitutive model is presented to model the cryogenic triaxal compression of saturated frozen soils. The constitutive theory proposed here provides a potential basis for modelling thermo-hydro-mechanical coupling interactions of saturated soils during the freezing process.

Keywords: Thermoporomechanics; Saturated freezing soils; Constitutive model; Elastoplastic theory;

Thermodynamics

1. Introduction

Frozen soils are compound materials consisting of solid mineral particles, ice crystals, liquid water (free water and tightly bound water), and gaseous inclusions (water vapor and air), whose mechanical and deformation features are distinct from other geological materials, such as soil, concrete, and rock at room temperature (Tsytovich, 1985; Andersland and Ladanyi, 2004). When the temperature falls below the freezing point, the in-pore water can be transformed to ice crystals. These ice crystals may gradually grow, accompanied by water migration to these frozen zones, while the interfaces between ice crystals and unfrozen water will move (Xu et al., 2010). This process may eventually lead to frost heave due to large ground displacements and deformations, which cannot be adequately described using infinitesimal deformation theory widely applied in existing research (Na et al., 2017). There are approximately $2.15 \times 10^6\,\mathrm{km}^2$ of permafrost regions and $5.14 \times 10^6\,\mathrm{km}^2$ of seasonally frozen regions in Western and Northern China (Zhou et al., 2000). With the increase in railway and oil line construction in permafrost and seasonally frozen regions, studies on the thermo-hydro-mechanical coupling interactions related to frost heave problems have become increasingly important. However, many existing studies on these problems are based on traditional theory of frozen soil mechanics (Thomas et al., 2009), in which the frozen soils are usually assimilated to deformable solid while the physical interactions of ice crystals and unfrozen water are ignored (Lai et al., 2013). In fact, frozen soils are porous media, in which the interactions of soil particle, ice crystals and unfrozen water have great influences on their deformation and mechanical properties (Coussy, 2004). Compared with other porous media, like hydrated cement at low temperature, soils during the freezing process can exhibit irreversible plastic deformations, which dominates their strength and mechanical behaviour (Lai et al.,

2009). Some poroelastic models for porous media exposed to freezing temperatures have been proposed (Coussy and Monteir, 2008), but few of them account for plastic deformations during the freezing process. Therefore, formulating a general elasto-plastic theory for saturated freezing soils based on thermoporomechanics is necessary. The presentation of such a general theory is the objective of this paper.

During the freezing process of soils, coupled thermo-hydro-mechanical interactions induce important changes on the distribution of stresses, strains, displacements and moisture contents, in particular due to formation of ice crystals and movement of interfaces between soil particles, ice crystals and unfrozen water. A number of experimental investigations have been carried out and theoretical models were developed to study the coupled thermo-hydro-mechanical behaviour of soils during the freezing process (Na et al., 2017). Lai et al. (1998) first derived a mathematical model on the coupled problem of temperature, seepage and stress fields accounting for phase change between liquid water and ice crystals. Their model was implemented in a finite element program to analyze the temperature and stress fields around tunnels in cold regions. Neaupane et al. (1999) proposed a numerical model of thermal-mechanical-fluid flow coupling system to simulate the laboratory freezing and thawing experiments on rocks, in which an anisotropic elastic stress-strain constitutive model was used and a two-dimensional numerical modelling performed. Later, this work (Neaupane and Yamabe, 2001) was extended to consider a nonlinear elasto-plastic simulation of freezing and thawing of rock. Li et al. (2000) established a heat-moisture-deformation (HMD) coupled model to simulate the frozen-soil foundation based on the equilibrium, continuity and energy principles of the multi-phase porous medium, which was also used to analyze the freezing and thawing processes of soil foundation. Yang et al. (2006) proposed an analysis model that couples the water freezing, temperature and stress fields,

which was also applied to an underground excavation problem of a corridor where ground freezing was used, and the numerical predictions were compared to field measurements. Boukpeti (2008) derived a solution to the problem of freezing of a poro-elastic material and analyzed in the case of one-dimensional deformation within the framework of thermo-poroelasticity of freezing materials, with special attention to the propagation of the freezing front boundary. Nishimura et al. (2009) presented a fully coupled thermo-hydro-mechanical finite element simulation of freezing and thawing of water-saturated soils, accounting explicitly for thermal, hydraulic and mechanical process as well as their interactions. Lu et al. (2011) proposed a model for saturated porous media undergoing phase transition using mixture theory and phase field theory. Zhou and Li (2012) proposed the concept of "separating void ratio" as a criterion for the formation of ice lenses, and established a coupled model of water, heat and stress transfer for saturated freezing soils. Zhou and Meschke (2013) proposed a three-phase finite element soil model based on the theory of poromechanics, in which solid particles, liquid water and ice crystals were considered as separate phases while temperature, liquid pressure, and solid displacement were the primary variables. In their model, Clapeyron's equation was applied in freezing soils to describe the relationship between temperature, water pressure and ice pressure when ice and water coexist in phase equilibrium. Sheng et al. (2014) proposed a simple quantitative model to simulate the pumping-enhanced frost heave, and the numerical results demonstrated that the proposed mechanism could indeed provide a rational explanation for the otherwise unexpected frost heave. Zhang (2014) developed a constitutive model for frozen soils based on the revised Cam-caly model, and implemented the model into a finite element system with a thermal-hydro-mechanical framework to simulate the multi-physical processes during freeze-thaw cycles. Na and Sun (2017) proposed a stabilized thermo-hydro-mechanical finite element model to investigate the freeze-thaw action of

frozen porous media in the domain of finite deformations. Mixture theory was used in their work and frozen soils were idealized as a three-phase composite consisting of solid grains, unfrozen water and ice crystals. Besides achievements of thermo-hydro-mechanical coupled interactions in the freezing process, there are many constitutive models proposed to describe the stress-strain behaviour of frozen soils and geological materials. These constitutive models for frozen soils, geological materials and other materials are based on elastic theory (Loria et al., 2017), plasticity (Khan et al., 1991; Muraleetharan et al., 2009; Kamrin, 2010; Zhang et al., 2012; Darabi et al., 2012; Yao et al., 2009, 2013, 2015; Xu et al., 2017; Liu et al., 2017), micromechanical modelling (Steinhauser et al., 2009; Collard et al., 2010; Zhu et al., 2010; Nicot et al., 2012; Yang et al., 2015; Shen and Shao, 2016), damage mechanics (Lai et al., 2010; de Sciarra, 2012) and thermodynamics (Al-Rub and Darabi, 2012; Henann and Kamrin, 2014; Krairi and Doghri, 2014; Lai et al., 2016; Zhang, 2017).

Even though some researchers proposed multi-physics theories to consider the coupling process of unsaturated soils with varying temperatures above zero (Lei et al., 2014; Sciarra, 2016), to the best of our knowledge, few studies have been performed on the elasto-plastic theory for saturated freezing soils within a rigorous theoretical framework based on well-proofed thermodynamic principles and fundamental physical laws. We will explore this in the present paper. In the following, firstly the equations of mass and momentum balance and the kinetic theorem for saturated frozen soils in Eulerian and Lagrangian formulations considering phase transition are presented, followed by the physical laws governing the behaviours of various components of a saturated frozen soil. Lastly, the constitutive framework for poro-elasto-plastic saturated frozen soils is proposed and verified with cryogenic triaxial compression test of saturated frozen soils.

2. Mass balance, momentum balance and the kinetic theorem for saturated frozen soils

A typical elementary volume of a saturated frozen soil is schematically represented in Fig. 1, which is treated as a porous medium with the superimposition of three continua, the soil skeleton, ice crystals and unfrozen water. Both the soil skeleton and the fluids including ice crystals and unfrozen water coincide with one another and the same geometrical point defined by position vector. At time $t = 0$, in its initial configuration (or "reference configuration"), the position of the soil particle in this elementary volume is represented by $\mathbf{X}$, or $X_i \boldsymbol{e}_i$ relative to a cartesian coordinate system. At time t, the soil particles will move and deform and lie in the current configuration, represented by $\mathbf{x}$, or $x_i(X_j, t)$. In other words:

$$\mathbf{X} = X_i \boldsymbol{e}_i \text{ and } \mathbf{x} = x_i(X_j, t)\boldsymbol{e}_i. \tag{1}$$

The deformation gradient $\mathbf{F}$ is expressed as follows,

$$\mathbf{F} = \nabla_x \mathbf{x} \text{ or } F_{ij} = \frac{\partial x_i}{\partial X_j}. \tag{2}$$

The displacement vector is $\boldsymbol{\xi}(\boldsymbol{X}, t)$, and we have

$$\mathbf{x} = \mathbf{X} + \boldsymbol{\xi};\ \mathbf{F} = \mathbf{1} + \nabla_x \boldsymbol{\xi}; \text{ and } F_{ij} = \delta_{ij} + \frac{\partial \xi_i}{\partial X_j}, \tag{3}$$

in which δ_{ij} is Kronecker delta and $\mathbf{1}$ unit tensor.

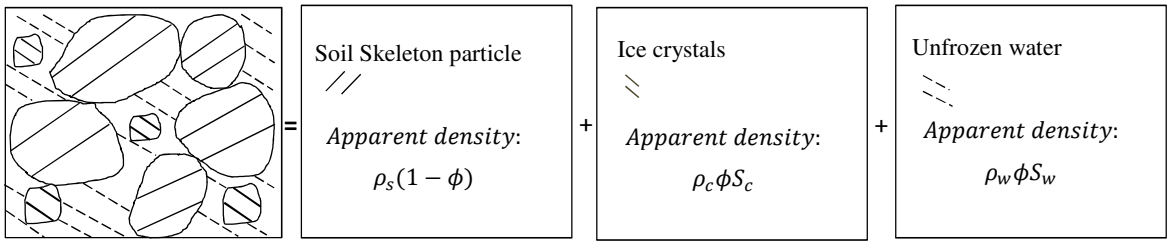

Fig. 1 Macroscopic model of the REV of saturated frozen soils

The volume of the undeformed element at the reference configuration $d\Omega_0$ and the volume of the deformed element in the current configuration $d\Omega$ are related to each other via the Jacobian J (Lai et al., 2010),

$$d\Omega = \det\mathbf{F} \cdot d\Omega_0 = J d\Omega_0. \tag{4}$$

The infinitesimal representative elementary volume (REV) of a porous continuum, as shown in Fig. 1,

consists of solid soil grains and a connected porous volume filled by ice crystals and unfrozen liquid water. Both the Eulerian porosity n and the Lagrangian porosity ϕ refer to the entirety of this connected volume (ice and water):

$$\phi \mathrm{d}\Omega_0 = n\mathrm{d}\Omega; \quad \phi = Jn. \tag{5}$$

In the undeformed reference configuration, the total porous volume is $\phi_0 \mathrm{d}\Omega_0$ with $\phi_0 = n_0$, and ϕ_0, n_0 are Lagrangian porosity and Eulerian porosity at undeformed reference configuration, respectively. At current time *t*, the porous volume is $\phi \mathrm{d}\Omega_0$.

For a REV of saturated frozen soil shown in Fig. 1, the overall Lagrangian porosity ϕ can be split into two partial porosities, ϕ_c (ice crystals) and ϕ_w (unfrozen water):

$$\phi = \phi_c + \phi_w. \tag{6}$$

The current partial porosities ϕ_α(α=*c*, *w*) may be written in the form as follows,

$$\phi_\alpha = \phi_0 S_\alpha + \varphi_\alpha, S_c + S_w = 1, \tag{7}$$

where S_α is the Langrangian saturation degree of phase α. The coefficients S_c et S_w reflect changes due to phase transformation and subsequent translation of the ice-water interface, whereas the coefficients φ_c et φ_w reflect the volume change due to deformation of the porous space. The overall change of the porous volume can only due to deformation of porous space, hence:

$$\phi - \phi_0 = \varphi_c + \varphi_w. \tag{8}$$

Based on (5) and (6), we can also define the Eulerian partial porosities by:

$$\phi_\alpha = Jn_\alpha, \tag{9}$$

so that $n_\alpha \mathrm{d}\Omega = \phi_\alpha \mathrm{d}\Omega_0$ represents the volume of α-phase in the current elementary volume $\mathrm{d}\Omega$. Similarly to (6), we have:

$$n = n_c + n_w, \tag{10}$$

The Eulerian saturation degrees are defined by:

$$n_c = ns_c,\ n_w = ns_w,\ s_c + s_w = 1, \tag{11}$$

in which $n_\alpha(\alpha = c, w)$ is Eulerian partial porosity of phase α, and $s_\alpha(\alpha = c, w)$ is Eulerian saturation degree of phase α.

2.1 Mass conservation

In the following, the mass-balance equations in the absence of phase change is presented first and then that considering phase change are given. For both cases, the Eulerian formulation is presented, followed by the Lagrangian formulation.

Let ρ_s and ρ_α (α=c, w) be the intrinsic mass densities of the solid matrix and the in-pore components, so that $\rho_s(1-n)d\Omega$ and $\rho_\alpha n s_\alpha d\Omega$ are respectively the mass of solid grains and that of the α-component currently contained in the material volume $d\Omega$. Accordingly, the macroscopic (or apparent) mass densities of the skeleton and α-component are respectively $\rho_s(1-n)$ and $\rho_\alpha n s_\alpha$. When phase change is absent, both for the skeleton and the in-phase components, the mass balance equations take the following form:

$$\frac{d^s}{dt}\int_\Omega \rho_s(1-n)\,\mathrm{d}\Omega = 0, \text{ and } \frac{d^s}{dt}(\rho_s(1-n)\mathrm{d}\Omega) = 0, \tag{12}$$

$$\frac{d^\alpha}{dt}\int_\Omega \rho_\alpha n s_\alpha\,\mathrm{d}\Omega = 0, \text{ and } \frac{d^\alpha}{dt}(\rho_\alpha n s_\alpha \mathrm{d}\Omega) = 0. \tag{13}$$

Therefore, the Eulerian continuity equations can be expressed as follows,

$$\frac{\partial(\rho_s(1-n))}{\partial t} + \nabla_x \cdot (\rho_s(1-n)\boldsymbol{V}^s) = 0, \tag{14}$$

and

$$\frac{\partial(\rho_\alpha n s_\alpha)}{\partial t} + \nabla_x \cdot (\rho_\alpha n s_\alpha \boldsymbol{V}^\alpha) = 0, \tag{15}$$

in which $\boldsymbol{V}^s$ and $\boldsymbol{V}^\alpha$ (α=c, w) are the velocities of solid grains and in-pore phases (ice crystals and unfrozen water) respectively, and can be expressed as follows,

$$\boldsymbol{V}^\pi(\mathbf{x}, t) = \frac{d^\pi \mathbf{x}}{dt} \quad (\pi = s, c, w). \tag{16}$$

where **x** refers to the common position of all the particles $(\pi = s, c, w)$ at the current time.

For the Lagrangian formulation, let m_α be the Lagrangian fluid mass content related to fluid α, we have:

$$m_\alpha = \rho_\alpha \phi_\alpha = \rho_\alpha \phi S_\alpha. \tag{17}$$

Following the derivation of saturated porous medium (Coussy, 1989), we can obtain the Lagrangian formulation of the mass conservation of in-pore phases (ice crystals or unfrozen water) as follows:

$$\frac{dm_\alpha}{dt} + \nabla_x \cdot \mathbf{M}_\alpha = 0, \text{ and } \quad \frac{\partial m_\alpha}{\partial t} + \frac{\partial \mathrm{M}_{\alpha i}}{\partial X_i} = 0, \tag{18}$$

where $\mathbf{M}_\alpha(X_i, t)$ is the Lagrangian flux attached to the initial configuration and linked to the Eulerian mass flux $\boldsymbol{w}_\alpha$ through the relations as follows,

$$\boldsymbol{w}_\alpha \cdot \boldsymbol{n} da = \boldsymbol{M}_\alpha \cdot \boldsymbol{N} dA, \tag{19}$$

$$\boldsymbol{M}_\alpha = J\boldsymbol{F}^{-1} \cdot \boldsymbol{w}_\alpha, \text{ and } M_{\alpha i} = J\frac{\partial X_i}{\partial x_j} \cdot w_{\alpha j}, \tag{20}$$

$$\nabla_x \cdot \mathbf{w}_\alpha \mathrm{d}\Omega = \nabla_X \cdot \boldsymbol{M}_\alpha \mathrm{d}\Omega_0, \text{ and } J\frac{\partial \mathrm{w}_{\alpha i}}{\partial x_i} = \frac{\partial M_{\alpha i}}{\partial X_i}. \tag{21}$$

Note that the liquid water mass flux writes: $\mathbf{w}_w(\mathbf{x}, t) = \rho_w \boldsymbol{\vartheta}$ with the filtration vector $\boldsymbol{\vartheta} = n(\boldsymbol{V}^w - \boldsymbol{V}^s)$ whereas $\mathbf{M}_w = \mathbf{w}_w = 0$ since ice crystals are attached to the solid skeleton with $\boldsymbol{V}^c = \boldsymbol{V}^s$. $\boldsymbol{N}$ is the unit normal of surface dA in initial configuration, and $\boldsymbol{n}$ the unit normal of surface da in current configuration.

The Lagrangian approach to the mass balance of the soil skeleton is as follows,

$$\rho_s(1-n)d\Omega = \rho_s^0(1-n_0)d\Omega_0, \tag{22}$$

in which ρ_s^0 is the initial matrix mass density, and $n_0 = \phi_0$ the initial porosity. Therefore, we can obtain the mass balance equation of the soil skeleton as follows,

$$m_s = J\rho_s(1-n) = m^0{}_s = \rho^0{}_s(1-\phi_0). \tag{23}$$

Note that phase change is not accounted for in the above derivation. The case where phase change

occurs for the open system is now considered. Assuming that phase change only concerns liquid water and ice crystals, the mass balance equation derived here-above for the solid matrix still applies. On the other hand, the mass balance equation for unfrozen water and ice crystals accounting for phase change now write as follows:

$$\frac{d^c}{dt}\int_\Omega \rho_c n_c d\Omega = \int_\Omega \Lambda_{w\to c} d\Omega, \tag{24}$$

$$\frac{d^w}{dt}\int_\Omega \rho_w n_w d\Omega = \int_\Omega \Lambda_{c\to w} d\Omega, \tag{25}$$

where $\Lambda_{w\to c}$ stands for the mass of water transforming into ice crystals per unit overall current volume and per unit time. The overall mass conservation requires that $\Lambda_{w\to c} = -\Lambda_{c\to w}$.

For any quantity Ξ, when the particle derivative applies to its volume integral, we have the following theorem:

$$\frac{d^\pi}{dt}\int_\Omega \Xi d\Omega = \int_\Omega \frac{d^\pi}{dt}(\Xi d\Omega), \tag{26}$$

so that

$$\frac{d^\pi}{dt}\int_\Omega \Xi d\Omega = \int_\Omega \left(\frac{\partial \Xi}{\partial \mathrm{t}} + \nabla_x \cdot (\Xi \mathbf{V}^\pi)\right) d\Omega. \tag{27}$$

On account of equation (26), the equations (24) and (25) can be rewritten as follows,

$$\frac{d^c}{dt}(\rho_c n_c d\Omega) = -\Lambda_{c\to w} d\Omega, \text{ and } \frac{d^w}{dt}(\rho_w n_w d\Omega) = \Lambda_{c\to w} d\Omega. \tag{28}$$

Using equation (27), we obtain the mass balance equations for the ice crystals and unfrozen water in Eulerian formulation as follows:

$$\frac{\partial(\rho_c n_c)}{\partial \mathrm{t}} + \nabla_x \cdot (\rho_c n_c \mathbf{V}^c) = -\Lambda_{c\to w}, \tag{29}$$

$$\frac{\partial(\rho_w n_w)}{\partial \mathrm{t}} + \nabla_x \cdot (\rho_w n_w \mathbf{V}^w) = \Lambda_{c\to w}. \tag{30}$$

Following the similar derivation of the previous Eulerian fluid continuity equations, the Lagrangian formulation of the continuum equations for ice crystals and unfrozen water can be obtained as follows,

$$\frac{d\mathrm{m}_c}{d\mathrm{t}} + \nabla_X \cdot \mathbf{M}_c = -\varpi_{c\to w}, \tag{31}$$

$$\frac{d\mathrm{m}_w}{d\mathrm{t}} + \nabla_X \cdot \mathbf{M}_w = \varpi_{c\to w}, \tag{32}$$

in which $m_\alpha = J\rho_\alpha n_\alpha = \rho_\alpha \phi_\alpha$; and $\varpi_{\alpha\to\beta} = J\Lambda_{\alpha\to\beta}$.

2.2 Momentum balance

With respect to purely mechanical considerations, the saturated frozen medium may be considered as the superposition of the ice crystals and unfrozen water in mechanical interaction. Therefore, the development of Coussy (1989, 1995) can be extended to saturated frozen soils to formulate the momentum balance. Using the definition of material derivatives, the variation of the linear momentum can now be expressed in terms of acceleration fields as follows,

$$\frac{d^s}{dt}\int_\Omega \rho_s(1-n)\boldsymbol{V}^s d\Omega + \sum_{\alpha=c,w}\frac{d^\alpha}{dt}\int_\Omega \rho_\alpha n_\alpha \boldsymbol{V}^\alpha d\Omega = \int_\Omega \left(\rho_s(1-n)\boldsymbol{\gamma}^s + \sum_{\alpha=c,w}\rho_\alpha n_\alpha \boldsymbol{\gamma}^\alpha\right) d\Omega + \int_\Omega \Lambda_{c\to w}(\boldsymbol{V^w} - \boldsymbol{V^c})\, d\Omega \ , \quad (33)$$

where $\rho_s(1-n)\boldsymbol{V}^s$ and $\rho_\alpha n_\alpha \boldsymbol{V}^\alpha (\alpha = c, w)$ represent the linear momentum of the soil skeleton, ice crystals and unfrozen water, respectively; $\boldsymbol{\gamma}^s$ and $\boldsymbol{\gamma}^\alpha$ are the accelerations of soil skeleton, ice crystals and unfrozen water, written as $\boldsymbol{\gamma}^\pi(\mathbf{x},t) = \frac{d^\pi \mathbf{V}}{dt}$ $(\pi = s, c, w)$; $\Lambda_{c\to w}(\boldsymbol{V^w} - \boldsymbol{V^c})$ accounts for the variation in linear momentum due to the mass rate exchanged between ice crystals and unfrozen water. On the other hand, the rate of change of linear momentum of all matters inside a material volume Ω is equal to the sum of all external forces acting on this matter (Lai et al., 2010). Therefore, the momentum balance with respect to all matters inside a generic porous domain Ω writes:

$$\frac{d^s}{dt}\int_\Omega \rho_s(1-n)\boldsymbol{V}^s d\Omega + \sum_{\alpha=c,w}\frac{d^\alpha}{dt}\int_\Omega \rho_\alpha n_\alpha \boldsymbol{V}^\alpha d\Omega = \int_\Omega \rho \boldsymbol{g}(\mathbf{x},\mathrm{t}) d\Omega + \int_{\partial\Omega} \boldsymbol{\sigma}\cdot\boldsymbol{n}\mathrm{d}a, \quad (34)$$

where $\rho = \rho_s(1-n) + \sum_{\alpha=c,w}\rho_\alpha n_\alpha$ is the total apparent mass density, $\boldsymbol{g}$ is the gravity and $\boldsymbol{\sigma}\cdot\boldsymbol{n}$ is the surface force acting on the boundary of the material domain Ω.

Combining Equations (33) and (34), we obtain the local equation of motion in Eulerian formulation as follows (Appendix I),

$$\nabla_x \cdot \boldsymbol{\sigma} + \rho_s(1-n)(\boldsymbol{g} - \boldsymbol{\gamma}^s) + \sum_{\alpha=c,w}\rho_\alpha n_\alpha(\boldsymbol{g} - \boldsymbol{\gamma}^\alpha) - \Lambda_{c\to w}(\boldsymbol{V^w} - \boldsymbol{V^c}) = 0. \quad (35)$$

To get the Lagrangian description, we introduce the Piola-Kirchhoff stress tensor $\boldsymbol{\pi}$ linked to the Cauchy stress $\boldsymbol{\sigma}$ as follows,

$$\boldsymbol{\pi} = J\boldsymbol{F}^{-1} \cdot \boldsymbol{\sigma} \cdot {}^{t}\boldsymbol{F}^{-1}. \tag{36}$$

A material surface element in the initial configuration $\mathrm{d}A$ and in the current configuration da (both contain the same set of solid skeleton particles) are linked to each other via the following equation:

$$\boldsymbol{F} \cdot \boldsymbol{\pi} \cdot \boldsymbol{N} dA = \boldsymbol{\sigma} \cdot \boldsymbol{n} da. \tag{37}$$

Considering the relation $\nabla_X \cdot \mathbf{V}\mathrm{d}\Omega_0 = \nabla_x \cdot \mathbf{v}\mathrm{d}\Omega$, the following expression can be obtained,

$$\nabla_X \cdot (\mathbf{F} \cdot \boldsymbol{\pi})\mathrm{d}\Omega_0 = \nabla_x \cdot \boldsymbol{\sigma}\mathrm{d}\Omega. \tag{38}$$

Therefore, the local equation of motion (35) in Eulerian formulation can be transformed to that in Lagrangian formulation as follows,

$$\nabla_X \cdot (\mathbf{F} \cdot \boldsymbol{\pi}) + m_s^0(\boldsymbol{g} - \boldsymbol{\gamma}^s) + \textstyle\sum_{\alpha=c,w} m_\alpha(\boldsymbol{g} - \boldsymbol{\gamma}^\alpha) - \varpi_{c\to w}(\boldsymbol{V}^w - \boldsymbol{V}^c) = 0. \tag{39}$$

2.3 Kinetic energy theorem

In the following, the kinetic energy theorem in Eulerian formulation is presented first. Favoring the motion of the soil skeleton by introducing the relative vector of fluid mass, $\boldsymbol{w}_\alpha = \rho_\alpha n_\alpha(\boldsymbol{V}^\alpha - \boldsymbol{V}^s)$ and the fluid pressure p_α. The work rate of the external body and surface forces of the RVE for saturated frozen soils in Eulerian form is as follows,

$$\mathrm{P_{f,T}}(\boldsymbol{V}^s, \boldsymbol{V}^\alpha) = \int_\Omega \left(\rho_s(1-n)\boldsymbol{g} \cdot \boldsymbol{V}^s + \boldsymbol{g} \cdot \textstyle\sum_{\alpha=c,w} \rho_\alpha n_\alpha \boldsymbol{V}^\alpha\right)d\Omega + \int_{\partial\Omega}\left(\boldsymbol{T}^s \cdot \boldsymbol{V}^s + \textstyle\sum_{\alpha=c,w}(\mathbf{T}^\alpha \cdot \boldsymbol{V}^\alpha)\right)da, \tag{40}$$

in which $\boldsymbol{T}^s$is the traction vector of soil solid grain, and $\mathbf{T}^\alpha$ the traction vector of fluid phase α.

The above equation can be rewritten as follows (referring to Appendix II),

$$\mathrm{P_{f,T}}(\boldsymbol{V}^s, \boldsymbol{V}^\alpha) = \int_\Omega \left(\rho\boldsymbol{g} \cdot \boldsymbol{V}^s + \boldsymbol{g} \cdot \textstyle\sum_{\alpha=c,w} \boldsymbol{w}^\alpha\right)d\Omega + \int_{\partial\Omega}\left(\mathbf{T} \cdot \boldsymbol{V}^s - \textstyle\sum_{\alpha=c,w}\left(\frac{p_\alpha}{\rho_\alpha}\boldsymbol{w}^\alpha\right) \cdot \mathbf{n}\right)da, \tag{41}$$

in which $\mathbf{T} = \boldsymbol{T}^s + \sum_{\alpha=c,w}\mathbf{T}^\alpha$ is the total traction vector.

For the RVE of saturated frozen soils, the kinetic energy associated with soil matrix and fluids

consisting of ice crystals and unfrozen water can be expressed as follows:

$$K_s = \frac{1}{2}\int_\Omega \rho_s(1-n)\,(\boldsymbol{V}^s)^2 d\Omega \text{ and } \sum_{\alpha=c,w} K_\alpha = \sum_{\alpha=c,w}\frac{1}{2}\int_\Omega \rho_\alpha n_\alpha\,(\boldsymbol{V}^\alpha)^2 d\Omega. \quad (42)$$

The above expression (42) of the kinetic energy does not account for the tortuosity effect (Biot, 1956). Therefore, the particle derivative of the kinetic energy of saturated frozen soils can be rewritten as follows (Appendix II),

$$\frac{d^s K_s}{dt} + \sum_{\alpha=c,w}\frac{d^\alpha K_\alpha}{dt} = \int_\Omega \left(\rho_s(1-n)\boldsymbol{\gamma}^s + \sum_{\alpha=c,w}\rho_\alpha n_\alpha \boldsymbol{\gamma}^\alpha\right)\cdot \boldsymbol{V}^s d\Omega + \int_\Omega \sum_{\alpha=c,w}\boldsymbol{\gamma}^\alpha\cdot\boldsymbol{w}^\alpha d\Omega +$$

$$\int_\Omega \frac{1}{2}\Lambda_{c\to w}((\boldsymbol{V}^w)^2 - (\boldsymbol{V}^c)^2)d\Omega \quad . (43)$$

Multiplying Equation (35) by $\boldsymbol{V}^s$ and integrating over the volume Ω while using Equation (43), we finally extend the kinetic energy theorem in Eulerian formulation as follows (Appendix II),

$$\mathrm{P}_{\mathrm{f,T}}(\boldsymbol{V}^s,\boldsymbol{V}^\alpha) = \mathrm{P}_{\mathrm{def}}(\boldsymbol{V}^s,\boldsymbol{V}^\alpha) + \frac{d^s K_s}{dt} + \sum_{\alpha=c,w}\frac{d^\alpha K_\alpha}{dt} - \int_\Omega \frac{1}{2}\Lambda_{c\to w}[(\boldsymbol{V}^w-\boldsymbol{V}^s)^2 - (\boldsymbol{V}^c-\boldsymbol{V}^s)^2]d\Omega, \quad (44)$$

where

$$\mathrm{P}_{\mathrm{def}}(\boldsymbol{V}^s,\boldsymbol{V}^\alpha) = \int_\Omega \boldsymbol{\sigma}:\mathbf{d}^s d\,\Omega - \int_\Omega \sum_{\alpha=c,w}\left[\nabla_x\cdot\left(\frac{p_\alpha}{\rho_\alpha}\boldsymbol{w}^\alpha\right) - (\boldsymbol{g}-\boldsymbol{\gamma}^\alpha)\cdot\boldsymbol{w}^\alpha\right] d\,\Omega. \quad (45)$$

The strain work rate $\mathrm{P}_{\mathrm{def}}(\boldsymbol{V}^s,\boldsymbol{V}^\alpha)$ is not a particle derivative and so the kinetic energy theorem cannot be interpreted as a conservation law. This theorem only expresses a balance of all the mechanical energies involved, without specifying the physical transformations affecting them.

In a similar way, the Kinetic energy theorem in Lagrangian formulation can be derived. The work rate of the external body and surface forces of the RVE for saturated frozen soils in Lagrangian form is as follows,

$$\mathcal{P}_{\mathrm{f,T}}(\boldsymbol{V}^s,\boldsymbol{V}^\alpha) = \int_{\Omega_0}\left(\rho_0\boldsymbol{g}\cdot\boldsymbol{V}^s + \boldsymbol{g}\cdot\frac{\boldsymbol{F}}{J}\cdot\sum_{\alpha=c,w}\boldsymbol{M}_\alpha\right)d\Omega_0 + \int_{\partial\Omega_0}\left(\boldsymbol{T}\cdot\boldsymbol{V}^s - \sum_{\alpha=c,w}\frac{\phi_\alpha p_\alpha}{m^\alpha}\frac{\boldsymbol{F}}{J}\cdot\boldsymbol{M}_\alpha\cdot\boldsymbol{N}\right)dA. \quad (46)$$

The kinetic energy associated with soil matrix and fluids consisting of ice crystals and unfrozen water can be expressed in Lagrangian formulation as follows,

$$\mathcal{K}_s = \frac{1}{2}\int_{\Omega_0}\rho_s^0\,(1-\phi)(\boldsymbol{V}^s)^2 d\Omega_0, \text{ and } \sum_{\alpha=c,w}\mathcal{K}_\alpha = \sum_{\alpha=c,w}\frac{1}{2}\int_{\Omega_0} m_\alpha\,(\boldsymbol{V}^\alpha)^2 d\Omega_0. \quad (47)$$

The strain work rate of the RVE for saturated frozen soils can be expressed in Lagrangian formulation as follows,

$$\mathcal{P}_{\mathrm{def}}(\boldsymbol{V}^s,\boldsymbol{V}^\alpha)=\int_{\Omega_0}\boldsymbol{\pi}:\frac{d\boldsymbol{\Delta}}{dt}d\Omega_0-\sum_{\alpha=c,w}\int_{\Omega_0}\left[\nabla_X\cdot\left(\frac{\phi_\alpha p_\alpha}{m^\alpha}\cdot\boldsymbol{M}_\alpha\right)-(\boldsymbol{g}-\boldsymbol{\gamma}^\alpha)\cdot\frac{\boldsymbol{F}}{J}\cdot\boldsymbol{M}_\alpha\right]d\Omega_0, \quad (48)$$

in which the Green-Lagrange strain tensor $\boldsymbol{\Delta}$ is defined as,

$$\boldsymbol{\Delta}=\frac{1}{2}\left({}^t\boldsymbol{F}\cdot\boldsymbol{F}-\mathbf{1}\right), \text{ and } \mathbf{d}^s={}^t\boldsymbol{F}^{-1}\cdot\frac{\mathrm{d}\boldsymbol{\Delta}}{dt}\cdot\boldsymbol{F}^{-1}. \quad (49)$$

Therefore, the kinetic energy theorem in Lagrangian formulation can be obtained as follows,

$$\mathcal{P}_{\mathrm{f,T}}(\boldsymbol{V}^s,\boldsymbol{V}^\alpha)=\mathcal{P}_{\mathrm{def}}(\boldsymbol{V}^s,\boldsymbol{V}^\alpha)+\frac{d^s\mathcal{K}_s}{dt}+\sum_{\alpha=c,w}\frac{d^\alpha\mathcal{K}_\alpha}{dt}-\int_{\Omega_0}\frac{1}{2}\,\varpi_{c\to w}[(\boldsymbol{V}^w-\boldsymbol{V}^s)^2-(\boldsymbol{V}^c-\boldsymbol{V}^s)^2]d\Omega_0. \quad (50)$$

3. Thermoporomechanics of saturated frozen soils

In this section, the thermodynamics of classic saturated porous media will be extended to saturated frozen soils taking into account the phenomenon of phase transformation (between liquid water and ice crystal). According to Coussy (1995), the extension of thermostatics to thermodynamics of continua can be obtained on the basis of the postulate of local state with regard to both time and space. With regard to time, the postulate of local state stipulates that the current state of internal energy of a homogeneous system in any (slow enough) evolution can be considered as crossing different equilibrium states such that at any time its state variables satisfy the state equations characterizing equilibrium states. With regard to space, the postulate of local state addresses the thermodynamics of a heterogeneous continuum by assuming that the material volume Ω can be considered as an ensemble of juxtaposed sub-systems or elementary material volumes $\mathrm{d}\Omega$ exchanging heat and mechanical work between them, each of them being in thermodynamic equilibrium hence verifies again the state equations. Note that an elementary material volume here is composed of the soil skeleton and of saturating "fluids" (we will use the term "fluid" as a convenient short-hand terminology when referring to the in-pore phases) of ice crystals and unfrozen water. Consequently, elementary thermodynamic

317 systems and the continua they form are open systems. As a consequence, the laws of thermodynamics
318 can be applied in an integral form to extensive quantities such as the energy, mass, momentum and
319 entropy. With the help of the local state postulate, it will be seen how to extend the thermodynamics of
320 closed continua to open continua composed of saturated frozen soils.

321 **3.1 The First law of thermodynamics principle**

322 **3.1.1 Energy conservation**

323 Based on the postulate of local state, the first law of thermodynamics states that the time rate of the
324 energy attached to the whole matter currently contained within the volume of saturated frozen soils is
325 equal to the sum of the work rate $\mathrm{P}_{\mathrm{f,T}}(\boldsymbol{V}^s, \boldsymbol{V}^\alpha)$ of the external forces acting upon this matter, and of the
326 rate Q^0 of external heat supply. When applied to a generic material volume of saturated frozen soils,
327 this leads to the energy balance equation as follows,

328 $$\frac{d^s}{dt}\int_\Omega \rho_s(1-n)\left(e_s+\frac{1}{2}(\boldsymbol{V}^s)^2\right)d\Omega+\sum_{\alpha=c,w}\frac{d^\alpha}{dt}\int_\Omega \rho_\alpha n_\alpha\left(e_\alpha+\frac{1}{2}(\boldsymbol{V}^\alpha)^2\right)d\Omega=\mathrm{P}_{\mathrm{f,T}}(\boldsymbol{V}^s,\boldsymbol{V}^\alpha)+Q^0, \quad (51)$$

329 in which e_s stands for the specific (i.e. per unit mass) internal energy of the soil matrix and e_α that of
330 the fluid phases. The total internal energy e per unit overall current volume can be expressed as
331 follows,

332 $$e=\rho_s(1-n)e_s+\sum_{\alpha=c,w}\rho_\alpha n_\alpha e_\alpha. \quad (52)$$

333 The internal energy e is a volume density, and not a density per mass unit as it is usually the case in
334 mechanics of closed continua. The particular choice of the volume density is more convenient here:
335 when following $d\Omega$ in the skeleton movement, $d\Omega$ will exchange fluid mass with its neighbours.
336 Thus, the quantity $ed\Omega$ always corresponds to the same set of solid particles but to different sets of
337 fluid particles at different times.

338 The rate of external heat supply can be written as follows,

$$Q^0 = \int_{\partial\Omega} \boldsymbol{J}_Q(\boldsymbol{x}, n, t)da + \int_\Omega \boldsymbol{r}_Q(\boldsymbol{x}, t)d\Omega, \quad (53)$$

in which $\boldsymbol{r}_Q$ is a volume density of the heat provided to Ω by an external heat sources, and $\boldsymbol{J}_Q$ is a surface rate of heat supply by conduction.

3.1.2 The energy equation

Use of the kinetic energy theorem of Equation (44) allows us to rewrite Equation (51) in the form as follows,

$$\frac{d^s}{dt}\int_\Omega \rho_s(1-n)e_s d\Omega + \sum_{\alpha=c,w}\frac{d^\alpha}{dt}\int_\Omega \rho_\alpha n_\alpha e_\alpha \, d\Omega = \mathrm{P}_{\mathrm{def}}(\boldsymbol{V}^s, \boldsymbol{V}^\alpha) - \int_\Omega \frac{1}{2}\Lambda_{c\to w}[(\boldsymbol{V}^w - \boldsymbol{V}^s)^2 - (\boldsymbol{V}^c - \boldsymbol{V}^s)^2]d\Omega + Q^0 \quad . \quad (54)$$

Combining Equation (52), the left side of Equation (54) can be rewritten as follows (Appendix III),

$$\frac{d^s}{dt}\int_\Omega \rho_s(1-n)e_s d\Omega + \sum_{\alpha=c,w}\frac{d^\alpha}{dt}\int_\Omega \rho_\alpha n_\alpha e_\alpha \, d\Omega = \int_\Omega \left[\frac{d^s e}{dt} + e\nabla_x\cdot\boldsymbol{V}^s + \sum_{\alpha=c,w}\nabla_x\cdot(e_\alpha \boldsymbol{w}^\alpha)\right]d\Omega. \quad (55)$$

Expression (45) for the strain work rate $\mathrm{P}_{\mathrm{def}}(\boldsymbol{V}^s, \boldsymbol{V}^\alpha)$, together with Equations (53)-(55), yields:

$$\int_\Omega \left[\frac{d^s e}{dt} + e\nabla_x\cdot\boldsymbol{V}^s + \sum_{\alpha=c,w}\nabla_x\cdot(e_\alpha \boldsymbol{w}^\alpha)\right]d\Omega = \int_\Omega \boldsymbol{\sigma}:\mathbf{d}^s d\,\Omega - \int_\Omega \sum_{\alpha=c,w}\left[\nabla_x\cdot\left(\frac{p_\alpha}{\rho_\alpha}\boldsymbol{w}^\alpha\right) - (\boldsymbol{g}-\boldsymbol{\gamma}^\alpha)\cdot\boldsymbol{w}^\alpha\right]d\,\Omega - \int_\Omega \frac{1}{2}\Lambda_{c\to w}[(\boldsymbol{V}^w - \boldsymbol{V}^s)^2 - (\boldsymbol{V}^c - \boldsymbol{V}^s)^2]d\Omega + Q^0 \quad . \quad (56)$$

The above equation (56) can be rewritten as follows,

$$\int_\Omega \left[\frac{d^s e}{dt} + e\nabla_x\cdot\boldsymbol{V}^s + \sum_{\alpha=c,w}\nabla_x\cdot\left(e_\alpha\boldsymbol{w}^\alpha + \frac{p_\alpha}{\rho_\alpha}\boldsymbol{w}^\alpha\right) - \boldsymbol{\sigma}:\mathbf{d}^s - (\boldsymbol{g}-\boldsymbol{\gamma}^\alpha)\cdot\boldsymbol{w}^\alpha\right]d\Omega + \int_\Omega \frac{1}{2}\Lambda_{c\to w}[(\boldsymbol{V}^w - \boldsymbol{V}^s)^2 - (\boldsymbol{V}^c - \boldsymbol{V}^s)^2]d\Omega = \int_{\partial\Omega}\boldsymbol{J}_Q(x,n,t)da + \int_\Omega \boldsymbol{r}_Q(x,t)d\Omega \quad , (57)$$

The surface rate $\boldsymbol{J}_\mathrm{Q}$ relies linearly on **n**, expressed as follows (Lai et al., 2010),

$$\boldsymbol{J}_Q = -\boldsymbol{q}\cdot\mathbf{n}. \quad (58)$$

where $\boldsymbol{q}$ is an outgoing heat flow vector.

Substitution of Eq. (58) into Eq. (57) provides the Euler energy equation as follows,

$$\int_\Omega \left[\frac{d^s e}{dt} + e\nabla_x\cdot\boldsymbol{V}^s + \sum_{\alpha=c,w}\nabla_x\cdot\left(e_\alpha\boldsymbol{w}^\alpha + \frac{p_\alpha}{\rho_\alpha}\boldsymbol{w}^\alpha\right) - \boldsymbol{\sigma}:\mathbf{d}^s - (\boldsymbol{g}-\boldsymbol{\gamma}^\alpha)\cdot\boldsymbol{w}^\alpha\right]d\Omega + \int_\Omega \frac{1}{2}\Lambda_{c\to w}[(\boldsymbol{V}^w -$$

$\boldsymbol{V}^s)^2 - (\boldsymbol{V}^c - \boldsymbol{V}^s)^2]d\Omega = \int_{\partial\Omega}(-\boldsymbol{q}\cdot\mathbf{n})da + \int_{\Omega}\boldsymbol{r}_Q(x,t)d\Omega$.(59)

Using the theorem of divergence, we can rewrite the above equation (59) as follows,

$\frac{d^s e}{dt} + e\nabla_x\cdot\boldsymbol{V}^s = \boldsymbol{\sigma}:\boldsymbol{d}^s - \sum_{\alpha=c,w}\nabla_x\cdot(h_\alpha\boldsymbol{w}^\alpha) - \nabla_x\cdot\boldsymbol{q} + \sum_{\alpha=c,w}(\boldsymbol{g}-\boldsymbol{\gamma}^\alpha)\cdot(\boldsymbol{w}^\alpha) + \boldsymbol{r}_Q - \frac{1}{2}\Lambda_{c\to w}[(\boldsymbol{V}^w -$

$\boldsymbol{V}^s)^2 - (\boldsymbol{V}^c - \boldsymbol{V}^s)^2]$, (60)

in which the fluid-specific enthalpy writes $h_\alpha = e_\alpha + \frac{p_\alpha}{\rho_\alpha}$ $(\alpha = c, w)$.

With the aim of transforming the energy equation (60) to the initial configuration of the soil skeleton, let E, $\boldsymbol{Q}$ and $\boldsymbol{R_Q}$ be respectively the overall Lagrangian densities of internal energy per unit of initial volume $\mathrm{d}\Omega_0$, the Lagrangian heat flow vector and volume rate density of the heat provided to Ω_0, such that:

$$\mathrm{E}\mathrm{d}\Omega_0 = e\mathrm{d}\Omega,\ \mathbf{Q}\cdot\mathbf{N}\mathrm{d}\mathrm{A} = \boldsymbol{q}\cdot\boldsymbol{n}\mathrm{d}\mathrm{a}, \text{ and } \boldsymbol{R}_Q\mathrm{d}\Omega_0 = \boldsymbol{r}_Q\mathrm{d}\Omega. \quad (61)$$

Considering the following equations (Coussy, 1995),

$\left(\frac{d^s e}{dt} + e\nabla_x\cdot\boldsymbol{V}^s\right)\mathrm{d}\Omega = \frac{d^s}{dt}(e\mathrm{d}\Omega) = \frac{d^s}{dt}(E\mathrm{d}\Omega_0),\ (\boldsymbol{\sigma}:\boldsymbol{d}^s)\mathrm{d}\Omega = \boldsymbol{\pi}:\frac{d\Delta}{dt}\mathrm{d}\Omega_0,\ \nabla_x\cdot\boldsymbol{q}\mathrm{d}\Omega = \nabla_X\cdot\boldsymbol{Q}\mathrm{d}\Omega_0,$

And $$\nabla_x\cdot(h_\alpha\boldsymbol{w}^\alpha)\mathrm{d}\Omega = \nabla_X\cdot(h_\alpha\boldsymbol{M}_\alpha)\mathrm{d}\Omega_0\ \ (\alpha = c, w), \quad (62)$$

and combining Equations (60), (61) and transport formulae derived in the previous sections, we can have the Lagrangian energy equation as follows,

$\frac{dE}{dt} = \boldsymbol{\pi}:\frac{d\Delta}{dt} - \sum_{\alpha=c,w}\nabla_X\cdot(h_\alpha\boldsymbol{M}_\alpha) - \nabla_X\cdot\boldsymbol{Q} + \sum_{\alpha=c,w}\left((\boldsymbol{g}-\boldsymbol{\gamma}^\alpha)\cdot\boldsymbol{F}\right)\cdot\boldsymbol{M}_\alpha + \boldsymbol{R}_Q - \frac{1}{2}\varpi_{c\to w}[(\boldsymbol{V}^w -$

$\boldsymbol{V}^s)^2 - (\boldsymbol{V}^c - \boldsymbol{V}^s)^2]$. (63)

3.2 The Second law of thermodynamics principle

3.2.1 The Clausius-Duhem inequality in Eulerian and Lagrangian formulations

There exists an extensive thermodynamic function, called entropy. According to the second principle of thermodynamics, during any process, the increase of entropy θ attached to any material subsystem Ω must be superior or at least equal to the rate of entropy externally supplied to it. Assuming that the

same temperature holds for the soil particle (or matrix), ice crystals and unfrozen water, the above entropy balance admits the following mathematical form:

$$\frac{d^s}{dt}\int_\Omega \rho_s(1-n)\theta_s d\Omega + \sum_{\alpha=c,w}\frac{d^\alpha}{dt}\int_\Omega \rho_\alpha n_\alpha \theta_\alpha d\Omega \geq \int_{\partial\Omega} -\frac{\boldsymbol{q}\cdot\boldsymbol{n}}{T} da + \int_\Omega \frac{r_Q}{T} d\Omega, \quad (64)$$

where θ_s, θ_c and θ_w stand for the specific entropy of the soil matrix, ice crystals and unfrozen water, respectively.

Using the theorem on material derivative, the left hand side of the above inequality can be written as follows (Appendix III),

$$\frac{d^s}{dt}\int_\Omega \rho_s(1-n)\theta_s d\Omega + \sum_{\alpha=c,w}\frac{d^\alpha}{dt}\int_\Omega \rho_\alpha n_\alpha \theta_\alpha d\Omega = \int_\Omega \left[\frac{d^s s}{dt} + \theta\nabla_x\cdot\boldsymbol{V}^s + \sum_{\alpha=c,w}\nabla_x\cdot(\theta_\alpha \boldsymbol{w}^\alpha)\right] d\Omega, \quad (65)$$

where θ is the total entropy per unit of overall current volume:

$$\theta = \rho_s(1-n)\theta_s + \sum_{\alpha=c,w}\rho_\alpha n_\alpha \theta_\alpha. \quad (66)$$

Substituting Equation (65) into Equation (64) and using theorem of divergence, we can obtain after some simplification:

$$\int_\Omega \left[\frac{d^s\theta}{dt} + \theta\nabla_x\cdot\boldsymbol{V}^s + \sum_{\alpha=c,w}\nabla_x\cdot(\theta_\alpha \boldsymbol{w}^\alpha)\right] d\Omega \geq \int_\Omega -\nabla_x\cdot\frac{\boldsymbol{q}}{T} d\Omega + \int_\Omega \frac{r_Q}{T} d\Omega. \quad (67)$$

Therefore, the following can be obtained,

$$\frac{d^s\theta}{dt} + \theta\nabla_x\cdot\boldsymbol{V}^s + \sum_{\alpha=c,w}\nabla_x\cdot(\theta_\alpha \boldsymbol{w}^\alpha) + \nabla_x\cdot\frac{\boldsymbol{q}}{T} - \frac{r_Q}{T} \geq 0. \quad (68)$$

Introducing the Helmholtz free energy $\psi = e - T\theta$, and combining Equation (60), we are led to the fundamental Clausius-Duhem inequality in Eulerian form (Appendix III),

$$\boldsymbol{\sigma}:\boldsymbol{d}^s - \sum_{\alpha=c,w}(g_\alpha\nabla_x\cdot\boldsymbol{w}^\alpha) - \theta\frac{dT}{dt} - \frac{d\psi}{dt} - \psi\nabla_x\cdot\boldsymbol{V}^s - \boldsymbol{w}^\alpha\cdot\sum_{\alpha=c,w}\left(\nabla_x g_\alpha + \theta_\alpha\nabla_x T - (\boldsymbol{g} - \boldsymbol{\gamma}^\alpha)\right) -$$

$$\frac{1}{2}\Lambda_{c\to w}[(\boldsymbol{V}^w - \boldsymbol{V}^s)^2 - (\boldsymbol{V}^c - \boldsymbol{V}^s)^2] - \frac{\boldsymbol{q}}{T}\cdot\nabla_x T \geq 0 \quad .(69)$$

To obtain the corresponding Lagrangian formulation, we introduce Lagrangian entropy density Θ defined by

$$\Theta d\Omega_0 = \theta d\Omega. \quad (70)$$

Therefore, Inequality (68) can be written in the Lagrangian formulation as follows (Appendix III),

$$\frac{d\Theta}{dt} + \sum_{\alpha=c,w} \nabla_X \cdot (\Theta_\alpha \boldsymbol{M}_\alpha) + \nabla_X \cdot \frac{\boldsymbol{Q}}{T} - \frac{\boldsymbol{R_Q}}{T} \geq 0. \quad (71)$$

Let Ψ be the Lagrangian free energy density which verifies:

$$\Psi d\Omega_0 = \psi d\Omega, \text{ and } \Psi = E - T\Theta. \quad (72)$$

By recalling the mass conservation (31) and (32), the Lagrangian energy equation (63), Inequality (71) can be written as follows (Appendix III),

$$\boldsymbol{\pi}: \frac{d\Delta}{dt} + \sum_{\alpha=c,w} g_\alpha \frac{dm_\alpha}{dt} - \Theta \frac{dT}{dt} - \frac{d\Psi}{dt} - (g_c - g_w)\varpi_{c\to w} - \frac{1}{2}\varpi_{c\to w}[(\boldsymbol{V}^w - \boldsymbol{V}^s)^2 - (\boldsymbol{V}^c - \boldsymbol{V}^s)^2] -$$

$$\sum_{\alpha=c,w}(\nabla_X g_\alpha + \Theta_\alpha \nabla_X T - (\boldsymbol{g} - \boldsymbol{\gamma}^\alpha) \cdot \boldsymbol{F}) \cdot \boldsymbol{M}_\alpha - \frac{\boldsymbol{Q}}{T} \cdot \nabla_X T \geq 0 \quad .(73)$$

The above is the Lagrangian formulation of the Clausius-Duhem inequality.

3.2.2 Identification of dissipation and Thermal equation

The left hand side of Inequality (73), which will be noted as Φ, is the total dissipation per unit of initial volume $d\Omega_0$. The second law requires the dissipation and the associated internal entropy produce Φ/T to be non-negative. Following Coussy (2004), the total dissipation Φ can be decomposed as the sum of different contributions of different physical origins while each one being non-negative as follows,

$$\Phi = \Phi_1 + \Phi_2 + \Phi_3 + \Phi_\rightarrow \ , \quad (74)$$

in which $$\Phi_1 = \boldsymbol{\pi}: \frac{d\Delta}{dt} + \sum_\alpha g_\alpha \frac{dm_\alpha}{dt} - \Theta \frac{dT}{dt} - \frac{d\Psi}{dt} \ , \quad (75)$$

$$\Phi_2 = -\frac{\boldsymbol{Q}}{T} \cdot \nabla_X T, \quad (76)$$

$$\Phi_3 = -\sum_{\alpha=c,w}(\nabla_X g_\alpha + \Theta_\alpha \nabla_X T - (\boldsymbol{g} - \boldsymbol{\gamma}^\alpha) \cdot \boldsymbol{F}) \cdot \boldsymbol{M}_\alpha, \quad (77)$$

$$\Phi_\rightarrow = -(g_c - g_w)\varpi_{c\to w} - \frac{1}{2}\varpi_{c\to w}[(\boldsymbol{V}^w - \boldsymbol{V}^s)^2 - (\boldsymbol{V}^c - \boldsymbol{V}^s)^2]. \quad (78)$$

Φ_1 is the intrinsic dissipation associated with the open system $d\Omega_0$, following the movement of the soil skeleton. On account of the local state postulate, all the quantities which appear in expression (75)

of Φ_1 depend only on the state variables which characterize the free energy $\Psi d\Omega_0$ of the open elementary system $d\Omega_0$. Thus, the terminology of intrinsic dissipation for Φ_1 is due to its dependence with regard to the other open elementary systems which constitute the continuum of saturated frozen soils. For the same reason, Φ_1/T is called the intrinsic entropy in internal production. The other contributions Φ_2, Φ_3 and $\Phi_{\rightarrow}$ are , respectively, the thermal dissipation associated with heat conduction, the dissipation associated with mass transport of in-pore phases, and the dissipation associated with phase change.

From Equation (72), we have

$$\frac{dE}{dt} = \frac{d\Psi}{dt} + T\frac{d\Theta}{dt} + \Theta\frac{dT}{dt}. \tag{79}$$

Combining energy equation (63), we can have (Appendix IV)

$$T\left(\frac{d\Theta}{dt} + \sum_{\alpha=c,w}\nabla_X\cdot(\Theta_\alpha \boldsymbol{M}_\alpha)\right) = \boldsymbol{R}_Q - \nabla_X\cdot\boldsymbol{Q} + \Phi_1 + \Phi_3 + \Phi_{\rightarrow} = \boldsymbol{R}_Q - \nabla_X\cdot\boldsymbol{Q} + \Phi_M + \Phi_{\rightarrow}, \tag{80}$$

in which $\Phi_M = \Phi_1 + \Phi_3$ is the mechanical dissipation due to irreversible matter movements. The equation (80) is called the Lagrangian thermal equation.

Substituting Equation (76) into Equation (80), we have

$$\frac{d\Theta}{dt}d\Omega_0 = \left[-\sum_{\alpha=c,w}\nabla_X\cdot(\Theta_\alpha\boldsymbol{M}_\alpha) + \left(\frac{\boldsymbol{R_Q}}{T} - \nabla_X\cdot\frac{\boldsymbol{Q}}{T}\right) + \frac{\Phi}{T}\right]d\Omega_0 = \left[-\sum_{\alpha=c,w}\nabla_X\cdot(\Theta_\alpha\boldsymbol{M}_\alpha)\right]d\Omega_0 + \left[\left(\frac{\boldsymbol{R_Q}}{T} - \nabla_X\cdot\frac{\boldsymbol{Q}}{T}\right)\right]d\Omega_0 + \frac{\Phi}{T}d\Omega_0 \tag{81}$$

Considering that $\frac{d}{dt}(\Theta d\Omega_0) = \Theta\frac{d}{dt}(d\Omega_0) + d\Omega_0\frac{d}{dt}(\Theta) = \frac{d\Theta}{dt}d\Omega_0$, so we have

$$\frac{d(\Theta d\Omega_0)}{dt} = -[\sum_\alpha\nabla_X\cdot(\Theta_\alpha\boldsymbol{M}_\alpha)]d\Omega_0 + \left(\frac{\boldsymbol{R_Q}}{T} - \nabla_X\cdot\frac{\boldsymbol{Q}}{T}\right)d\Omega_0 + \frac{\Phi}{T}d\Omega_0. \tag{82}$$

Hence, the thermal equation (80), or equivalently Equation (82), corresponds to a balance in entropy for the elementary open system $d\Omega_0$. The term $d(\Theta d\Omega_0)$ is the entropy variation which could be recorded, during the time interval d*t*, by an observer attached to the open system $d\Omega_0$ following the

movement of the soil skeleton. Equation (82) stipulates that this variation must be equal to the external supply plus the internal entropy production within the system, during the same time interval.

The above is the Lagrangian formulation of the thermal equation. Let φ_i be the Eulerian dissipation volume densities defined by

$$\varphi_i d\Omega = \Phi_i d\Omega_0 \quad \text{and} \quad J\varphi_i = \Phi_i \ . \tag{83}$$

The dissipations in Eulerian formulation are as follows,

$$\varphi = \varphi_1 + \varphi_2 + \varphi_3 + \varphi_{\rightarrow}, \tag{84}$$

and

$$\varphi_1 = \boldsymbol{\sigma}: \boldsymbol{d}^s - \sum_\alpha (g_\alpha \nabla_x \cdot \boldsymbol{w}^\alpha) - \theta \frac{dT}{dt} - \frac{d\psi}{dt} - \psi \nabla_x \cdot \boldsymbol{V}^s \ , \tag{85}$$

$$\varphi_2 = -\frac{\boldsymbol{q}}{T} \cdot \nabla_x T \quad , \tag{86}$$

$$\varphi_3 = -\boldsymbol{w}^\alpha \cdot \sum_\alpha \left(\nabla_x g_\alpha + \theta_\alpha \nabla_x T - (\boldsymbol{g} - \boldsymbol{\gamma}^\alpha) \right) \ , \tag{87}$$

$$\varphi_{\rightarrow} = -\frac{1}{2} \Lambda_{c \rightarrow w} [(\boldsymbol{V}^w - \boldsymbol{V}^s)^2 - (\boldsymbol{V}^c - \boldsymbol{V}^s)^2]. \tag{88}$$

From the definition that $\psi = e - T\theta$, we can obtain

$$\mathrm{d}e = \mathrm{d}\psi + Td\theta + \theta dT \ \text{ and } \ \frac{\mathrm{d}e}{dt} = \frac{\mathrm{d}\psi}{dt} + T\frac{d\theta}{dt} + \theta \frac{dT}{dt}. \tag{89}$$

From Equation (80), we can deduce the following Eulerian thermal balance equation (Appendix IV),

$$T\frac{d\theta}{dt} + T\theta \nabla_x \cdot \boldsymbol{V}^s + T \sum_\alpha \nabla_x \cdot (\theta_\alpha \boldsymbol{w}^\alpha) = \boldsymbol{r}_Q - \nabla_x \cdot \boldsymbol{q} + \varphi_1 + \varphi_3 + \varphi_{\rightarrow}. \tag{90}$$

3.3 Heat conduction and mass transport for in-pore phases

3.3.1 Darcy's Law

For the fluids ($\alpha = c, w$), their fluid-specific free enthalpy can be expressed as follows,

$$g_\alpha = g_\alpha(p, T): \frac{1}{\rho_\alpha} = \frac{\partial g_\alpha}{\partial p_\alpha}; \theta_\alpha = -\frac{\partial g_\alpha}{\partial T}. \tag{91}$$

φ_3 in Equation (91) denotes the dissipation associated with fluid mass transport or conduction through the porous medium. From Equation (91), we have

$$\nabla_x g_\alpha = \frac{\partial g_\alpha}{\partial p} \nabla_x p_\alpha + \frac{\partial g_\alpha}{\partial T} \nabla_x T. \tag{92}$$

Substituting Equation (92) into Equation (87), we have

$$\varphi_3 = -\boldsymbol{w}^{\alpha} \cdot \sum_{\alpha}\left(\nabla_x g_{\alpha} + \theta_{\alpha}\nabla_x T - (\boldsymbol{g} - \boldsymbol{\gamma}^{\alpha})\right) = \sum_{\alpha} \frac{\boldsymbol{w}^{\alpha}}{\rho_{\alpha}} \cdot \left(-\nabla_x p_{\alpha} + \rho_{\alpha}(\boldsymbol{g} - \boldsymbol{\gamma}^{\alpha})\right) \geq 0. \tag{93}$$

For the ice crystals or unfrozen water, the dissipation can be assumed to be non-negative, expressed as follows,

$$\frac{\boldsymbol{w}^{\alpha}}{\rho_{\alpha}} \cdot \left(-\nabla_x p_{\alpha} + \rho_{\alpha}(\boldsymbol{g} - \boldsymbol{\gamma}^{\alpha})\right) = \boldsymbol{v}_{\alpha} \cdot \boldsymbol{\ell}_{\alpha} \geq 0, \tag{94}$$

in which $\boldsymbol{v}_{\alpha} = \frac{\boldsymbol{w}^{\alpha}}{\rho_{\alpha}}$ and $\boldsymbol{\ell}_{\alpha} = -\nabla_x p_{\alpha} + \rho_{\alpha}(\boldsymbol{g} - \boldsymbol{\gamma}^{\alpha})$.

At the quasistatic limit where the inertia forces can be neglected, and in the absence of body forces, Inequality (93) implies that the fluid mass transport takes place from high to low fluid pressures. Again, the assumption of the normality of the associated dissipative mechanism leads one to postulate the existence of a dissipation potential $D_{3\alpha}\left(\frac{\boldsymbol{w}^{\alpha}}{\rho_{\alpha}}\right)$ such that (Lemaitre et al., 1994)

$$-\nabla_x p_{\alpha} + \rho_{\alpha}(\boldsymbol{g} - \boldsymbol{\gamma}^{\alpha}) = \frac{\partial D_{3\alpha}}{\partial \frac{\boldsymbol{w}^{\alpha}}{\rho_{\alpha}}}. \tag{95}$$

If the potential $D_{3\alpha}\left(\frac{\boldsymbol{w}^{\alpha}}{\rho_{\alpha}}\right)$ is chosen as a positively defined quadratic function as follows,

$$D_{3\alpha}\left(\frac{\boldsymbol{w}^{\alpha}}{\rho_{\alpha}}\right) = \frac{1}{2}\frac{\boldsymbol{w}^{\alpha}}{\rho_{\alpha}} \cdot \mathbf{k}_{\alpha}^{-1} \cdot \frac{\boldsymbol{w}^{\alpha}}{\rho_{\alpha}}, \tag{96}$$

where $\mathbf{k}_{\boldsymbol{\alpha}}$ is a symmetric tensor which corresponds to a positively defined bilinear form, Eqs. (95) and (96) yield the linear mass fluid conduction law or Darcy's law as follows,

$$\frac{\boldsymbol{w}^{\alpha}}{\rho_{\alpha}} = \mathbf{k}_{\alpha} \cdot \left(-\nabla_x p_{\alpha} + \rho_{\alpha}(\boldsymbol{g} - \boldsymbol{\gamma}^{\alpha})\right), \tag{97}$$

where $\mathbf{k}_{\alpha}$ is then identified as the permeability tensor, relative to the current configuration.

For the Lagrangian equations, corresponding to Equations (93)-(97), we can have the following equations,

$$\Phi_3 = -\sum_{\alpha}(\nabla_X g_{\alpha} + \Theta_{\alpha}\nabla_X T - (\boldsymbol{g} - \boldsymbol{\gamma}^{\alpha}) \cdot \boldsymbol{F}) \cdot M^{\alpha} = -\sum_{\alpha} \frac{\boldsymbol{M}^{\alpha}}{\rho_{\alpha}}(\nabla_X p_{\alpha} - (\boldsymbol{g} - \boldsymbol{\gamma}^{\alpha}) \cdot \boldsymbol{F}) \geq 0, \tag{98}$$

which is assumed to be non-negative, expressed as follows,

$$\frac{\boldsymbol{M}_{\alpha}}{\rho_{\alpha}}(\nabla_X p_{\alpha} - (\boldsymbol{g} - \boldsymbol{\gamma}^{\alpha}) \cdot \boldsymbol{F}) = \boldsymbol{\mathcal{V}}_{\alpha} \cdot \boldsymbol{\mathcal{L}}_{\alpha} \geq 0, \tag{99}$$

494 in which $\boldsymbol{\mathcal{V}}_\alpha = \frac{\boldsymbol{M}_\alpha}{\rho_\alpha}$ and $\boldsymbol{\mathcal{L}}_\alpha = \nabla_X p_\alpha - (\boldsymbol{g} - \boldsymbol{\gamma}^\alpha) \cdot \boldsymbol{F}$. (100)

495 Choosing the dissipation potential $D_{3\alpha}\left(\frac{\boldsymbol{M}_\alpha}{\rho_\alpha}\right)$ as follows,

496 $$D_{3\alpha}\left(\frac{\boldsymbol{M}_\alpha}{\rho_\alpha}\right) = \frac{1}{2}\frac{\boldsymbol{M}^\alpha}{\rho_\alpha} \cdot \mathbf{K}_\alpha^{-1} \cdot \frac{\boldsymbol{M}_\alpha}{\rho_\alpha}, \quad (101)$$

497 so we have

498 $$\nabla_X p - (\boldsymbol{g} - \boldsymbol{\gamma}^\alpha) \cdot \boldsymbol{F} = \frac{\partial D_{3\alpha}}{\partial \frac{\boldsymbol{M}^\alpha}{\rho_\alpha}}, \quad (102)$$

499 and $$\frac{\boldsymbol{M}_\alpha}{\rho_\alpha} = \mathbf{K}_\alpha \cdot (\nabla_X p_\alpha - (\boldsymbol{g} - \boldsymbol{\gamma}^\alpha) \cdot \boldsymbol{F}), \quad (103)$$

500 where $\mathbf{K}_\alpha$ is the convective transportee of $\mathbf{k}_\alpha$, with $\mathbf{K}_\alpha = J\boldsymbol{F}^{-1} \cdot \mathbf{k}_\alpha \cdot {}^t\boldsymbol{F}^{-1}$.

501 **3.3.2 Fourier's Law**

502 The decoupling hypothesis (84) requires the non-negativity of thermal dissipation φ_2, which reads

503 $$\varphi_2 = -\frac{\boldsymbol{q}}{T} \cdot \nabla_x T = -\boldsymbol{L}_{q/T} \cdot \frac{\boldsymbol{q}}{T} \geq 0 \quad \text{and} \quad \boldsymbol{L}_{q/T} = -\frac{\boldsymbol{q}}{T}. \quad (104)$$

504 Equations (104) associates, through the thermal dissipation, the entropy efflux vector $\boldsymbol{q}/T$ and the

505 thermodynamic force $-\nabla_x T$. According to the above inequality, the heat flows spontaneously from

506 high to low temperatures. A simple law that verifies automatically Inequality (104) is the Fourier law,

507 $$\boldsymbol{q} = -\boldsymbol{\kappa} \cdot \nabla_x T \quad (105)$$

508 where $\boldsymbol{\kappa}$ is identified as the thermal conductivity tensor, relative to the current configuration, which

509 must be symmetric and definitie positive.

510 In a Lagrangian approach, we have

511 $$\boldsymbol{Q} = -\boldsymbol{K} \cdot \nabla_X T, \quad (106)$$

512 where $\boldsymbol{K}$ is the convective transportee of $\boldsymbol{\kappa}$, with $\boldsymbol{K} = J\boldsymbol{F}^{-1} \cdot \boldsymbol{\kappa} \cdot {}^t\boldsymbol{F}^{-1}$.

513 # 4 Poro-elastoplastic constitutive model for saturated frozen soils

514 ## 4.1 Solid-fluid interface energy and the Lagrangian saturation

515 In the following, the infinitesimal transformations and quasistatic deformations are assumed, and

Lagrangian and Eulerian formulations are indifferent.

When the acceleration is ignored, the internal dissipation $\phi_{int} = \phi_1 + \phi_{\rightarrow}$ can be simplified as follows,

$$\phi_{int} = \boldsymbol{\sigma}:\frac{d\boldsymbol{\varepsilon}}{dt} + \sum_\alpha g_\alpha \frac{dm_\alpha}{dt} - \theta\frac{dT}{dt} - \frac{d\Psi}{dt} - (g_c - g_m)m_{c\to w}. \quad (107)$$

In Equation (107), $g_\alpha dm_\alpha = (\psi_\alpha + p_\alpha/\rho_\alpha)dm_\alpha$ accounts for the free energy supplied to the open system of volume $\mathrm{d}\Omega$ due to the fluid mass dm_α supplied to the system. $\psi_\alpha dm_\alpha$ is the free energy carried by this fluid mass supply while $p_\alpha/\rho_\alpha dm_\alpha$ is the mechanical work required to inject this additional mass into the elementary volume $\mathrm{d}\Omega$. $\boldsymbol{\varepsilon}$ is the strain tensor. However, the energy required to insert the fluid mass $\mathrm{d}m_\alpha$ into the volume $\mathrm{d}\Omega$ does not always reduce to the mechanical work $p_\alpha \mathrm{d}m_\alpha/\rho_\alpha$. For instance, non-local interaction forces can exist between the saturation solution and the solid walls of the porous space (Coussy, 2004). Let μ_α be the specific chemical potential of the saturating solution so that $\mu_\alpha dm_\alpha$ is the free energy supply associated with the introduction of mass dm_α, accounting for the non-local interaction forces at work. Instead of Equation (107), we now write:

$$\phi_{int} = \boldsymbol{\sigma}:\frac{d\boldsymbol{\varepsilon}}{dt} + \sum_\alpha \mu_\alpha \frac{dm_\alpha}{dt} - \theta\frac{dT}{dt} - \frac{d\Psi}{dt} - (\mu_c - \mu_m)m_{c\to w}. \quad (108)$$

The last term in Equation (108) accounts for the dissipation possibly occurring during phase transformation. A zero dissipation of the phase transformation implies thermodynamic equilibrium between the co-existing phases of the same components, hence the equality of their chemical potentials, $\mu_c = \mu_w$. For the ice crystals and unfrozen water, the following relationship can be obtained when considering the simplifying assumption of $\mu_\alpha = g_\alpha$,

$$d\mu_\alpha = \frac{\mathrm{d}p_\alpha}{\rho_\alpha} - \theta_\alpha dT. \quad (109)$$

Now let Ψ_s and θ_s be the skeleton free energy and entropy densities defined by

$$\Psi_s = \Psi - \sum_\alpha m_\alpha \Psi_\alpha, \quad (110)$$

538 and $$\theta_s = \theta - \sum_\alpha m_\alpha \theta_\alpha. \quad (111)$$

539 Combining Equations (109)-(111) and $m_\alpha = \rho_\alpha \phi_\alpha$, we get the Clasusius-Duhem inequality stating the

540 non-negativity of the dissipation related to the skeleton only, that is (Appendix V),

541 $$\boldsymbol{\sigma}: \frac{d\boldsymbol{\varepsilon}}{dt} + \sum_{\alpha=c,w} p_\alpha \frac{d\phi_\alpha}{dt} - \theta_s \frac{dT}{dt} - \frac{d\Psi_s}{dt} \geq 0. \quad (112)$$

542 Since only the bulk phases have been removed, the 'skeleton' does still include the moving interfaces

543 between the different constituents. Advancement of constituent interfaces, and, consequently, changes

544 in the partial porosities ϕ_α, result from two different processes. The first is the growth of ice crystals,

545 accompanied by the creation of new interfaces between ice crystals, liquid water, and the solid matrix.

546 The second process is related only to the skeleton deformation, hence change of pore volume, due to

547 pressures exerted by ice crystals and liquid water on the internal walls of the porous network. The

548 simultaneous action of these two processes is reflected in Equation (7) on the volumetric evolutions of

549 in-pore phases.

550 Consistently the currently (Lagrangian) overall porosity ϕ, which eventually concerns the skeleton

551 only, is given by

552 $$\phi = \phi_c + \phi_w = \phi_0 S_c + \varphi_c + \phi_0 S_w + \varphi_w = \phi_0 + \varphi_c + \varphi_w. \quad (113)$$

553 Being associated with the creation/modification of interfaces between constituents, the saturation

554 degrees S_α vary from 0 to 1, and, thereby, undergo finite changes. In contrast, reflecting the

555 infinitesimal deformation of the porous network, the partial porosities φ_α undergo infinitesimal

556 changes only. Confining our attention to infinitesimal changes of the liquid density ρ_w, the saturation

557 degree of unfrozen water S_w can conceptually be maintained constant, by preventing any migration of

558 liquid water inside the porous space and maintaining the temperature constant too in order to prevent

559 any liquid-crystal transformation. Insofar as $S_w = 1 - S_c$ is held constant, and henceforth controlled,

560 the subsequent changes of ϕ_c and ϕ_w reduce to the changes of φ_c and φ_w, respectively.

561 In general, the Lagrangian saturation degrees S_w and S_c do not remain constant with time. The

562 references state may be conveniently chosen as fully saturated by one of them, the unfrozen water, for

563 instance, so that we have $S_w = 1$. The associated initial pore-water pressure is generally equal to the

564 atmospheric pressure taken as the reference datum. If the ice crystals grow hence the saturation degree

565 of ice crystals p_c increases, the pressure difference $p_c - p_w$ also increases in consequence. The

remaining unfrozen water is simultaneously expulsed (due to volume expansion during phase transformation) and S_w decreases in consequence according to the last of relations (113). During this process, the porous network simultaneously deforms.

Substituting (113) into (112), we obtain,

$$\sigma_{ij} d\varepsilon_{ij} + \sum_\alpha p_\alpha d\varphi_\alpha - \phi_0 (p_c - p_w) dS_w - \theta_s dT - d\Psi_s \geq 0. \quad (114)$$

In Expression (114), the first three items represent the strain work supplied to the porous solid between time t and $t + dt$. The fourth term identifies with the work done against the interfacial forces in order to create new interfaces between ice crystals and the solid matrix which accompanies the propagation of liquid water front inside the porous volume, resulting in the change of ice volume $-\phi_0 dS_w = \phi_0 dS_c$. The free energy of soil skeleton, which includes soil matrix and interfaces, thereby changes. This change is induced not only by the deformation of the porous solid, but also by the creation/destruction of interfaces between the ice crystal, the liquid water, and the solid matrix. Owing to its extensive character, the skeleton free energy Ψ_s can be expressed as follows,

$$\Psi_s = W_s\left(\varepsilon_{ij}, \varphi_c, \varphi_w, T; \varepsilon_{ij}^p, \varphi_c^p, \varphi_w^p, \chi_J\right) + \phi U(S_w, \phi, T), \quad (115)$$

in which $\varepsilon_{ij}^p, \varphi_c^p, \varphi_w^p$ are plastic strain, plastic porosities of ice and unfrozen water, respectively. The first term stands for the free energy of the solid matrix. The second represents the contribution from the interfaces and depends on the current partition of the porous volume between unfrozen water, ice crystals and soil matrix. W_s can also be decomposed into two parts, one of which is the elastic energy and the other is the locked energy due to irreversible (mechanical) processes. This locked energy is assumed to only depend on a hardening variable χ_J for simplicity. The term $\phi U(S_w, \phi, T)$ accounts for the current values of the interfaces between ice crystals, unfrozen water and soil matrix. Here we assume that the interface energy does not significantly vary as the porous solid deforms. Accordingly, U is assumed independent of ε_{ij}. Moreover, it does not depend separately upon φ_c and φ_w, but additively through ϕ.

4.2 Thermo-poro-elasticity for saturated frozen soils

Under linear elastic behaviour, previous expression of the free energy Ψ_s is reduced to the following form:

$$\Psi_s = W_s\left(\varepsilon_{ij}, \varphi_c, \varphi_w, T\right) + \phi U(S_w, \phi, T). \quad (116)$$

Therefore, we have,

595 $$d\Psi_s = \frac{\partial W_s}{\partial \varepsilon_{ij}} d\varepsilon_{ij} + \frac{\partial W_s}{\partial \varphi_c} d\varphi_c + \frac{\partial W_s}{\partial \varphi_w} d\varphi_w + \left(\frac{\partial W_s}{\partial T} + \phi \frac{\partial U}{\partial T}\right) dT + U d\phi + \phi \left(\frac{\partial U}{\partial S_w} dS_w + \frac{\partial U}{\partial \phi} d\phi\right). \quad (117)$$

596 Substituting Equation (117) into Equation (114), we deduce that:

597 $$\left(\sigma_{ij} - \frac{\partial W_s}{\partial \varepsilon_{ij}}\right) d\varepsilon_{ij} + \left(p_c - \frac{\partial W_s}{\partial \varphi_c}\right) d\varphi_c + \left(p_w - \frac{\partial W_s}{\partial \varphi_w}\right) d\varphi_w - \left(\theta_s + \frac{\partial W_s}{\partial T} + \phi \frac{\partial U}{\partial T}\right) dT - \left(\phi_0 (p_c - p_w) +$$

598 $$\phi \frac{\partial U}{\partial S_w}\right) dS_w - \left(U + \frac{\partial U}{\partial \phi}\right) d\phi \geq 0. \quad (118)$$

599 From Equation (113), we have $d\phi = d\varphi_c + d\varphi_w$, so we have:

600 $$\left(\sigma_{ij} - \frac{\partial W_s}{\partial \varepsilon_{ij}}\right) d\varepsilon_{ij} + \left(p_c - \frac{\partial W_s}{\partial \varphi_c} - \frac{\partial U}{\partial \phi}\right) d\varphi_c + \left(p_w - \frac{\partial W_s}{\partial \varphi_w} - \frac{\partial U}{\partial \phi}\right) d\varphi_w - \left(\theta_s + \frac{\partial W_s}{\partial T} + \phi \frac{\partial U}{\partial T}\right) dT -$$

601 $$\left(\phi_0 (p_c - p_w) + \phi \frac{\partial U}{\partial S_w}\right) dS_w - U d\phi \geq 0. \quad (119)$$

602 Conceptually, the skeleton and pore space deformations as well as temperature can vary
603 independently of water saturation. Restricting our attentions momentarily to processes at constant water
604 saturation, the inequality sign becomes equality for elastic behaviour and we are led to the following
605 state equations:

606 $$\sigma_{ij} = \frac{\partial W_s}{\partial \varepsilon_{ij}}, p_c = \frac{\partial W_s}{\partial \varphi_c} + \frac{\partial U}{\partial \phi}, \; p_w = \frac{\partial W_s}{\partial \varphi_w} + \frac{\partial U}{\partial \phi}, \text{ and } \theta_s = -\frac{\partial W_s}{\partial T} - \phi \frac{\partial U}{\partial T}. \quad (120)$$

607 The entropy θ_s for the soil skeleton consists of two parts, in which $\theta_m = -\frac{\partial W_s}{\partial T}$ is the entropy of
608 solid matrix and $S_{int} = -\phi \frac{\partial U}{\partial T}$ is the interface entropy.

609 Substituting relations (120) into Equation (119), we get:

610 $$\Phi_{hys} = -\left(\phi_0 (p_c - p_w) + \phi \frac{\partial U}{\partial S_w}\right) dS_w - U d\phi \geq 0, \quad (121)$$

611 in which Φ_{hys} represents the hysteretic dissipation of freezing-thaw cycles. For simplicity, this
612 hysteretic phenomenon is neglected here and left to a further study. Under such conditions, inequality
613 (121) becomes an equality, leading after accounting for the assumption of small strains $(\phi - \phi_0)/$
614 $\phi_0 \ll 1$ to the following state equation:

615 $$p_{cap} = (p_c - p_w) = -\frac{dU}{dS_w}. \quad (122)$$

616 The thermodynamic equilibrium between ice crystals and unfrozen water requires equality of their
617 chemical potentials. Neglecting higher order terms, this condition implies:

618 $$p_{cap} = (p_c - p_w) = \Sigma_m (T_m - T), \quad (123)$$

619 where T_m and Σ_m stand respectively for the melting temperature and the melting entropy. The
620 water-ice equilibrium equation (123) and state equation (122) combine to reveal the existence of a

thermodynamic state function, linking bijectively the liquid saturation degree S_w to the current temperature T as follows,

$$S_w = \wp(T_m - T). \tag{124}$$

If the interfacial energy U is assumed to take the following form (Coussy, 2004):

$$U = \phi^{-1/3}\Gamma(S_w, T) \;\; ; \;\; \frac{\partial(\phi U)}{\partial \phi} = \frac{2}{3}U. \tag{125}$$

The ice pressure p_c and water pressure p_w then satisfy the following state equations:

$$\bar{p}_c = \frac{\partial W_s}{\partial \varphi_c}, \;\; \bar{p}_w = \frac{\partial W_s}{\partial \varphi_w}, \tag{126}$$

where $\bar{p}_\alpha = p_\alpha - \frac{2}{3}U \; (\alpha = c, w)$ represents the in-pore fluid pressures effectively transmitted to the solid skeleton. The term $-\frac{2}{3}U$ accounts for the capillary forces arising from the interfaces.

The state equations obtained previously for thermo-poro-elasticity of saturated frozen soils can be summarized as follows,

$$\sigma_{ij} = \frac{\partial W_s}{\partial \varepsilon_{ij}}, \;\; \bar{p}_c = \frac{\partial W_s}{\partial \varphi_c}, \;\; \bar{p}_w = \frac{\partial W_s}{\partial \varphi_w} \text{ and } \theta_m = -\frac{\partial W_s}{\partial T}. \tag{127}$$

Introducing the Legendre-Fenchel transform W_s^* of W_s with respect to φ_J:

$$W_s^* = W_s - \bar{p}_c\varphi_c - \bar{p}_w\varphi_w. \tag{128}$$

State equations (127) can be partially inverted in the form as follows,

$$\sigma_{ij} = \frac{\partial W_s^*}{\partial \varepsilon_{ij}}, \;\; \varphi_c = \frac{\partial W_s^*}{\partial \bar{p}_c}, \;\; \varphi_w = \frac{\partial W_s^*}{\partial \bar{p}_w}, \text{ and } \theta_m = -\frac{\partial W_s^*}{\partial T}. \tag{129}$$

We know that in linear poro-elasticity W_s^* is a quadratic form of its arguments, namely ε_{ij}, $\bar{p}_c$, $\bar{p}_w$ and $T_m - T$. For isotropic linear thermo-poro-elasticity, W_s^* has the following form,

$$W_s^* = \frac{1}{2}(K - 2G/3)(\varepsilon_{kk})^2 + G\varepsilon_{ij}\varepsilon_{ji} - 3\alpha K\varepsilon_{kk}(T - T_m) - \sum_{J,K=c,w}\left(b_J\,\bar{p}_J\varepsilon_{kk} - 3\alpha_J\,\bar{p}_J(T - T_m) + \frac{\bar{p}_J\,\bar{p}_K}{2N_{JK}}\right) - \frac{C_T}{2T_m}(T - T_m)^2. \tag{130}$$

And thus, we have

$$\sigma_{ij} = (\mathrm{K} - 2\mathrm{G}/3)(\varepsilon_{kk})\delta_{ij} + 2G(\varepsilon_{ij}) - b_c\,\bar{p}_c\delta_{ij} - b_w\,\bar{p}_w\delta_{ij} - 3\alpha K(T - T_m)\delta_{ij}, \tag{131}$$

$$\varphi_c = b_c\varepsilon_{kk} + \frac{\bar{p}_c}{N_{CC}} + \frac{\bar{p}_w}{N_{CW}} - 3\alpha_C(T - T_m), \tag{132}$$

$$\varphi_w = b_w\varepsilon_{kk} + \frac{\bar{p}_c}{N_{CW}} + \frac{\bar{p}_w}{N_{WW}} - 3\alpha_w(T - T_m), \tag{133}$$

$$\theta_m = 3\alpha K\varepsilon_{kk} - 3\alpha_C\,\bar{p}_c - 3\alpha_w\,\bar{p}_w + \frac{C_T}{T_m}(T - T_m), \tag{134}$$

in which ε_{kk} is the volumetric dilation; K, G and α are the bulk modulus, the shear modulus and the

thermal volumetric dilation coefficient of the solid skeleton, respectively, which are the ones related to the empty porous materials subject to conditions $\bar{p}_c = \bar{p}_w = 0$. b_J and N_{JK} are the generalized Biot coefficients and the generalized Biot coupling moduli (Biot, 1941), with $N_{JK} = N_{KJ}$ owing to the Maxwell's symmetry relations. α_J and C_T are the thermal dilation of the pore volume occupied by phase *J* and the heat capacity of the soil matrix.

4.3 Thermo-poro-elasto-plasticity for saturated frozen soils

When plastic deformations occur, mechanical dissipation will be generated. The skeleton free energy Ψ_s can be decomposed additively into the recoverable elastic free energy of soil skeleton, the locked (or frozen) energy and the free energy of interfaces:

$$\Psi_s = W_s\left(\varepsilon_{ij}, \varphi_c, \varphi_w, T; \varepsilon_{ij}^p, \varphi_c^p, \varphi_w^p, \chi_J\right) + \phi U(S_w, \phi, T). \tag{135}$$

Therefore, we have,

$$d\Psi_s = \frac{\partial W_s}{\partial \varepsilon_{ij}} d\varepsilon_{ij} + \frac{\partial W_s}{\partial \varphi_c} d\varphi_c + \frac{\partial W_s}{\partial \varphi_w} d\varphi_w + \frac{\partial W_s}{\partial T} dT + \frac{\partial W_s}{\partial \varepsilon_{ij}^p} d\varepsilon_{ij}^p + \frac{\partial W_s}{\partial \varphi_c^p} d\varphi_c^p + \frac{\partial W_s}{\partial \varphi_w^p} d\varphi_w^p + \frac{\partial W_s}{\partial \chi_J} d\chi_J + U d\phi + \phi\left(\frac{\partial U}{\partial S_w} dS_w + \frac{\partial U}{\partial \phi} d\phi + \frac{\partial U}{\partial T} dT\right). \tag{136}$$

Substituting Equation (136) into Inequality (114) and accounting for the identity $d\phi = d\varphi_c + d\varphi_w$, we have:

$$\left(\sigma_{ij} - \frac{\partial W_s}{\partial \varepsilon_{ij}}\right) d\varepsilon_{ij} + \left(p_c - \frac{\partial W_s}{\partial \varphi_c} - \frac{\partial U}{\partial \phi}\right) d\varphi_c + \left(p_w - \frac{\partial W_s}{\partial \varphi_w} - \frac{\partial U}{\partial \phi}\right) d\varphi_c - \left(S_s + \frac{\partial W_s}{\partial T} + \phi \frac{\partial U}{\partial T}\right) dT - \left[\phi_0(p_c - p_w) + \phi \frac{\partial U}{\partial S_w}\right] dS_w - U d\phi - \frac{\partial W_s}{\partial \varepsilon_{ij}^p} d\varepsilon_{ij}^p - \frac{\partial W_s}{\partial \varphi_c^p} d\varphi_c^p - \frac{\partial W_s}{\partial \varphi_w^p} d\varphi_w^p - \frac{\partial W_s}{\partial \chi_J} d\chi_J \geq 0 \tag{137}$$

.

In view of the state equations (120) and (121), we deduce the following form of the plastic dissipation:

$$-\frac{\partial W_s}{\partial \varepsilon_{ij}^p} d\varepsilon_{ij}^p - \frac{\partial W_s}{\partial \varphi_c^p} d\varphi_c^p - \frac{\partial W_s}{\partial \varphi_w^p} d\varphi_w^p - \frac{\partial W_s}{\partial \chi_J} d\chi_J \geq 0. \tag{138}$$

In the following, we will discuss ideal plasticity and hardening plasticity for saturated frozen soils, respectively.

4.3.1 Ideal plasticity

For ideal plasticity, it can be defined by the absence of hardening variable χ_J. Hence, no variables are χ_J involved in the expression of W_s^*. From equation (130) a suitable expression for W_s^* under ideal plasticity can be expressed as follows,

$$W_s^* = \frac{1}{2}\left(K - \frac{2G}{3}\right)\left(\varepsilon_{kk} - \varepsilon_{kk}^p\right)^2 + G\left(\varepsilon_{ij} - \varepsilon_{ij}^p\right)\left(\varepsilon_{ji} - \varepsilon_{ji}^p\right) - 3\alpha K\left(\varepsilon_{kk} - \varepsilon_{kk}^p\right)(T - T_m)$$

$$-\sum_{J,K=c,w}\left(b_J\,\bar{p}_J\left(\varepsilon_{kk}-\varepsilon_{kk}^p\right)-3\alpha_J\,\bar{p}_J(T-T_m)+\frac{\bar{p}_J\,\bar{p}_K}{2N_{JK}}\right)-\frac{C_T}{2T_m}(T-T_m)^2. \quad (139)$$

So, we have

$$\sigma_{ij}=\left(\mathrm{K}-\frac{2\mathrm{G}}{3}\right)\left(\varepsilon_{kk}-\varepsilon_{kk}^p\right)\delta_{ij}+2G\left(\varepsilon_{ij}-\varepsilon_{ij}^p\right)-b_c\,\bar{p}_c\delta_{ij}-b_w\,\bar{p}_w\delta_{ij}-3aK(T-T_m)\delta_{ij}, \quad (140)$$

$$\varphi_c=b_c\left(\varepsilon_{kk}-\varepsilon_{kk}^p\right)+\frac{\bar{p}_c}{N_{CC}}+\frac{\bar{p}_w}{N_{CW}}-3\alpha_C(T-T_m)+\varphi_c^p\ , \quad (141)$$

$$\varphi_w=b_w\left(\varepsilon_{kk}-\varepsilon_{kk}^p\right)+\frac{\bar{p}_c}{N_{CW}}+\frac{\bar{p}_w}{N_{WW}}-3\alpha_w(T-T_m)+\varphi_w^p, \quad (142)$$

$$\theta_m=3\alpha K\left(\varepsilon_{kk}-\varepsilon_{kk}^p\right)-3\alpha_C\,\bar{p}_c-3\alpha_w\,\bar{p}_w+\frac{C_T}{T_m}(T-T_m)\ . \quad (143)$$

Therefore, the plastic dissipation of (138) can be rewritten as follows,

$$\sigma_{ij}d\varepsilon_{ij}^p+\bar{p}_c d\varphi_c^p+\bar{p}_w d\varphi_w^p\geq 0, \quad (144)$$

and the following relationships have been used, $\bar{p}_c=-\frac{\partial W_s}{\partial\varphi_c^p}=\frac{\partial W_s}{\partial\varphi_c}$, $\bar{p}_w=-\frac{\partial W_s}{\partial\varphi_w^p}=\frac{\partial W_s}{\partial\varphi_w}$, $\sigma_{ij}=-\frac{\partial W_s}{\partial\varepsilon_{ij}^p}=\frac{\partial W_s}{\partial\varepsilon_{ij}}$.

Equation (144) shows that the thermodynamical forces associated with the plastic strain, plastic porosities of ice crystal and unfrozen water are, respectively,σ_{ij}, $\bar{p}_c$ and $\bar{p}_w$. Now standard principles of ideal plasticity can be applied, namely the maximal plastic work principle introduced by Hill (1950). More precisely, let us note by

$$f\left(\sigma_{ij},\,\bar{p}_c,\,\bar{p}_w\right)\leq 0, \quad (145)$$

the equation delimiting in the stress-pressure space the elastic domain which is assumed to be independent of the temperature. Let $\left(\sigma_{ij},\,\bar{p}_c,\,\bar{p}_w\right)$ be the current stress-pressure state satisfying (145) and $\left(\sigma^*{}_{ij},\overline{p}_c^*,\overline{p}_w^*\right)$ another couple satisfying (145). Then the maximal plastic work principle implies

$$\left(\sigma_{ij}-\sigma^*{}_{ij}\right)d\varepsilon_{ij}^p+\left(\bar{p}_c-\overline{p}_c^*\right)d\varphi_c^p+\left(\bar{p}_w-\overline{p}_w^*\right)d\varphi_w^p\geq 0. \quad (146)$$

From (146), assuming for simplicity the smoothness of the yield locus $f\left(\sigma_{ij},\,\bar{p}_c,\,\bar{p}_w\right)=0$ (no vertex effects), it can be standardly shown (Hill, 1950) that $f\left(\sigma_{ij},\,\bar{p}_c,\,\bar{p}_w\right)$ must be a convex function and that

$$\begin{aligned}&\text{if } f\left(\sigma_{ij},\,\bar{p}_c,\,\bar{p}_w\right)=0 \text{ and } df=\left(\partial f/\partial\sigma_{ij}\right)d\sigma_{ij}+(\partial f/\partial\,\bar{p}_c)d\,\bar{p}_c+(\partial f/\partial\,\bar{p}_w)\,\bar{p}_w=0,\\&\text{then: } d\varepsilon_{ij}^p=d\lambda\left(\partial f/\partial\sigma_{ij}\right),\ d\varphi_c^p=d\lambda(\partial f/\partial\,\bar{p}_c) \text{ and } d\varphi_w^p=d\lambda(\partial f/\partial\,\bar{p}_w),\ d\lambda\geq 0,\end{aligned} \quad (147)$$

while in the other cases, $f<0$ or $f=0$ and $df<0$(respectively, elastic state or local unloading state) $d\varepsilon_{ij}^p=0$, $d\varphi_c^p=0$ and $d\varphi_w^p=0$. Equation (147) implies that f can be considered as an associated plastic potential, the flow rule given by (147) being associated with the plastic yield locus f.

4.3.2 Hardening plasticity

For hardening plasticity at isothermal conditions, the hardening variables χ_J are now present in the expression of W_s^*. Therefore, the plastic dissipation of (138) can be rewritten as follows,

$$\sigma_{ij} d\varepsilon_{ij}^p + \bar{p}_c d\varphi_c^p + \bar{p}_w d\varphi_w^p - \frac{\partial W_s}{\partial \chi_J} d\chi_J \geq 0. \tag{148}$$

To introduce hardening plasticity, we will follow the presentation of Halphen and Nguyen (1974) which generalizes the maximal plastic work principle. We assume that W_s is a strictly (smooth hardening) convex (positive hardening) function and we note

$$\xi_J = -\frac{\partial W_s}{\partial \chi_J}, \ \left(\sigma_{ij} d\varepsilon_{ij}^p + \bar{p}_c d\varphi_c^p + \bar{p}_w d\varphi_w^p + \xi_J d\chi_J \geq 0\right). \tag{149}$$

Furthermore, let us introduce a strictly (smooth plasticity) convex function $f(\sigma_{ij}, \bar{p}_c, \bar{p}_w, \xi_J)$, the current elastic domain being given by $f(\sigma_{ij}, \bar{p}_c, \bar{p}_w, \xi_J) \leq 0$. The generalization of the results stated for ideal plasticity yields:

$$d\varepsilon_{ij}^p = d\lambda\left(\partial f/\partial \sigma_{ij}\right), \ d\varphi_c^p = d\lambda(\partial f/\partial \bar{p}_c), \ d\varphi_w^p = d\lambda(\partial f/\partial \bar{p}_w), \ d\chi_J = d\lambda\left(\partial f/\partial \xi_J\right), \tag{150}$$

$d\lambda \geq 0$ if $f = 0$ and $df = 0$, and $d\lambda = 0$ if $f < 0$ or $df < 0$.

Now, following Halphen and Nguyen (1974) one can retrieve the standard theory of hardening plasticity. From (135) and (144), one obtains that:

if $f = 0 \ and \ df_\zeta > 0$, $d\varepsilon_{ij}^p = (1/\mathcal{H})\left(\partial f/\partial \sigma_{ij}\right) df_\zeta$,

$$d\varphi_c^p = (1/\mathcal{H})(\partial f/\partial \bar{p}_c) df_\zeta,$$

$$d\varphi_w^p = (1/\mathcal{H})(\partial f/\partial \bar{p}_w) df_\zeta, \tag{151}$$

$$\text{and } d\chi_J = (1/\mathcal{H})\left(\partial f/\partial \xi_J\right) df_\zeta;$$

if $f < 0 \ or \ f = 0 \ and \ df_\zeta \leq 0$, $d\varepsilon_{ij}^p = d\varphi_c^p = d\varphi_w^p = d\chi_J = 0$, (152)

where $\mathcal{H} = -\frac{\partial f}{\partial \xi_J}\frac{\partial \xi_J}{\partial \chi_J}\frac{d\chi_J}{d\lambda} = \frac{\partial f}{\partial \xi_J} \cdot \left(\frac{\partial^2 W_s}{\partial \chi^2{}_J}\right) \cdot \frac{\partial f}{\partial \xi_J}$ and $df_\zeta = \left(\partial f/\partial \sigma_{ij}\right) d\sigma_{ij} + (\partial f/\partial \bar{p}_c) d\bar{p}_c + (\partial f/\partial \bar{p}_w) d\bar{p}_w$. $\mathcal{H}$ is the hardening modulus of the phenomenological theory of hardening plasticity.

For saturated frozen soils, they may exhibit the property that their experimental results do not confirm the validity of the maximal work principle. In this case normality does not hold, with that the plastic strain rate is not normal to the yield locus and f cannot be considered as a plastic potential. Nevertheless, we can standardly introduce a non-associated plastic potential $h(\sigma_{ij}, \bar{p}_c, \bar{p}_w, \xi_J)$, such that the flow rule under this condition is as follows,

if $f(\sigma_{ij}, \bar{p}_c, \bar{p}_w, \xi_J) = 0$ and $df_\zeta \geq 0$,

then $d\varepsilon_{ij}^p = (1/\mathbb{H})\left(\partial h/\partial \sigma_{ij}\right) df_\zeta$,

$$d\varphi_c^p = (1/\mathbb{H})(\partial h/\partial\, \bar{p}_c) df_\zeta, \quad (153)$$

$$d\varphi_w^p = (1/\mathbb{H})(\partial h/\partial\, \bar{p}_w) df_\zeta,$$

$$\text{and } d\chi_J = (1/\mathbb{H})\left(\partial h/\partial \xi_J\right) df_\zeta;$$

$$\text{if } f < 0 \text{ or } f = 0 \text{ and } df_\zeta < 0,\ d\varepsilon_{ij}^p = d\varphi_c^p = d\varphi_w^p = d\chi_J = 0, \quad (154)$$

where $\mathbb{H}$ is the hardening modulus, and $\mathbb{H} = -\frac{\partial f}{\partial \xi_J}\frac{\partial \xi_J}{\partial \chi_J}\frac{d\chi_J}{d\lambda} = \left(\partial f/\partial \xi_J\right)\cdot\frac{\partial^2 W_s}{\partial {\chi^2}_J}\cdot\frac{\partial h}{\partial \xi_J}$. When the principle of maximum plastic work does not apply, the plastic strains do not achieve a maximum production of entropy. Accordingly, the positivity of the plastic work is not guaranteed and has to be checked.

4.4 Modelling the cryogenic triaxial compression tests of frozen soils

4.4.1 Effective stress in cryogenic triaxial stress state

For saturated frozen soils under cryogenic triaxial compression conditions, the stress and strain can be described by $\sigma_m = \frac{1}{3}(\sigma_a + 2\sigma_c)$, $\sigma_s = \left(\frac{3}{2}s_{ij}s_{ij}\right)^{1/2} = \sigma_a - \sigma_c$, $\varepsilon_s = \left(\frac{2}{3}e_{ij}e_{ij}\right)^{1/2} = \frac{2}{3}(\varepsilon_a - \varepsilon_c)$, and $\varepsilon_v = \frac{1}{3}(\varepsilon_a + 2\varepsilon_c)$, in which σ_a, σ_c, σ_m and σ_s are the axial stress, confining pressure, mean stress and generalized shear stress, respectively; e_{ij}, $s_{ij}$are the strain deviator tensor and stress deviator tensor , respectively; ε_a, ε_c, ε_s are the axial strain, radial strain, and shear strain, respectively.

When performing the laboratory test on saturated frozen soils using cryogenic triaxial apparatus, we can only measure the strain (ε_a, ε_v), axial stress σ_a and confining pressure σ_c. Under these conditions, the strains measured for the samples are the same as those of soil skeleton, but the stresses (σ_a, σ_c) measured are the total stresses applied on the surface of samples. Therefore, considering the theory presented in the paper, the yield criterion should be expressed as stress undergone by soil skeleton, which can be expressed in terms of stress, water pressure, ice pressure. The soil skeleton deforms subjected to the combining actions of external load, pore pressures of water pressure and ice pressure. When formulating the elasto-plastic constitutive model, we have to make some assumptions here. It is assumed that solid soil grains are plastic incompressible, meaning that plasticity are solely due to irreversible sliding between un-deformable solid soil grains, and implies that $d\varepsilon_v^p = -d\varphi_c^p - d\varphi_w^p$. By introducing a coefficient χ ranging from 0 to 1, we can also assume that

$$d\varphi_c^p = -(1-\chi)d\varepsilon_v^p;\ d\varphi_w^p = -\chi d\varepsilon_v^p. \quad (155)$$

This factor χ is not easy to be determined, varying with $S_\alpha(\alpha = c, w)$, which needs further study.

The dissipation (148) can be expressed in triaxial conditions as follows (Appendix VI),

$$\mathrm{D} = -(\sigma_m - \bar{p}_c)d\varphi_c^p - (\sigma_m - \bar{p}_w)d\varphi_w^p + \sigma_s d\varepsilon_s^p + \xi_J d\chi_J \geq 0. \quad (156)$$

Substituting (155) into (156), we have

$$\mathrm{D} = [\sigma_m - (1-\chi)\,\bar{p}_c - \chi\,\bar{p}_w]d\varepsilon_v^p + \sigma_s d\varepsilon_s^p + \xi_J d\chi_J \geq 0. \quad (157)$$

Let $\sigma_m^E = \sigma_m - (1-\chi)\,\bar{p}_c - \chi\,\bar{p}_w$, which is the effective stress combining the influence of total stress, water pressure and ice crystal pressure, we can have

$$\mathrm{D} = \sigma_m^E d\varepsilon_v^p + \sigma_s d\varepsilon_s^p + \xi_J d\chi_J \geq 0. \quad (158)$$

Let p_{por} express the combining pore pressure of water pressure and ice pressure, we have

$$\mathrm{p}_{por} = (1-\chi)\,\bar{p}_c + \chi\,\bar{p}_w, \quad (159\text{-}1)$$

and

$$\sigma_m^E = \sigma_m - \mathrm{p}_{por}. \quad (159\text{-}2)$$

When χ is selected as saturation of ice crystals S_w, p_{por} is the similar expression used by other researchers (Nishimura et al., 2009; Zhou and Meschke, 2013; Shen et al. 2014), but the influence of interface energy is considered in the paper. Under the assumption of incompressibility of solid soil grain forming soil skeleton, σ_m^E is the effective stress controlling the deformation and strength of soil skeleton of saturated frozen soils, which plays the similar role as Terzaghi's effective stress for saturated soils or Bishop's effective stress for unsaturated soils under unfreezing states.

Therefore, under triaxial stress conditions for saturated frozen soils, the current elastic domain can be given by

$$f\left(\sigma_m^E, \sigma_s, \xi_J\right) \leq 0, \quad (160)$$

in which f is the loading function. Combining (151) and (152) for associated plastic criterion or (153) and (154) for non-associated plastic criterion, the stress-strain relationship for saturated frozen soils can be formulated when $f\left(\sigma_m^E, \sigma_s, \xi_J\right)$ or $h\left(\sigma_m^E, \sigma_s, \xi_J\right)$ are determined.

4.4.2 Formulation of constitutive equations

The frozen soils usually behave strain softening at lower confining pressure and gradually transfer to strain hardening with increasing confining pressure, and the volumetric strain contract first, followed by dilatancy at lower confining pressure, but contract all the time at higher confining pressure. For example, the stress-strain curves for frozen sand with 1.0 MPa confining pressure at -1℃ to -10℃ was published by Xu et al. (2016) and those for saturated frozen saline sandy soils at -6℃ by Lai et al. (2016). Therefore, when formulating the special constitutive model for frozen soils, these mechanical features should be taken into account.

In order to formulate a constitutive model reflecting the main mechanical features of frozen soils

with strain softening accompanied by volumetric contraction followed by dilatancy at lower confining pressure, and strain hardening accompanied by volumetric contraction at higher confining pressure, the yield function *f* used is as follows,

$$f\left(\sigma_m^E, \sigma_s, \xi_\alpha, \xi_\beta\right) = \frac{\sigma_m^E}{1-(\eta/\xi_\alpha)^z} - \xi_\beta = 0, \tag{161}$$

where $\eta = \sigma_s/\sigma_m^E$, $\xi_\alpha\left(\varepsilon_s^p\right)$, $\xi_\beta\left(\varepsilon_v^p\right)$ are hardening parameters, and *z* is a material parameter.

These hardening parameters, $\xi_\alpha\left(\varepsilon_s^p\right)$ and $\xi_\beta\left(\varepsilon_v^p\right)$, are expressed as follows,

$$\xi_\alpha\left(\varepsilon_s^p\right) = \alpha_m\left(1.0 - \kappa exp\left(-\frac{\varepsilon_s^p}{\gamma_1}\right)\right), \tag{162}$$

$$\xi_\beta\left(\varepsilon_v^p\right) = \sigma_{mr}^E \exp\left(\beta\varepsilon_v^p\right), \tag{163}$$

in which $\alpha_m, \kappa, \gamma_1, \beta$ are material parameters, and σ_{mr}^E is a reference pressure.

The plastic potential function *h* has the same form as yield function, expressed as follows

$$h = \frac{\sigma_m^E}{1-(\eta/\xi_{\alpha 1})^{z_1}} - \xi_{\beta 1} = 0, \tag{164}$$

with

$$\xi_{\alpha 1}\left(\varepsilon_s^p\right) = \alpha_{m1}\left(1.0 - \kappa_1 exp\left(-\frac{\varepsilon_s^p}{\gamma_2}\right)\right), \tag{165}$$

$$\xi_{\beta 1}\left(\varepsilon_v^p\right) = \sigma_{mr}^E \exp\left(\beta_1\varepsilon_v^p\right), \tag{166}$$

in which z_1, $\alpha_{m1}, \kappa_1, \gamma_2, \beta_1$ are material parameters.

The incremental ε_v^p and ε_s^p can be obtained as follows,

$$d\varepsilon_v^p = d\lambda\frac{\partial h}{\partial \sigma_m^E}, \tag{167-1}$$

$$d\varepsilon_s^p = d\lambda\frac{\partial h}{\partial \sigma_s}. \tag{167-2}$$

From consistency conditions, $d\lambda$ can be expressed as follows,

$$d\lambda = \frac{1}{H}\left(\frac{\partial f}{\partial \sigma_m^E}d\sigma_m^E + \frac{\partial f}{\partial \sigma_s}d\sigma_s\right), \tag{166}$$

in which

$$H = -\frac{\partial f}{\partial \xi_\alpha}\frac{\partial \xi_\alpha}{\partial \chi_\alpha}\frac{d\chi_\alpha}{d\lambda} - \frac{\partial f}{\partial \xi_\beta}\frac{\partial \xi_\beta}{\partial \chi_\beta}\frac{d\chi_\beta}{d\lambda}. \tag{167}$$

Substituting $d\chi_\alpha = d\varepsilon_s^p = d\lambda\frac{\partial h}{\partial \sigma_s}$ and $d\chi_\beta = d\varepsilon_v^p = d\lambda\frac{\partial h}{\partial \sigma_m^E}$ into (167), we have

$$H = -\frac{\partial f}{\partial \xi_\alpha}\frac{\partial \xi_\alpha}{\partial \chi_\alpha}\frac{\partial h}{\partial \sigma_s} - \frac{\partial f}{\partial \xi_\beta}\frac{\partial \xi_\beta}{\partial \chi_\beta}\frac{\partial h}{\partial \sigma_m^E}. \tag{168}$$

Therefore, the incremental form of volumetric strain and shear strain can be expressed as follows (Appendix VI),

$$d\varepsilon_v = d\varepsilon_v^e + d\varepsilon_v^p = \mathrm{A}_1 d\sigma_m^E + \mathrm{B}_1 d\sigma_s, \tag{169-1}$$

$$d\varepsilon_s = d\varepsilon_s^e + d\varepsilon_s^p = \mathrm{A}_2 d\sigma_m^E + \mathrm{B}_2 d\sigma_s, \quad (169\text{-}2)$$

where $\mathrm{A}_1 = \frac{1}{K} + \frac{1}{H}\frac{\partial f}{\partial \sigma_m^E}\frac{\partial h}{\partial \sigma_m^E}$, $\mathrm{B}_1 = \frac{1}{H}\frac{\partial f}{\partial \sigma_s}\frac{\partial h}{\partial \sigma_m^E}$, $\mathrm{A}_2 = \frac{1}{H}\frac{\partial f}{\partial \sigma_m^E}\frac{\partial h}{\partial \sigma_s}$, $\mathrm{B}_2 = \frac{1}{3G} + \frac{1}{H}\frac{\partial f}{\partial \sigma_s}\frac{\partial h}{\partial \sigma_s}$. The non-associated plastic potential function used here can assure the dissipation (158) $\mathrm{D} \geq 0$.

The approaches for determining the model parameters are described as follows. K and G are elastic parameters, which can be determined by unloading tests or use of initial loading stage within a small axial strain range, and these elastic parameters can be expressed as function of stress level and temperature. $S_c, S_w, \Sigma_m, U, T_m, k_s, b_\alpha, \phi_0$ can be determined for particular frozen soils under cryogenic triaxial tests. The other parameters in the model are related to yield function, plastic potential, and hardening parameters, in which z and z_1 denote the shape of yield surface and plastic potential surface, $\alpha_m \, or \, \alpha_{m1}$, κ, κ_1, $\gamma_1 \, or \, \gamma_2$ denote the evolution of hardening parameters of ξ_α and $\xi_{\alpha 1}$, and σ_{mr}^E, $\beta or \beta_1$ denote the evolution of hardening parameters of ξ_β and $\xi_{\beta 1}$, and these parameters of parameters do not have clear physical meanings can be determined by trial and error approach. The sensitivity analyses of these parameters are done in Section 4.4.4, from which we know the influences of their variations on stress-strain relationships of frozen soils.

4.4.3 Validation of the proposed constitutive model

Considering the thermodynamic equilibrium between ice crystals and unfrozen water, we can express equation (123) as follows,

$$p_c - p_w = \overline{p_c} - \overline{p_w} = \Sigma_m (T_m - T). \quad (170)$$

It is obvious that at constant T, the differences between p_c, p_w (or $\overline{p_c}, \overline{p_w}$) are constant for special freezing materials with determined values of melting entropy Σ_m and melting temperature T_m.

For the frozen soils tested under cryogenic triaxial compression conditions (Xu et al., 2016; Lai et al., 2016), the water is prevented from escaping from the frozen soil sample upon loading, and the total mass of water and ice crystals $\rho_c\phi_c + \rho_w\phi_w$ remains constantly equal to the initial mass of water and ice crystals at the start of loading. Therefore, we have

$$\mathrm{d}(\rho_c\phi_c + \rho_w\phi_w) = \mathrm{d}(\rho_c\varphi_c + \rho_w\varphi_w) = 0. \quad (171)$$

Combining Equations (132), (133) and (171) with neglecting the variation of densities of ice crystal and unfrozen water within the small range of pressure at isothermal conditions, we can have the relation between $\mathrm{d}\overline{p_w}$ (or $\mathrm{d}\overline{p_c}$) with $d\varepsilon_v$ (or $d\sigma_m^E$) as follows,

$$(b_c + b_w)d\varepsilon_v + \left(\frac{1}{N_{CC}} + \frac{1}{N_{CW}}\right)d\bar{p}_c + \left(\frac{1}{N_{CW}} + \frac{1}{N_{WW}}\right)d\bar{p}_w = 0. \quad (172)$$

From the tested results, we can have the values of ε_v and ε_s for different confining pressures, and thus combining (170) and (172) we can obtain $\bar{p}_c$ and $\bar{p}_w$. Therefore, in the process of loading we can have p_{por} and σ_m^E by use of (159-1) and (159-2).

Fig. 2 (a) and (b) present the comparison of tested and simulated results of frozen sand soil at -1℃, -5℃ and -10℃ with 1MPa confining pressure. Under triaxial compression conditions, the generalized shear stress equals the deviatoric stress. The triaxial compression tests were performed on frozen sand under 1MPa confining pressure at temperatures of -1℃, -5℃ and -10℃ (Xu et al., 2016). The parameters used are as follows (Lee et al., 2002; Coussy, 2004, 2008; Xu et al., 2016): $K = K_0 p_a \left(\frac{\sigma_m^E}{p_a}\right)^{m_1}$, $G = G_0 p_a \left(\frac{\sigma_m^E}{p_a}\right)^{m_2}$, $K_0 = 1666.13|T|^{0.5721}$ MPa, $G_0 = 1741.48e^{0.1094|T|}$ MPa, $m_1 = 0.0404|T|^{0.6584}$, $m_2 = 0.06$, and p_a is standard atmospheric pressure; $S_c = 0.95$, $S_w = 0.05$, $\Sigma_m = 1.2$MPa.K^{-1}, $U = 5.21$MPa, $T_m = 273$K, $k_s = 42400MPa$, $b_0 = 1 - K/k_s$, $b_\alpha = b_0 S_\alpha (\alpha = c, w)$, $\frac{1}{N_{CC}} + \frac{1}{N_{CW}} = \frac{b_c - \phi_0 S_c}{k_s}$, $\frac{1}{N_{WW}} + \frac{1}{N_{WC}} = \frac{b_w - \phi_0 S_w}{k_s}$, $\phi_0 = 0.465$; $\alpha_m = \alpha_{m1} = 3.56$, $\kappa = -0.066ln|T| + 0.4281$, $\gamma_1 = 0.0389T + 0.541$, $\sigma_{mr}^E = 66.649e^{0.0398|T|}$, $\beta = \beta_1 = 445.3ln|T| + 69.259$, $z = z_1 = -0.591ln|T| + 2.754$, $\kappa_1 = 0.5348|T|^{-0.176}$, $\gamma_2 = -0.0198T + 0.3779$. From Fig. 2, we can see that the proposed constitutive model can simulate the stress-strain properties of frozen sand at different temperatures, and with decreasing temperature the soil samples behave strain hardening transforming to strain softening slightly; the lower the temperature, the smaller the volumetric compaction and the higher the temperature, the smaller the volumetric dilatancy at failure. Fig. 2 (c) presents the predicted curves of volumetric strain and pore pressure in the process of shear loading, indicating that the pore pressure increases gradually in the whole loading process.

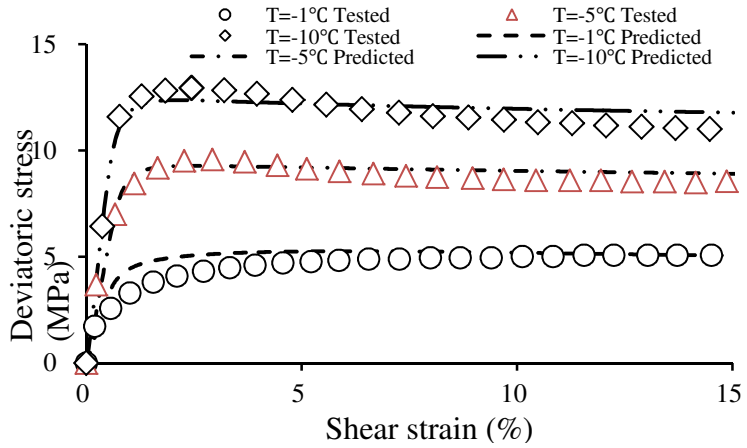

(a) Deviatoric stress-shear strain curves

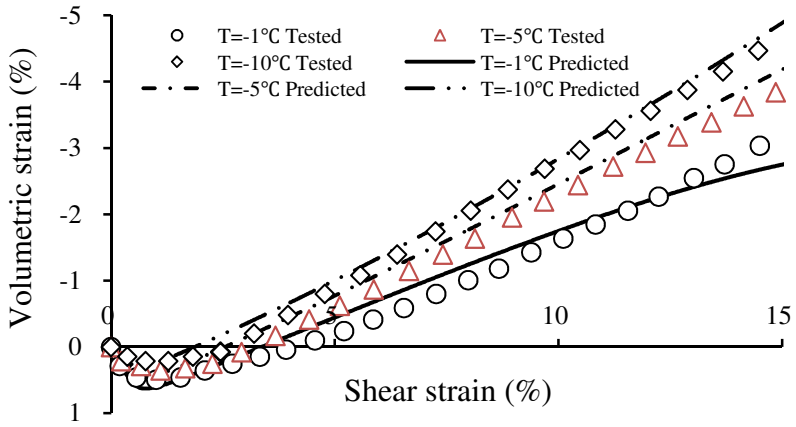

(b) Volumetric strain-shear strain curves

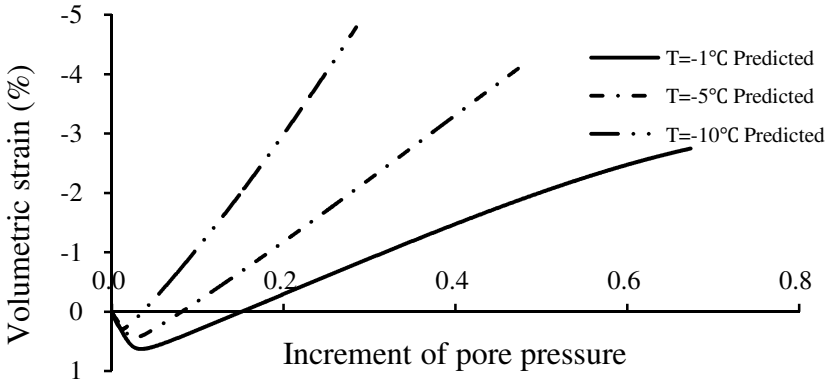

(c) Predicted volumetric strain- pore pressure curves

Fig. 2 Comparisons of tested and simulated results of frozen sand soil at -1℃, -5℃ and -10℃ with 1MPa confining pressure

Fig. 3 (a) and (b) show another comparison of tested and simulated results of saline frozen sand soil at -6℃ with 1.0MPa to 10.0 MPa confining pressures (Lai et al., 2016). The parameters used are as

follows (Lee et al., 2002; Coussy, 2004, 2008; Lai et al., 2016): $K = K_0 p_a \left(\frac{\sigma_m^E}{p_a}\right)^{m_1}$, $G = G_0 p_a \left(\frac{\sigma_m^E}{p_a}\right)^{m_2}$, $K_0 = 200$ MPa, $G_0 = 2733.2\mathfrak{Y}^{-1.387}$ MPa, $m_1 = 0.4051\ln\mathfrak{Y} - 0.1304$, $m_2 = -\frac{0.2991}{\mathfrak{Y}} + 0.3127$; $S_c = 0.951$, $S_w = 0.049$, $\Sigma_m = 1.2$ MPa.K^{-1}, $U = 5.21$ MPa, $T_m = 273$K, $k_s = 42400MPa$, $b_0 = 1 - K/k_s$, $b_\alpha = b_0 S_\alpha (\alpha = c, w)$, $\frac{1}{N_{CC}} + \frac{1}{N_{CW}} = \frac{b_c - \phi_0 S_c}{k_s}$, $\frac{1}{N_{WW}} + \frac{1}{N_{WC}} = \frac{b_w - \phi_0 S_w}{k_s}$, $\phi_0 = 0.4652$; $\alpha_m = \alpha_{m1} = 1.9925ln\mathfrak{Y} + 1.389$, $\kappa = 0.4081\left(\frac{1}{\mathfrak{Y}}\right)^{0.7037}$, $\gamma_1 = 0.1007\mathfrak{Y} - 0.1418$, $\sigma_{mr}^E = 5.5997e^{1.2587\mathfrak{Y}}$, $\beta = \beta_1 = 832.1ln\mathfrak{Y} - 117.32$, $z = z_1 = 2.5$, $\kappa_1 = 1.5199ln\mathfrak{Y} + 1.5757$, $\gamma_2 = \frac{1}{-5.8072\mathfrak{Y} + 15.909}$, and $\mathfrak{Y} = \sigma_s/\sigma_m$ is the stress ratio at peak stress state for samples with strain softening or failure state for samples with strain hardening. From the compared results, it is obvious that the stress-strain features of frozen saline sands can be duplicated by the constitutive model proposed here at different confining pressures with -6℃. The samples behave slight strain softening and volumetric compaction first followed by dilatancy with increasing axial strain at lower confining pressures, and strain hardening and volumetric compaction all the time at higher confining pressures, which can be simulated relatively well by the proposed constitutive model. Fig. 3 (c) presents the predicted curves of volumetric strain and pore pressure in the process of shear loading, which indicates that the higher the confining pressure, the bigger the pore pressure generated at failure for the frozen samples.

4.4.4 Analysis of parameter sensitivity and discussions

Figs. 4-11 present the simulated results with varying values of model parameters, including $\alpha_m(=\alpha_{m1})$, κ, γ_1, σ_{mr}^E, $\beta(=\beta_1)$, $z(=z_1)$, κ_1 and γ_2, with 2 MPa confining pressure at -6℃. From these simulated results, we can find that the main mechanical features of frozen soils can be duplicated. For example, with increasing $\alpha_m(=\alpha_{m1})$, κ, σ_{mr}^E, $z(=z_1)$, κ_1, and γ_2, the samples behave strain softening slightly to strain hardening; while with increasing γ_1 and $\beta(=\beta_1)$, the samples behave strain hardening slightly to strain softening. For the volumetric strain, with increasing $\alpha_m(=\alpha_{m1})$, σ_{mr}^E, $\beta(=\beta_1)$, $z(=z_1)$, κ_1, and γ_2, the samples compact more heavily; with increasing γ_1, the samples dilate more greatly, and the bigger κ, the smaller the samples contract and dilate. All the stress paths of σ_m^E-σ_s with varying these parameters, the samples exhibit the similar pattern with increasing pore pressure during the process of shear loading.

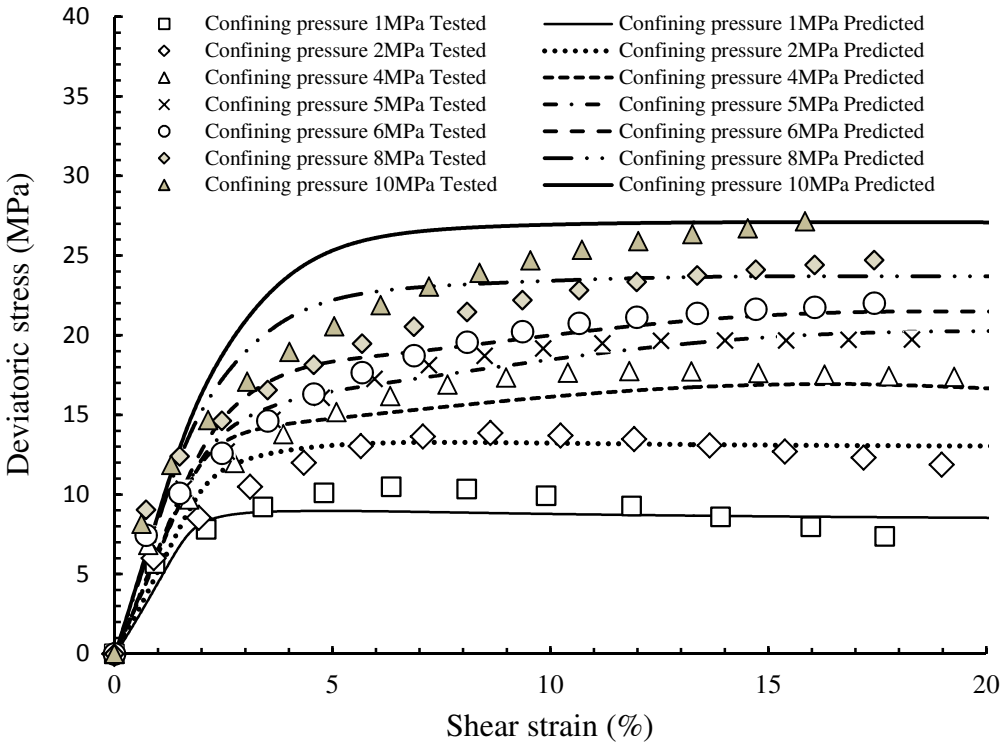

(a) Deviatoric stress-shear strain curves

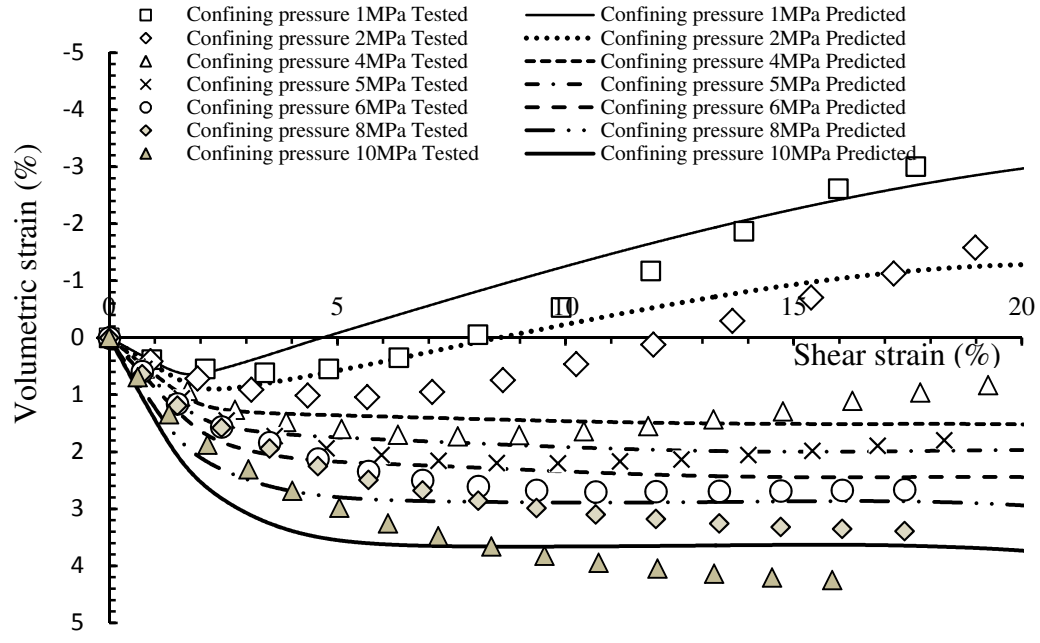

(b) Volumetric strain-shear strain curves

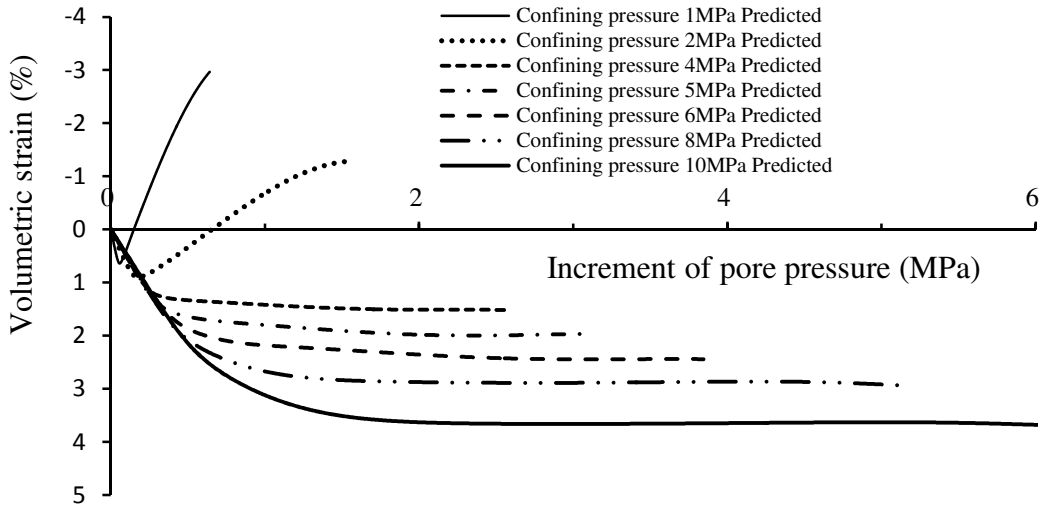

909

910 (c) Predicted volumetric strain- pore pressure curves

911 Fig. 3 Comparisons of tested and simulated results of frozen saline sand soil at -6℃with 1MPa-10MPa

912 confining pressures

913

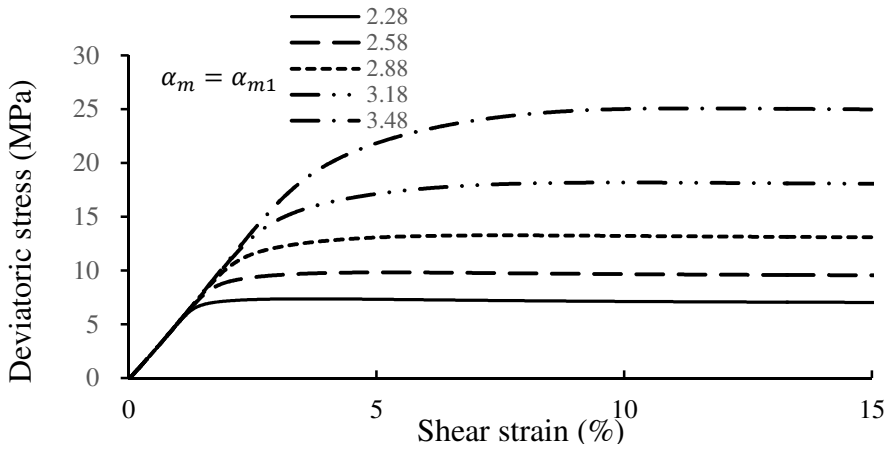

914

915 (a) Deviatoric stress-shear strain curves

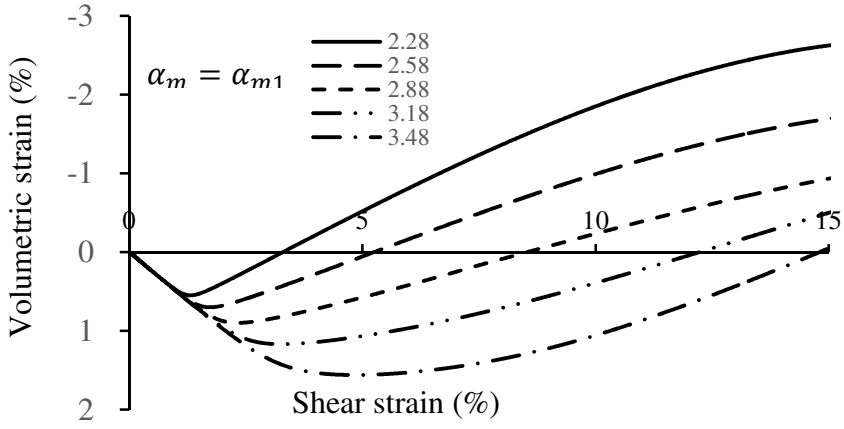

916

917 (b) Volumetric strain-shear strain curves

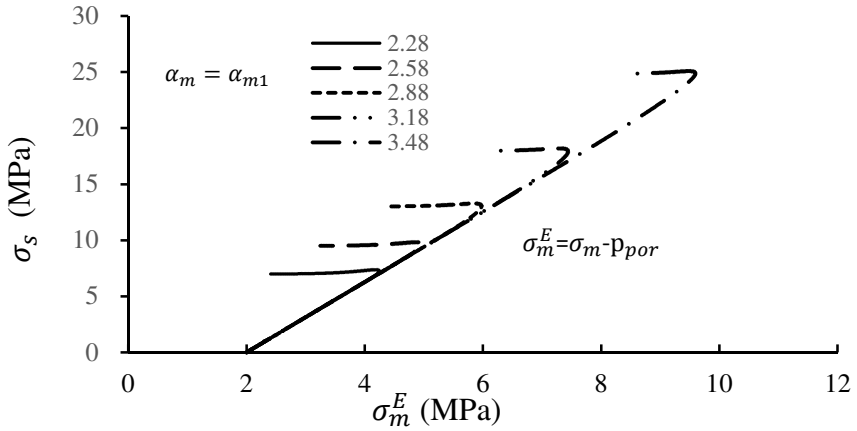

(c) Stress path of σ_m^E-σ_s

Fig. 4 Simulated results with varying $\alpha_m = \alpha_{m1}$ at 2.0MPa confining pressures

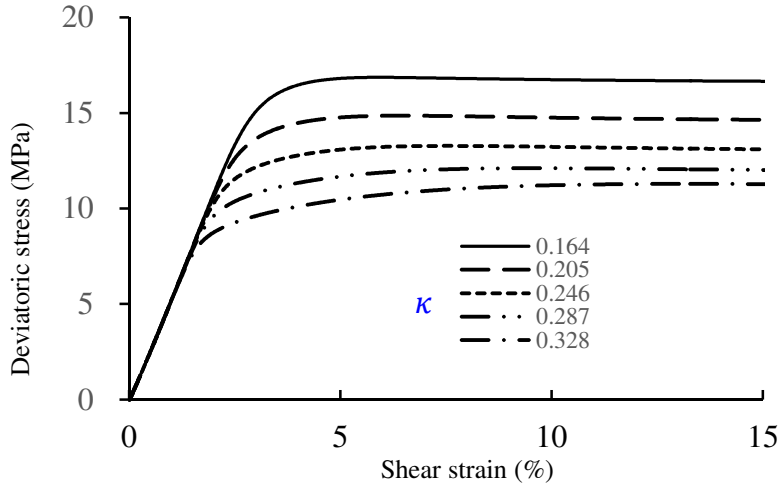

(a) Deviatoric stress-shear strain curves

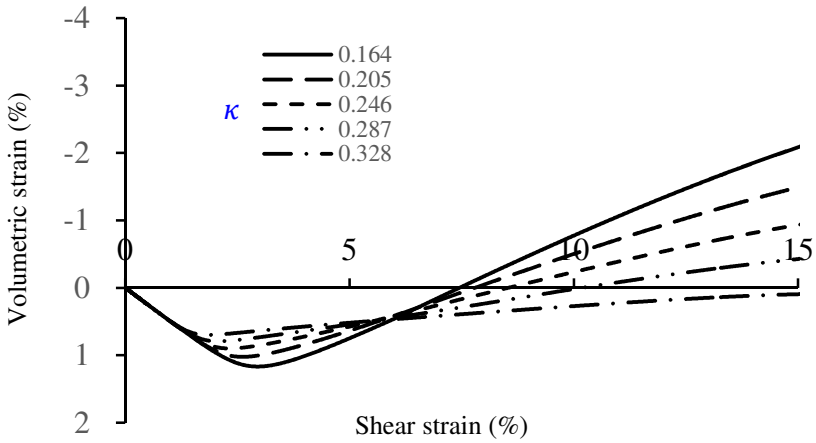

(b) Volumetric strain-shear strain curves

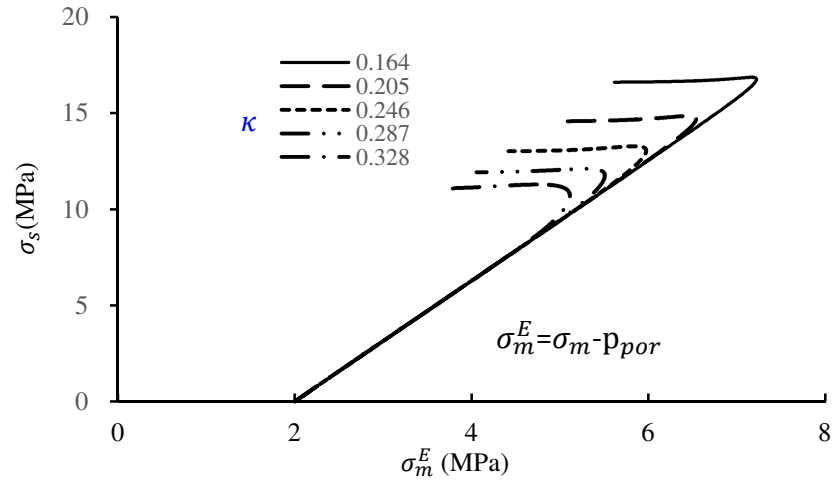

925

926 (c) Stress path of σ_m^E-σ_s

927 Fig. 5 Simulated results with varying κ at 2.0MPa confining pressures

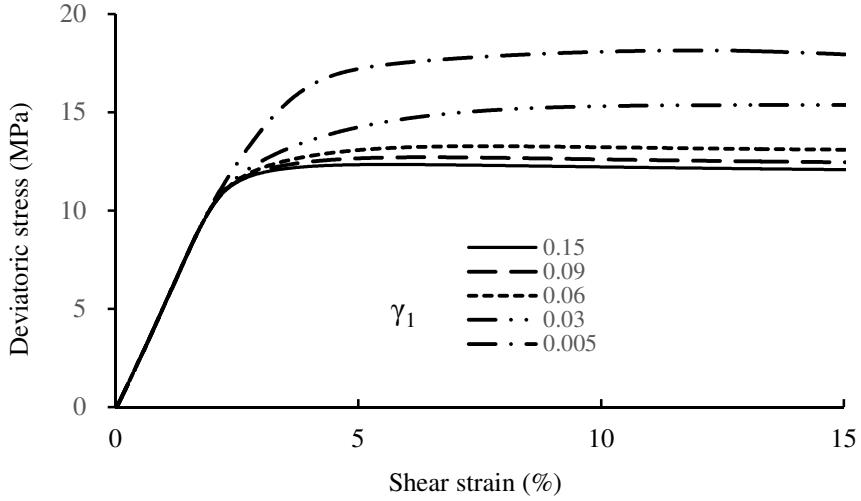

928

929 (a) Deviatoric stress-shear strain curves

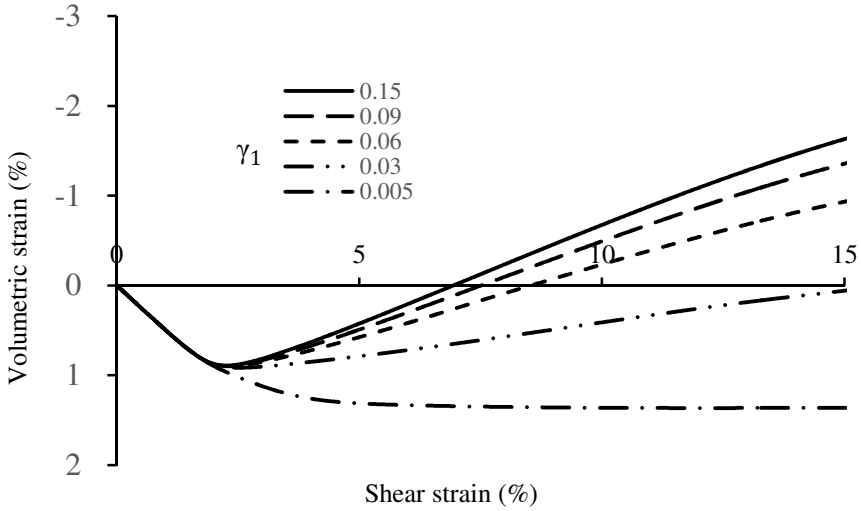

930

931 (b) Volumetric strain-shear strain curves

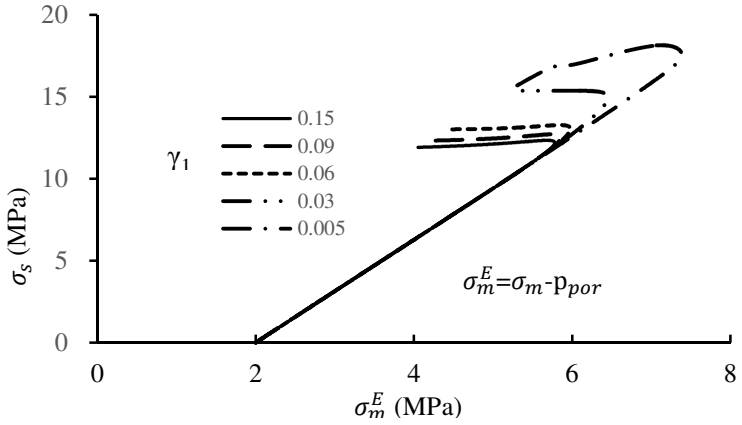

932

933 (c) Stress path of σ_m^E-σ_s

934 Fig. 6 Simulated results with varying γ_1 at 2.0MPa confining pressures

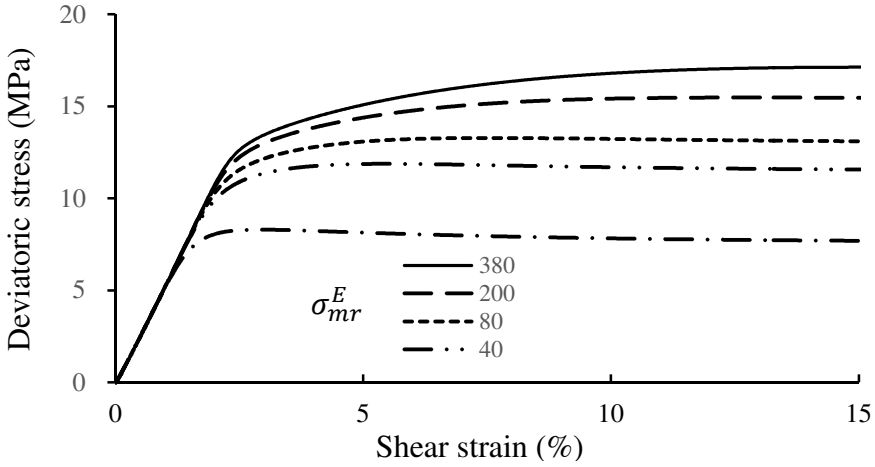

935

936 (a) Deviatoric stress-shear strain curves

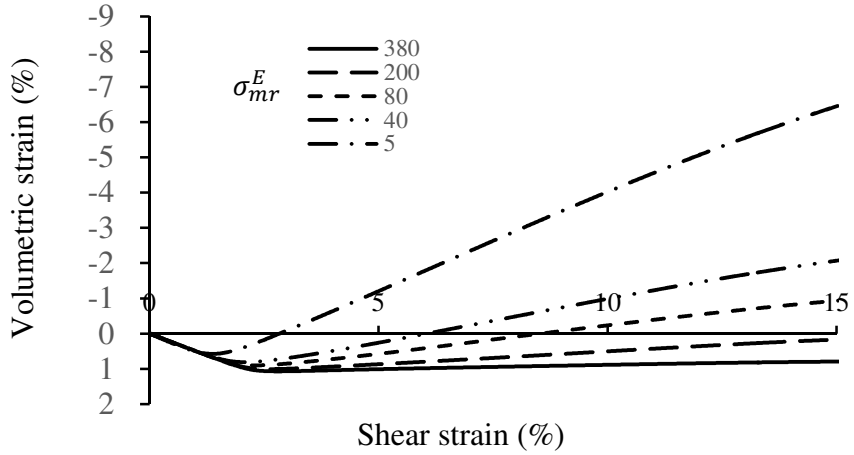

937

938 (b) Volumetric strain-shear strain curves

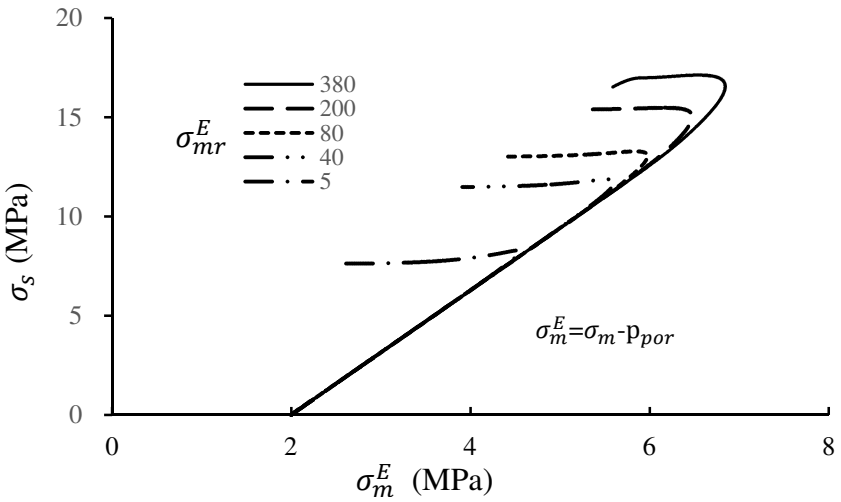

939

940 (c) Stress path of σ_m^E-σ_s

941 Fig. 7 Simulated results with varying σ_{mr}^E at 2.0MPa confining pressures

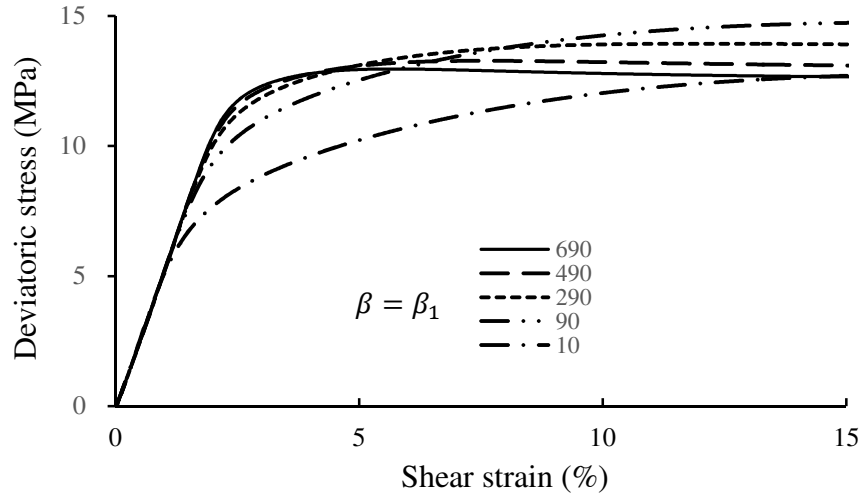

942

943 (a) Deviatoric stress-shear strain curves

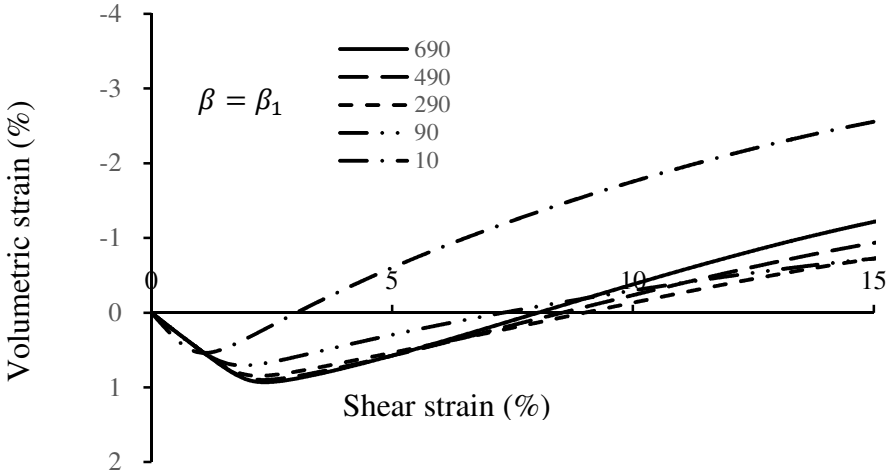

944

945 (b) Volumetric strain-shear strain curve

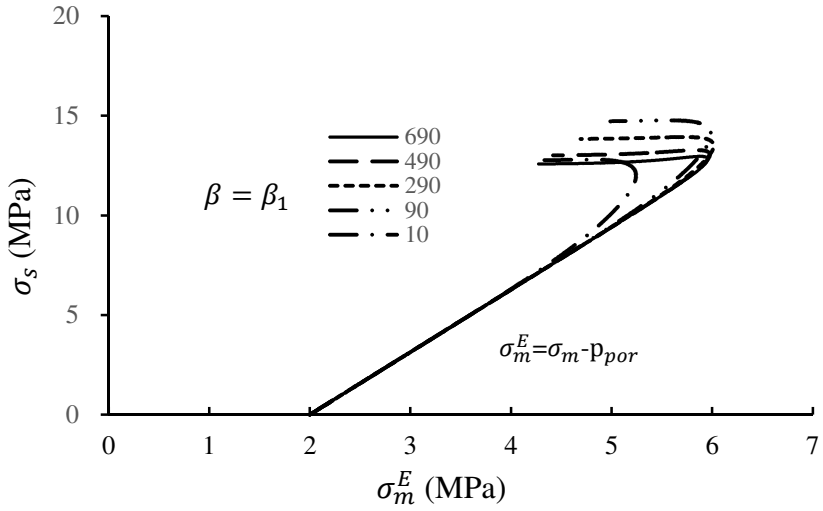

946

947 (c) Stress path of σ_m^E-σ_s

948 Fig. 8 Simulated results with varying $\beta = \beta_1$ at 2.0MPa confining pressures

949

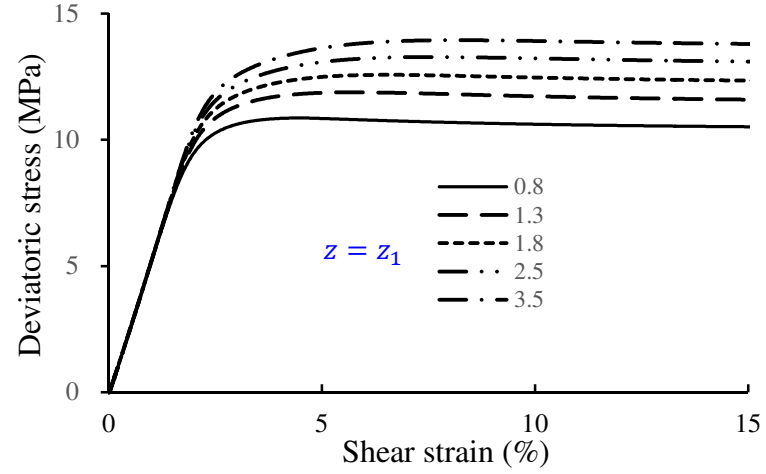

950

951 (a) Deviatoric stress-shear strain curves

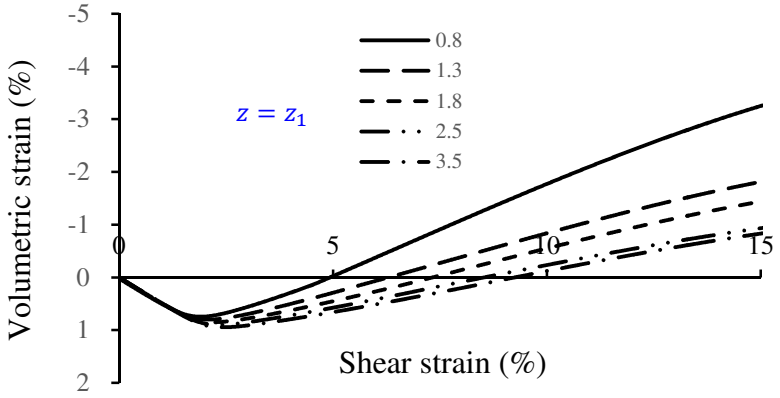

952

953 (b) Volumetric strain-shear strain curves

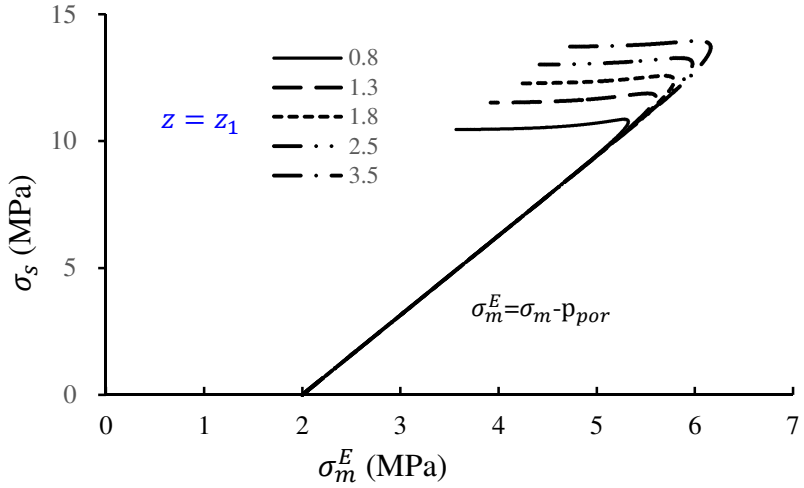

954

955 (c) Stress path of σ_m^E-σ_s

956 Fig. 9 Simulated results with varying $z = z_1$ at 2.0MPa confining pressures

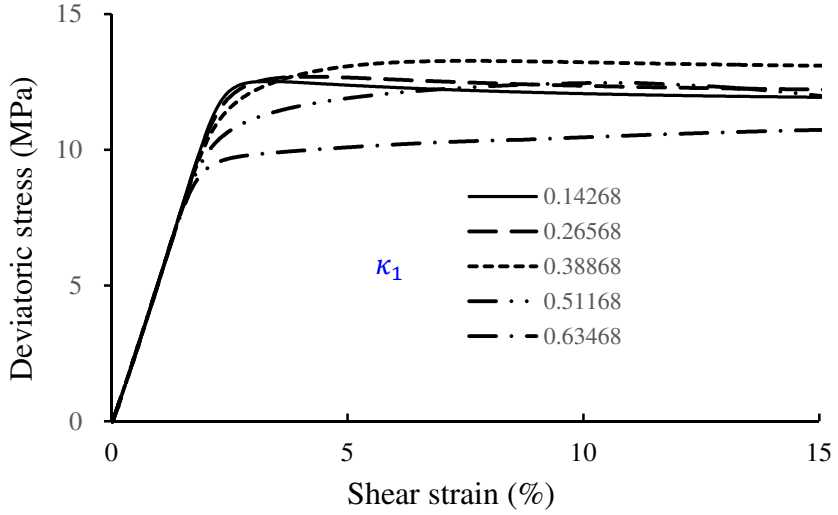

957

958 (a) Deviatoric stress-shear strain curves

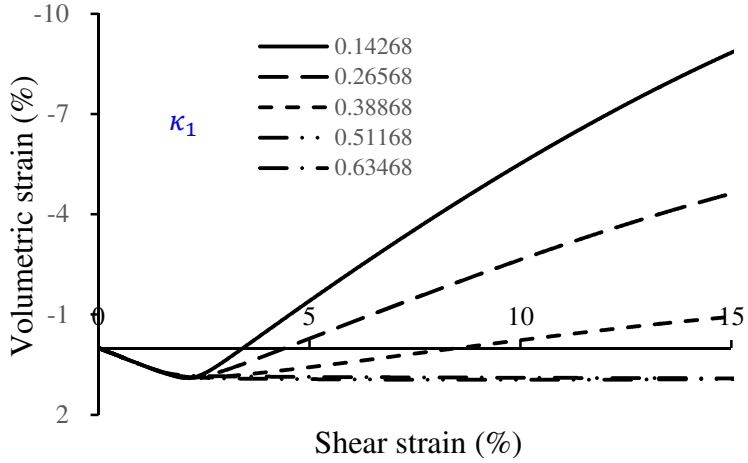

959

960 (b) Volumetric strain-shear strain curves

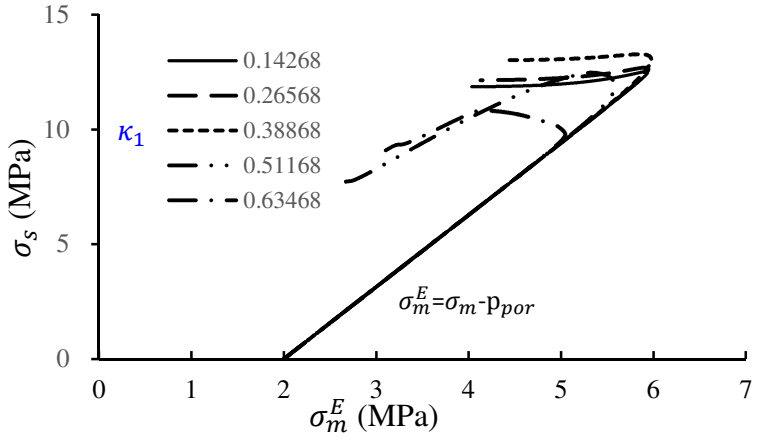

961

962 (c) Stress path of σ_m^E-σ_s

963 Fig. 10 Simulated results with varying κ_1 at 2.0MPa confining pressures

964

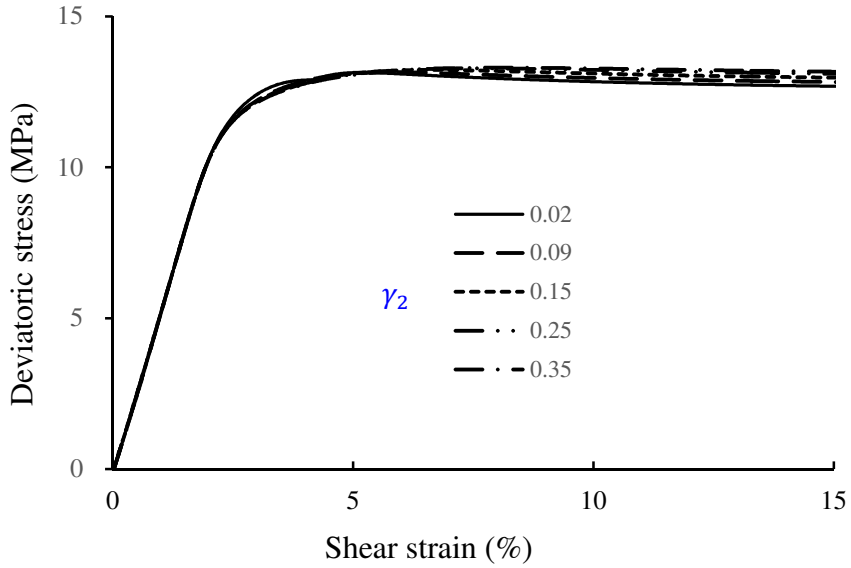

965

966 (a) Deviatoric stress-shear strain curves

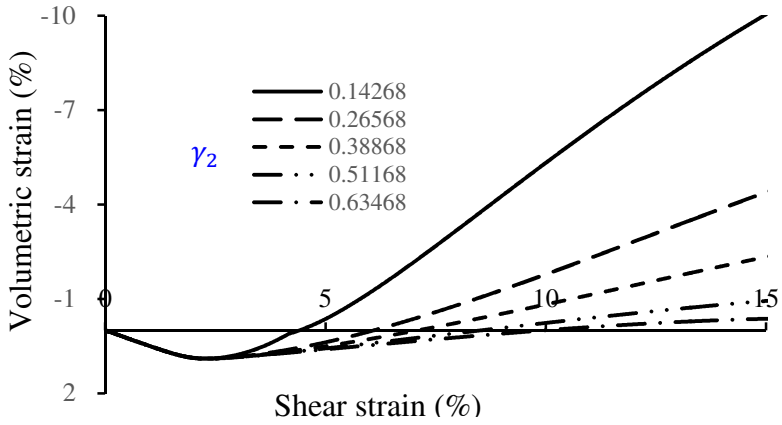

967

968 (b) Volumetric strain-shear strain curves

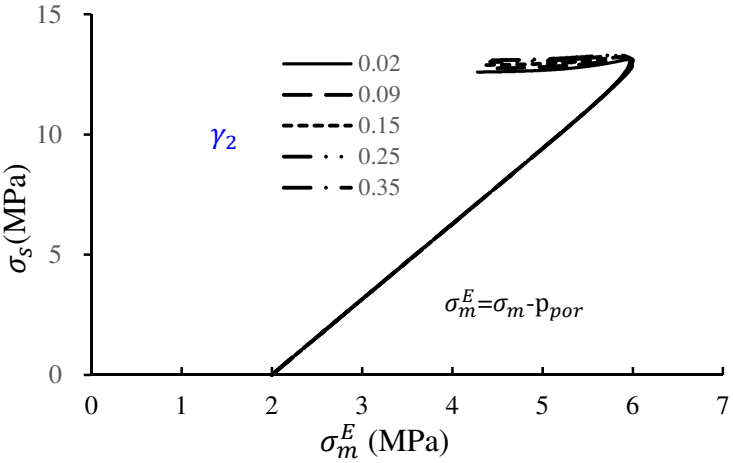

(c) Stress path of σ_m^E-σ_s

Fig. 11 Simulated results with varying γ_2 at 2.0MPa confining pressures

For geological materials, there are some constitutive models formulated with associated plastic flow rule, such as Cam-clay model for remoulded clay, while some others formulated with non-associated plastic flow rule, such as revised Lade-Duncan model for sand. For frozen soils, we can also use the associated plastic flow rule or non-associated plastic flow rule. In the simulated examples, we use here the non-associated flow rule for frozen soils, with the same form of yield function and plastic potential functions.

For the method proposed here, the stress states of $f\left(\sigma_{ij},\ \bar{p}_c,\ \bar{p}_w, \xi_J\right)$ satisfies the maximal plastic work principle, which means the yield locus $f = 0$ (no vertex effects) must be a convex function. Therefore, $d\varepsilon_{ij}^p$, $d\varphi_c^p$ and $d\varphi_w^p$ in Equations (151) or (153) in Section 4.3.2 can be obtained following the method proposed by Hill (1950). The incremental directions of $d\varepsilon_{ij}^p$, $d\varphi_c^p$ and $d\varphi_w^p$ are determined by $\partial h/\partial\sigma_{ij}$, $\partial h/\partial\,\bar{p}_c$ and $\partial h/\partial\,\bar{p}_w$, respectively, which means an non-associated plastic flow rule is used. When the associated or non-associated plastic flow rule is used, the plastic dissipation inequality (158) must be satisfied. For frozen soils tested, we can select a yield function f and a plastic potential function h and a free energy function, and then determine the corresponding parameters when deriving the incremental generalized stress strain relationships. We supplement a constitutive model with a non-associated plastic rule to simulate the relationships of deviatoric stress-shear strain and volumetric strain-shear strain under cryogenic triaxial loading conditions in Section 4.4.3. When formulating the elasto-plastic constitutive model, we have to make some assumptions. For different soil samples, there are different plastic criteria assumed by different researchers within the corresponding theoretical framework (Khan et al., 1991; Muraleetharan et al.,

2009; Kamrin, 2010; Zhang et al., 2012; Darabi et al., 2012; Yao et al., 2009, 2015; Xu et al., 2017). Although the constitutive model proposed here can present the simulated results agreeing relatively well with the test results, as shown in Figs. 2 and Fig.3 for frozen soils under triaxial compression conditions, further studies have to be done in the future to give less model parameters or easily methods to determine these parameters.

5. Conclusions

On the basis of thermoporomechanics, an elastoplastic model for saturated frozen soils are formulated in the paper. The saturated frozen soils are described as an open thermodynamics continuum. When phase change occurs, the equations of conservation of mass, momentum, and energy, and the Clausius-Duhem inequality are presented in both Lagrangian and Eulerian formulations. By considering the solid-fluid interface energy and the lagrangian saturation, the constitutive relationships in both elastic and ideal plasticity are given, and for hardening plasticity, the general form of stress-strain relationship is also presented and a hardening elastic-plastic constitutive is also proposed to simulate the cryogenic traixal compression properties of saturated frozen soils. The theory framework put forward here is an investigation on the extending of poroelasticty to poroelasoplasticity considering phase change between liquid water and ice crystals during the freezing process, which can be applied to study the frost heave of freezing ground in further numerical study.

Appendix I: Deriving the local equation of motion in Eulerian formulation.

From Equation (33) and Equation (34), we have

$$\frac{d^s}{dt}\int_\Omega \rho_s(1-n)\boldsymbol{V}^s d\Omega + \sum_{\alpha=c,w}\frac{d^\alpha}{dt}\int_\Omega \rho_\alpha n_\alpha \boldsymbol{V}^\alpha d\Omega = \int_\Omega \left(\rho_s(1-n)\boldsymbol{\gamma}^s + \sum_{\alpha=c,w}\rho_\alpha n_\alpha \boldsymbol{\gamma}^\alpha\right) d\Omega +$$

$$\int_\Omega \Lambda_{c\to w}(\boldsymbol{V}^w - \boldsymbol{V}^c)\, d\Omega = \int_\Omega \rho \boldsymbol{g}(\mathrm{x},\mathrm{t}) d\Omega + \int_{\partial\Omega} \mathbf{T}(\mathrm{x},\mathrm{t},\mathrm{n}) d\mathrm{a}. \quad \text{(I-1)}$$

Considering that $\mathbf{T}(\mathrm{x},\mathrm{t},\mathrm{n}) = \boldsymbol{\sigma}\cdot\mathbf{n}$ and $\rho = \rho_s(1-n) + \sum_{\alpha=c,w}\rho_\alpha n_\alpha$, so we have

$$\int_\Omega \rho \boldsymbol{g}(\mathrm{x},\mathrm{t}) d\Omega + \int_{\partial\Omega} \mathbf{T}(\mathrm{x},\mathrm{t},\mathrm{n}) d\mathrm{a} = \int_\Omega \rho \boldsymbol{g}(\mathrm{x},\mathrm{t}) d\Omega + \int_{\partial\Omega} \boldsymbol{\sigma}\cdot\mathbf{n} d\mathrm{a} = \int_\Omega \left(\rho_s(1-n) + \sum_{\alpha=c,w}\rho_\alpha n_\alpha\right)\boldsymbol{g} d\Omega +$$

$$\int_\Omega \nabla\cdot\boldsymbol{\sigma} d\Omega. \quad \text{(I-2)}$$

Combining (I-1) and (I-2), we can have the following,

$$\int_\Omega \left(\rho_s(1-n)\boldsymbol{\gamma}^s + \sum_{\alpha=c,w}\rho_\alpha n_\alpha \boldsymbol{\gamma}^\alpha\right) d\Omega + \int_\Omega \Lambda_{c\to w}(\boldsymbol{V}^w - \boldsymbol{V}^c)\, d\Omega$$

$$= \int_\Omega \left(\rho_s(1-n) + \sum_{\alpha=c,w}\rho_\alpha n_\alpha\right)\boldsymbol{g} d\Omega + \int_\Omega \nabla_x\cdot\boldsymbol{\sigma} d\Omega \quad \text{(I-3)}$$

Therefore, the local equation (35) can be obtained as follows,

$$\nabla_x \cdot \boldsymbol{\sigma} + \rho_s(1-n)(\boldsymbol{g} - \boldsymbol{\gamma}^s) + \sum_{\alpha=c,w} \rho_\alpha n_\alpha (\boldsymbol{g} - \boldsymbol{\gamma}^\alpha) - \Lambda_{c\to w}(\boldsymbol{V}^w - \boldsymbol{V}^c) = 0. \quad \text{(I-4) or (35)}$$

Appendix II: Deriving kinetic energy theorem.

From $\boldsymbol{w}_\alpha = \rho_\alpha n_\alpha (\boldsymbol{V}^\alpha - \boldsymbol{V}^s)$, we can have

$$\boldsymbol{V}^\alpha = \frac{\boldsymbol{w}_\alpha}{\rho_\alpha n_\alpha} + \boldsymbol{V}^s. \quad \text{(II-1)}$$

Use of Equation (II-1), the following can be obtained,

$$\rho_s(1-n)\boldsymbol{g}\cdot\boldsymbol{V}^s + \boldsymbol{g}\cdot\sum_{\alpha=c,w}\rho_\alpha n_\alpha \boldsymbol{V}^\alpha = \rho_s(1-n)\boldsymbol{g}\cdot\boldsymbol{V}^s + \boldsymbol{g}\cdot\sum_{\alpha=c,w}\rho_\alpha n_\alpha\left(\frac{\mathbf{w}_\alpha}{\rho_\alpha n_\alpha} + \boldsymbol{V}^s\right) = \rho_s(1-n)\boldsymbol{g}\cdot\boldsymbol{V}^s + \boldsymbol{g}\cdot\sum_{\alpha=c,w} g_\alpha + \boldsymbol{g}\cdot\sum_{\alpha=c,w}\rho_\alpha n_\alpha \boldsymbol{V}^s \quad \text{. (II-2)}$$

The total apparent mass density $\rho = \rho_s(1-n) + \sum_{\alpha=c,w}\rho_\alpha n_\alpha$, therefore, (II-2) can be rewritten as follows,

$$\rho_s(1-n)\boldsymbol{g}\cdot\boldsymbol{V}^s + \boldsymbol{g}\cdot\sum_{\alpha=c,w}\rho_\alpha n_\alpha \boldsymbol{V}^\alpha = \rho\boldsymbol{g}\cdot\boldsymbol{V}^s + \boldsymbol{g}\cdot\sum_{\alpha=c,w}\mathbf{w}_\alpha. \quad \text{(II-3)}$$

$$\mathbf{T}^s\cdot\boldsymbol{V}^s + \sum_{\alpha=c,w}(\mathbf{T}^\alpha\cdot\boldsymbol{V}^\alpha) = \mathbf{T}^s\cdot\boldsymbol{V}^s + \sum_{\alpha=c,w}\left(\mathbf{T}^\alpha\cdot\left(\frac{\mathbf{w}_\alpha}{\rho_\alpha n_\alpha} + \boldsymbol{V}^s\right)\right) = \mathbf{T}^s\cdot\boldsymbol{V}^s + \sum_{\alpha=c,w}\mathbf{T}^\alpha\cdot\boldsymbol{V}^s + \sum_{\alpha=c,w}\mathbf{T}^\alpha\cdot\frac{\mathbf{w}_\alpha}{\rho_\alpha n_\alpha} \quad \text{. (II-4)}$$

Applying the momentum balance separately to the soil skeleton and to the fluids (the ice crystals and unfrozen water), we can obtain the separate existence of a partial volumetric stress $\boldsymbol{\sigma}^s$ related to the soil skeleton and a partial volumetric stress tensor $\boldsymbol{\sigma}^\alpha(\alpha = c, w)$ related to the fluids, such as:

$$\mathbf{T}^s(\mathrm{x}, t, \mathrm{n}) = (1-n)\boldsymbol{\sigma}^s\cdot\mathbf{n}; \text{ and } \mathbf{T}^\alpha(\mathrm{x}, t, \mathrm{n}) = n_\alpha\boldsymbol{\sigma}^\alpha\cdot\mathbf{n}\ (\alpha = c, w), \quad \text{(II-5)}$$

in which n, $n_\alpha(\alpha = c, w)$ are the porosities, $\mathbf{n}$ is the normal vector of the surface da. The intrinsic averaged stress within the fluids can be addressed through a spherical tensor as follows,

$$\boldsymbol{\sigma}^\alpha = -p_\alpha\mathbf{1}. \quad \text{(II-6)}$$

Substituting (II-5) and (II-6) into (II-4), we can have

$$\mathbf{T}^s\cdot\boldsymbol{V}^s + \sum_{\alpha=c,w}(\mathbf{T}^\alpha\cdot\boldsymbol{V}^\alpha) = \mathbf{T}^s\cdot\boldsymbol{V}^s + \sum_{\alpha=c,w}\mathbf{T}^\alpha\cdot\boldsymbol{V}^s + \sum_{\alpha=c,w}(-n_\alpha p_\alpha)\mathbf{n}\cdot\frac{\boldsymbol{w}_\alpha}{\rho_\alpha n_\alpha} = \mathbf{T}\cdot\boldsymbol{V}^s - \sum_{\alpha=c,w}\frac{\mathbf{w}_\alpha}{\rho_\alpha}\cdot\mathbf{n} \quad \text{. (II-7)}$$

Therefore, substituting Equations (II-4) and (II-7) into Equation (40), we can have

$$\mathrm{P_{f,T}}(\boldsymbol{V}^s, \boldsymbol{V}^\alpha) = \int_\Omega\left(\rho\boldsymbol{g}\cdot\boldsymbol{V}^s + \boldsymbol{g}\cdot\sum_{\alpha=c,w}\boldsymbol{w}^\alpha\right)d\Omega + \int_{\partial\Omega}\left(\mathbf{T}\cdot\boldsymbol{V}^s - \sum_{\alpha=c,w}\left(\frac{p_\alpha}{\rho_\alpha}\boldsymbol{w}^\alpha\right)\cdot\mathbf{n}\right)da. \text{(II-8) or (41)}$$

From the kinetic energy of soil skeleton K_s in Equation (42), we can obtain its particle derivative as follows,

$$\frac{d^s K_s}{dt} = \frac{1}{2}\frac{d}{dt}\int_\Omega \rho_s(1-n)(\boldsymbol{V}^s)^2 d\Omega = \frac{1}{2}\int_\Omega \frac{d}{dt}(\rho_s(1-n)(\boldsymbol{V}^s)^2 d\Omega) = \frac{1}{2}\int_\Omega \left[(\boldsymbol{V}^s)^2 \frac{d}{dt}(\rho_s(1-n)d\Omega) + 2\rho_s(1-n)d\Omega\frac{d\boldsymbol{V}^s}{dt}\cdot\boldsymbol{V}^s\right] = \int_\Omega [\rho_s(1-n)\boldsymbol{\gamma}^s\cdot\boldsymbol{V}^s]d\Omega \quad , \text{(II-9)}$$

in which the mass balance of soil skeleton is used.

In a similar way, from the kinetic energy of ice crystals and unfrozen water of saturated frozen soils, we can also obtain the particle derivative as follows,

$$\frac{d^\alpha}{dt}\sum_{\alpha=c,w} K_\alpha = \sum_{\alpha=c,w}\frac{d^\alpha}{dt}\left\{\frac{1}{2}\int_\Omega \rho_\alpha n_\alpha (\boldsymbol{V}^\alpha)^2 d\Omega\right\} = \sum_{\alpha=c,w}\frac{1}{2}\left\{\frac{d^\alpha}{dt}\left(\int_\Omega \rho_\alpha n_\alpha (\boldsymbol{V}^\alpha)^2 d\Omega\right)\right\} = \sum_{\alpha=c,w}\frac{1}{2}\int_\Omega \left\{\left[\left((\boldsymbol{V}^\alpha)^2\frac{d}{dt}(\rho_\alpha n_\alpha d\Omega)\right) + 2\rho_\alpha n_\alpha d\Omega\frac{d\boldsymbol{V}^\alpha}{dt}\cdot\boldsymbol{V}^\alpha\right]\right\} \quad . \text{(II-10)}$$

Combining Equations (28) and (II-1), we can rewrite the above equation (II-10) as follows,

$$\frac{d^\alpha}{dt}\sum_{\alpha=c,w} K_\alpha = \int_\Omega \frac{1}{2}\Lambda_{c\to w}((\boldsymbol{V}^w)^2 - (\boldsymbol{V}^c)^2)d\Omega + \sum_{\alpha=c,w}\int_\Omega \left(\rho_\alpha n_\alpha \boldsymbol{\gamma}^\alpha\cdot\left(\frac{\mathbf{w}_\alpha}{\rho_\alpha n_\alpha} + \boldsymbol{V}^s\right)\right)d\Omega = \int_\Omega \frac{1}{2}\Lambda_{c\to w}((\boldsymbol{V}^w)^2 - (\boldsymbol{V}^c)^2)d\Omega + \sum_{\alpha=c,w}\int_\Omega (\rho_\alpha n_\alpha \boldsymbol{\gamma}^\alpha\cdot\boldsymbol{V}^s + \boldsymbol{\gamma}^\alpha\cdot\mathbf{w}_\alpha)d\Omega. \quad \text{(II-11)}$$

Combining (II-9) and (II-10), we can obtain the particle derivative of the kinetic energy of saturated frozen soils as follows,

$$\frac{d^s K_s}{dt} + \sum_{\alpha=c,w}\frac{d^\alpha K_\alpha}{dt} = \int_\Omega \left(\rho_s(1-n)\boldsymbol{\gamma}^s + \sum_{\alpha=c,w}\rho_\alpha n_\alpha \boldsymbol{\gamma}^\alpha\right)\cdot\boldsymbol{V}^s d\Omega + \int_\Omega \sum_{\alpha=c,w}\boldsymbol{\gamma}^\alpha\cdot\boldsymbol{w}^\alpha d\Omega + \int_\Omega \frac{1}{2}\Lambda_{c\to w}((\boldsymbol{V}^w)^2 - (\boldsymbol{V}^c)^2)d\Omega \quad . \text{(II-12) or (43)}$$

From Equation (16), the Eulerian strain rate tensor $\mathbf{d}^\pi$ is defined as follows,

$$\mathbf{d}^\pi = \frac{1}{2}\left(\nabla_x \boldsymbol{V}^\pi + {}^t\nabla_x \boldsymbol{V}^\pi\right) \quad (\pi = s, c, w) \quad . \quad \text{(II-13)}$$

From Equations (41) and (43), we can have

$$\mathrm{P_{f,T}}(\boldsymbol{V}^s, \boldsymbol{V}^\alpha) - \frac{d^s K_s}{dt} - \sum_{\alpha=c,w}\frac{d^\alpha K_\alpha}{dt} = \int_\Omega \left(\rho\boldsymbol{g}\cdot\boldsymbol{V}^s + \boldsymbol{g}\cdot\sum_{\alpha=c,w}\boldsymbol{w}^\alpha\right)d\Omega + \int_{\partial\Omega}\left(\mathbf{T}\cdot\boldsymbol{V}^s - \sum_{\alpha=c,w}\left(\frac{p_\alpha}{\rho_\alpha}\boldsymbol{w}^\alpha\right)\cdot\mathbf{n}\right)da - \int_\Omega \left(\rho_s(1-n)\boldsymbol{\gamma}^s + \sum_{\alpha=c,w}\rho_\alpha n_\alpha\boldsymbol{\gamma}^\alpha\right)\cdot\boldsymbol{V}^s d\Omega - \int_\Omega \sum_{\alpha=c,w}\boldsymbol{\gamma}^\alpha\cdot\boldsymbol{w}^\alpha d\Omega - \int_\Omega \frac{1}{2}\Lambda_{c\to w}((\boldsymbol{V}^w)^2 - (\boldsymbol{V}^c)^2)d\Omega \quad .\text{(II-14)}$$

Using the divergence theorem, we have

$$\int_{\partial\Omega}\left(\mathbf{T}\cdot\boldsymbol{V}^s - \sum_{\alpha=c,w}\left(\frac{p_\alpha}{\rho_\alpha}\boldsymbol{w}^\alpha\right)\cdot\mathbf{n}\right)da = \int_{\partial\Omega}\left(\mathbf{n}\cdot\boldsymbol{\sigma}\cdot\boldsymbol{V}^s - \sum_{\alpha=c,w}\left(\frac{p_\alpha}{\rho_\alpha}\boldsymbol{w}^\alpha\right)\cdot\mathbf{n}\right)da = \int_\Omega \left(\boldsymbol{\sigma}:\mathbf{d}^s + \boldsymbol{V}^s\cdot(\nabla_x\cdot\boldsymbol{\sigma}) - \sum_{\alpha=c,w}\nabla_x\cdot\left(\frac{p_\alpha}{\rho_\alpha}\boldsymbol{w}^\alpha\right)\right)d\Omega \quad .\text{(II-15)}$$

Substituting (II-15) into (II-14), we can obtain the following expression,

$$P_{f,T}(\boldsymbol{V}^s,\boldsymbol{V}^\alpha)-\frac{d^sK_s}{dt}-\sum_{\alpha=c,w}\frac{d^\alpha K_\alpha}{dt}=\int_\Omega\left(\rho\boldsymbol{g}\cdot\boldsymbol{V}^s+\boldsymbol{g}\cdot\sum_{\alpha=c,w}\boldsymbol{w}^\alpha\right)d\Omega+\int_\Omega\Big(\boldsymbol{\sigma}:\mathbf{d}^s+\boldsymbol{V}^s\cdot(\nabla_x\cdot\boldsymbol{\sigma})-\sum_{\alpha=c,w}\nabla_x\cdot\left(\frac{p_\alpha}{\rho_\alpha}\boldsymbol{w}^\alpha\right)\Big)d\Omega-\int_\Omega\left(\rho_s(1-n)\boldsymbol{\gamma}^s+\sum_{\alpha=c,w}\rho_\alpha n_\alpha\boldsymbol{\gamma}^\alpha\right)\cdot\boldsymbol{V}^s d\Omega-\int_\Omega\sum_{\alpha=c,w}\boldsymbol{\gamma}^\alpha\cdot\boldsymbol{w}^\alpha d\Omega-\int_\Omega\frac{1}{2}\Lambda_{c\to w}((\boldsymbol{V}^w)^2-(\boldsymbol{V}^c)^2)d\Omega \quad .(II\text{-}16)$$

Considering that

$$\int_\Omega(\rho\boldsymbol{g}\cdot\boldsymbol{V}^s)d\Omega+\int_\Omega\left(\boldsymbol{V}^s\cdot(\nabla_x\cdot\boldsymbol{\sigma})\right)d\Omega-\int_\Omega\left(\rho_s(1-n)\boldsymbol{\gamma}^s+\sum_{\alpha=c,w}\rho_\alpha n_\alpha\boldsymbol{\gamma}^\alpha\right)\cdot\boldsymbol{V}^s d\Omega=\int_\Omega\Big[\big(\rho_s(1-n)+\sum_{\alpha=c,w}\rho_\alpha n_\alpha\big)(\boldsymbol{g}\cdot\boldsymbol{V}^s)\Big]d\Omega+\int_\Omega\left(\boldsymbol{V}^s\cdot(\nabla_x\cdot\boldsymbol{\sigma})\right)d\Omega-\int_\Omega\left(\rho_s(1-n)\boldsymbol{\gamma}^s+\sum_{\alpha=c,w}\rho_\alpha n_\alpha\boldsymbol{\gamma}^\alpha\right)\cdot\boldsymbol{V}^s d\Omega=\int_\Omega\left((\nabla_x\cdot\boldsymbol{\sigma})\cdot\boldsymbol{V}^s\right)d\Omega+\int_\Omega\Big[\big(\rho_s(1-n)(\boldsymbol{g}-\boldsymbol{\gamma}^s)\big)\cdot\boldsymbol{V}^s\Big]d\Omega+\int_\Omega\left(\sum_{\alpha=c,w}\rho_\alpha n_\alpha(\boldsymbol{g}-\boldsymbol{\gamma}^s)\right)\cdot\boldsymbol{V}^s d\Omega=\int_\Omega\Lambda_{c\to w}(\boldsymbol{V}^w-\boldsymbol{V}^c)\cdot\boldsymbol{V}^s d\Omega \quad .(II\text{-}17)$$

Expression (II-16) can be rewritten as follows,

$$P_{f,T}(\boldsymbol{V}^s,\boldsymbol{V}^\alpha)-\frac{d^sK_s}{dt}-\sum_{\alpha=c,w}\frac{d^\alpha K_\alpha}{dt}=\int_\Omega\Lambda_{c\to w}(\boldsymbol{V}^w-\boldsymbol{V}^c)\cdot\boldsymbol{V}^s d\Omega-\int_\Omega\frac{1}{2}\Lambda_{c\to w}((\boldsymbol{V}^w)^2-(\boldsymbol{V}^c)^2)d\Omega+\int_\Omega(\boldsymbol{\sigma}:\mathbf{d}^s)\,d\Omega-\int_\Omega\sum_{\alpha=c,w}\nabla_x\cdot\left(\frac{p_\alpha}{\rho_\alpha}\boldsymbol{w}^\alpha\right)d\Omega+\int_\Omega\sum_{\alpha=c,w}(\boldsymbol{g}-\boldsymbol{\gamma}^\alpha)\cdot\boldsymbol{w}^\alpha d\Omega=\int_\Omega(\boldsymbol{\sigma}:\mathbf{d}^s)\,d\Omega-\int_\Omega\sum_{\alpha=c,w}\left[\nabla_x\cdot\left(\frac{p_\alpha}{\rho_\alpha}\boldsymbol{w}^\alpha\right)-(\boldsymbol{g}-\boldsymbol{\gamma}^\alpha)\cdot\boldsymbol{w}^\alpha\right]d\Omega-\int_\Omega\frac{1}{2}\Lambda_{c\to w}[(\boldsymbol{V}^w-\boldsymbol{V}^s)^2-(\boldsymbol{V}^c-\boldsymbol{V}^s)^2]d\Omega \quad .(II\text{-}18)$$

Therefore, the kinetic energy theorem in Eulerian form can be obtained as follows,

$$P_{f,T}(\boldsymbol{V}^s,\boldsymbol{V}^\alpha)=P_{def}(\boldsymbol{V}^s,\boldsymbol{V}^\alpha)+\frac{d^sK_s}{dt}+\sum_{\alpha=c,w}\frac{d^\alpha K_\alpha}{dt}-\int_\Omega\frac{1}{2}\Lambda_{c\to w}[(\boldsymbol{V}^w-\boldsymbol{V}^s)^2-(\boldsymbol{V}^c-\boldsymbol{V}^s)^2]d\Omega, \quad (II\text{-}19)\text{ or }(44)$$

and $$P_{def}(\boldsymbol{V}^s,\boldsymbol{V}^\alpha)=\int_\Omega\boldsymbol{\sigma}:\mathbf{d}^s d\,\Omega-\int_\Omega\sum_{\alpha=c,w}\left[\nabla_x\cdot\left(\frac{p_\alpha}{\rho_\alpha}\boldsymbol{w}^\alpha\right)-(\boldsymbol{g}-\boldsymbol{\gamma}^\alpha)\cdot\boldsymbol{w}^\alpha\right]d\,\Omega. \quad (II\text{-}20)\text{or }(45)$$

Appendix III: Deriving the energy equation and Clausius-Duhem inequality.

From Equation (54), we have

$$\frac{d^s}{dt}\int_\Omega\rho_s(1-n)e_s d\Omega+\sum_{\alpha=c,w}\frac{d^\alpha}{dt}\int_\Omega\rho_\alpha n_\alpha e_\alpha\,d\Omega=\int_\Omega\left[\frac{d^s(\rho_s(1-n)e_s)}{dt}+\rho_s(1-n)e_s\nabla_x\cdot\boldsymbol{V}^s\right]d\Omega+\sum_{\alpha=c,w}\int_\Omega\left[\frac{d^\alpha(\rho_\alpha n_\alpha e_\alpha)}{dt}+\rho_\alpha n_\alpha e_\alpha\nabla_x\cdot\boldsymbol{V}^\alpha\right]d\Omega \quad .(III\text{-}1)$$

Considering that the particulate derivative of a field respect to the soil skeleton as follows (Coussy, 1995),

$$\frac{d^\alpha(\rho_\alpha n_\alpha e_\alpha)}{dt}=\frac{d^s(\rho_\alpha n_\alpha e_\alpha)}{dt}+\nabla_x(\rho_\alpha n_\alpha e_\alpha)\cdot(\boldsymbol{V}^\alpha-\boldsymbol{V}^s), \quad (III\text{-}2)$$

and Equation (II-1), Expression (III-1) can be rewritten as follows,

$$\frac{d^s}{dt}\int_\Omega \rho_s(1-n)e_s d\Omega + \sum_{\alpha=c,w}\frac{d^\alpha}{dt}\int_\Omega \rho_\alpha n_\alpha e_\alpha \, d\Omega = \int_\Omega \left[\frac{d^s(\rho_s(1-n)e_s)}{dt} + \rho_s(1-n)e_s\nabla_x\cdot\boldsymbol{V}^s\right]d\Omega +$$

$$\sum_{\alpha=c,w}\int_\Omega \left[\frac{d^s(\rho_\alpha n_\alpha e_\alpha)}{dt} + \nabla_x(e_\alpha)\cdot\boldsymbol{w}_\alpha + e_\alpha\nabla_x\cdot\boldsymbol{w}^\alpha + \rho_\alpha n_\alpha e_\alpha\nabla_x\cdot\boldsymbol{V}^s\right]d\Omega = \int_\Omega \left[\frac{d^s e}{dt} + e\nabla_x\cdot\boldsymbol{V}^s + \right.$$

$$\left.\sum_{\alpha=c,w}[\nabla_x(e_\alpha)\cdot\boldsymbol{w}_\alpha + e_\alpha\nabla_x\cdot\boldsymbol{w}^\alpha]\right]d\Omega \quad . \text{(III-3)}$$

Therefore, the following can be obtained,

$$\frac{d^s}{dt}\int_\Omega \rho_s(1-n)e_s d\Omega + \sum_{\alpha=c,w}\frac{d^\alpha}{dt}\int_\Omega \rho_\alpha n_\alpha e_\alpha \, d\Omega = \int_\Omega \left[\frac{d^s e}{dt} + e\nabla_x\cdot\boldsymbol{V}^s + \sum_{\alpha=c,w}\nabla_x\cdot(e_\alpha\boldsymbol{w}^\alpha)\right]d\Omega.$$

(III-4) or (55)

According to Equation (27), the left side of Equation (64) can be written as follows,

$$\frac{d^s}{dt}\int_\Omega \rho_s(1-n)\theta_s d\Omega + \sum_{\alpha=c,w}\frac{d^\alpha}{dt}\int_\Omega \rho_\alpha n_\alpha\theta_\alpha d\Omega = \int_\Omega \left[\frac{d^s(\rho_s(1-n)\theta_s)}{dt} + \rho_s(1-n)\theta_s\nabla_x\cdot\boldsymbol{V}^s\right]d\Omega +$$

$$\sum_{\alpha=c,w}\int_\Omega \left[\frac{d^\alpha(\rho_\alpha n_\alpha\theta_\alpha)}{dt} + \rho_\alpha n_\alpha\theta_\alpha\nabla_x\cdot\boldsymbol{V}^\alpha\right]d\Omega \quad . \text{(III-5)}$$

Considering the particulate derivative of a field respect to the soil skeleton, we have

$$\sum_{\alpha=c,w}\int_\Omega \left[\frac{d^\alpha(\rho_\alpha n_\alpha\theta_\alpha)}{dt} + \rho_\alpha n_\alpha\theta_\alpha\nabla_x\cdot\boldsymbol{V}^\alpha\right]d\Omega = \sum_{\alpha=c,w}\int_\Omega \left[\frac{d^s(\rho_\alpha n_\alpha\theta_\alpha)}{dt} + \nabla_x(\theta_\alpha)\cdot\boldsymbol{w}_\alpha + \theta_\alpha\nabla_x\cdot\right.$$

$$\left.\boldsymbol{w}^\alpha + \rho_\alpha n_\alpha\theta_\alpha\nabla_x\cdot\boldsymbol{V}^s\right]d\Omega \quad . \text{(III-6)}$$

Therefore, we have

$$\frac{d^s}{dt}\int_\Omega \rho_s(1-n)\theta_s d\Omega + \sum_{\alpha=c,w}\frac{d^\alpha}{dt}\int_\Omega \rho_\alpha n_\alpha\theta_\alpha d\Omega$$

$$= \int_\Omega \left[\frac{d^s(\rho_s(1-n)\theta_s)}{dt} + \sum_{\alpha=c,w}\frac{d^s(\rho_\alpha n_\alpha\theta_\alpha)}{dt} + \rho_s(1-n)\theta_s\nabla_x\cdot\boldsymbol{V}^s + \sum_{\alpha=c,w}\rho_\alpha n_\alpha\theta_\alpha\nabla_x\cdot\boldsymbol{V}^s\right.$$

$$\left. + \sum_{\alpha=c,w}(\nabla_x(\theta_\alpha)\cdot\boldsymbol{w}_\alpha + \theta_\alpha\nabla_x\cdot\boldsymbol{w}^\alpha)\right]d\Omega$$

$$= \int_\Omega \left[\frac{d^s\theta}{dt} + \theta\nabla_x\cdot\boldsymbol{V}^s + + \sum_{\alpha=c,w}\nabla_x\cdot(\theta_\alpha\boldsymbol{w}^\alpha)\right]d\Omega \ . \quad \text{(III-7) or (65)}$$

Considering that $$\nabla_x\cdot\frac{\boldsymbol{q}}{T} = \frac{1}{T}\nabla_x\cdot\boldsymbol{q} - \frac{\boldsymbol{q}}{T^2}\cdot\nabla_x T \quad ,\text{(III-8)}$$

we can rewrite Inequality (68) as follows,

$$\mathrm{T}\frac{d^s\theta}{dt} + T\theta\nabla_x\cdot\boldsymbol{V}^s + T\sum_{\alpha=c,w}\nabla_x\cdot(\theta_\alpha\boldsymbol{w}^\alpha) + \nabla_x\cdot\boldsymbol{q} - \frac{\boldsymbol{q}}{T}\cdot\nabla_x T - \boldsymbol{r}_Q \geq 0. \quad \text{(III-9)}$$

Combining Equation (60), we can have

$$\mathrm{T}\frac{d^s\theta}{dt} + T\theta\nabla_x\cdot\boldsymbol{V}^s + T\sum_{\alpha=c,w}\nabla_x\cdot(\theta_\alpha\boldsymbol{w}^\alpha) - \frac{\boldsymbol{q}}{T}\cdot\nabla_x T - \frac{d^s e}{dt} - e\nabla_x\cdot\boldsymbol{V}^s + \boldsymbol{\sigma}:\boldsymbol{d}^s - \sum_{\alpha=c,w}\nabla_x\cdot(h_\alpha\boldsymbol{w}^\alpha) +$$

$$\sum_{\alpha=c,w}(\boldsymbol{g}-\boldsymbol{\gamma}^\alpha)\cdot(\boldsymbol{w}^\alpha) - \frac{1}{2}\Lambda_{c\to w}[(\boldsymbol{V}^w-\boldsymbol{V}^s)^2 - (\boldsymbol{V}^c-\boldsymbol{V}^s)^2] \geq 0 \quad .\text{(III-10)}$$

Substituting $\mathrm{d}\psi = de - Td\theta - \theta dT$ into the above inequality (III-10), we can have

$$\boldsymbol{\sigma}:\boldsymbol{d}^s + \sum_{\alpha=c,w}(\boldsymbol{g}-\boldsymbol{\gamma}^\alpha)\cdot\boldsymbol{w}^\alpha + \mathrm{T}\frac{d^s\theta}{dt} - \left(\frac{\mathrm{d}\psi}{dt} + T\frac{d\theta}{dt} + \theta\frac{dT}{dt}\right) - \psi\nabla_x\cdot\boldsymbol{V}^s + T\sum_{\alpha=c,w}\nabla_x\cdot(\theta_\alpha\boldsymbol{w}^\alpha) -$$

$$\sum_{\alpha=c,w}\nabla_x\cdot(h_\alpha\boldsymbol{w}^\alpha) - \frac{1}{2}\Lambda_{c\to w}[(\boldsymbol{V}^w-\boldsymbol{V}^s)^2 - (\boldsymbol{V}^c-\boldsymbol{V}^s)^2] - \frac{\boldsymbol{q}}{T}\cdot\nabla_x T \geq 0 \quad \text{,(III-11)}$$

Considering that the fluid-specific free enthalpy $g_\alpha = h_\alpha - T\theta_\alpha$ ($\alpha = c, w$), and $\nabla_x\cdot(\theta_\alpha\boldsymbol{w}^\alpha) = \boldsymbol{w}^\alpha\cdot\nabla_x\theta_\alpha + \theta_\alpha\nabla_x\cdot\boldsymbol{w}^\alpha$, we can have

$$T\sum_{\alpha=c,w}\nabla_x\cdot(\theta_\alpha\boldsymbol{w}^\alpha) - \sum_{\alpha=c,w}\nabla_x\cdot(h_\alpha\boldsymbol{w}^\alpha) = -\boldsymbol{w}^\alpha\cdot\sum_{\alpha=c,w}(\nabla_x g_\alpha + \theta_\alpha\nabla_x T) - \sum_{\alpha=c,w}(g_\alpha\nabla_x\cdot\boldsymbol{w}^\alpha). \text{(III-12)}$$

Substituting (III-12) into (III-11), we obtain so-called Clausius-Duhem inequality in Eulerian form as follows,

$$\boldsymbol{\sigma}:\boldsymbol{d}^s - \sum_{\alpha=c,w}(g_\alpha\nabla_x\cdot\boldsymbol{w}^\alpha) - \theta\frac{dT}{dt} - \frac{d\psi}{dt} - \psi\nabla_x\cdot\boldsymbol{V}^s - \boldsymbol{w}^\alpha\cdot\sum_{\alpha=c,w}\left(\nabla_x g_\alpha + \theta_\alpha\nabla_x T - (\boldsymbol{g}-\boldsymbol{\gamma}^\alpha)\right) -$$

$$\frac{1}{2}\Lambda_{c\to w}[(\boldsymbol{V}^w-\boldsymbol{V}^s)^2 - (\boldsymbol{V}^c-\boldsymbol{V}^s)^2] - \frac{\boldsymbol{q}}{T}\cdot\nabla_x T \geq 0 \quad \text{.(III-13) or (69)}$$

The time rate of the entropy associated with the matter contained in Ω_0 of saturated frozen soils can be expressed as follows,

$$\frac{D\Theta}{Dt} = \frac{D}{Dt}\int_{\Omega_0}\Theta d\Omega_0 = \int_{\Omega_0}\frac{d\Theta}{dt}d\Omega_0 + \sum_{\alpha=c,w}\int_{\Omega_0}\nabla_X\cdot(\Theta_\alpha\boldsymbol{M}_\alpha)d\Omega_0. \quad \text{(III-14)}$$

Therefore, the second law of thermodynamics in Lagrangian formulation can be expressed as follows,

$$\int_{\Omega_0}\frac{d\Theta}{dt}d\Omega_0 + \sum_{\alpha=c,w}\int_{\Omega_0}\nabla_X\cdot(\Theta_\alpha\boldsymbol{M}_\alpha)d\Omega_0 \geq -\int_{\partial\Omega_0}\frac{\boldsymbol{Q}\cdot\boldsymbol{N}}{T}d\mathrm{A} + \int_{\Omega_0}\frac{\boldsymbol{R_Q}}{T}d\Omega_0 \ . \quad \text{(III-15)}$$

By using the theorem of divergence, inequality (III-15) can be written in the Lagrangian formulation as follows,

$$\int_{\Omega_0}\frac{d\Theta}{dt}d\Omega_0 + \sum_{\alpha=c,w}\int_{\Omega_0}\nabla_X\cdot(\Theta_\alpha\boldsymbol{M}_\alpha)d\Omega_0 \geq -\int_{\Omega_0}\nabla_X\cdot\frac{\boldsymbol{Q}}{T}d\Omega_0 + \int_{\Omega_0}\frac{\boldsymbol{R_Q}}{T}d\Omega_0 \ . \text{(III-16)}$$

Therefore, the following can be obtained,

$$\frac{d\Theta}{dt} + \sum_{\alpha=c,w}\nabla_X\cdot(\Theta_\alpha\boldsymbol{M}_\alpha) + \nabla_X\cdot\frac{\boldsymbol{Q}}{T} - \frac{\boldsymbol{R_Q}}{T} \geq 0. \quad \text{(III-17) or (71)}$$

Substituting $\nabla_X\cdot\frac{\boldsymbol{Q}}{T} = \frac{1}{T}\nabla_X\cdot\boldsymbol{Q} - \frac{\boldsymbol{Q}}{T^2}\cdot\nabla_X T$ into Inequality (71), we can have

$$\frac{d\Theta}{dt} + \sum_{\alpha=c,w}\nabla_X\cdot(\Theta_\alpha\boldsymbol{M}_\alpha) + \frac{1}{T}\nabla_X\cdot\boldsymbol{Q} - \frac{\boldsymbol{Q}}{T^2}\cdot\nabla_X T - \frac{\boldsymbol{R_Q}}{T} \geq 0 \ , \quad \text{(III-18)}$$

which can be rewritten as follows,

$$T\frac{d\Theta}{dt} + T\sum_{\alpha=c,w}\nabla_X\cdot(\Theta_\alpha\boldsymbol{M}_\alpha) + \nabla_X\cdot\boldsymbol{Q} - \frac{\boldsymbol{Q}}{T}\cdot\nabla_X T - \boldsymbol{R}_Q \geq 0. \quad \text{(III-19)}$$

Combining Equations (63) and (III-19), we have

$$T\frac{d\Theta}{dt} + T\sum_{\alpha=c,w}\nabla_X\cdot(\Theta_\alpha\boldsymbol{M}_\alpha) - \frac{dE}{dt} + \boldsymbol{\pi}:\frac{d\Delta}{dt} - \sum_{\alpha=c,w}\nabla_X\cdot h_\alpha\boldsymbol{M}_\alpha - \nabla_X\cdot\boldsymbol{Q} + \sum_{\alpha=c,w}\left((\boldsymbol{g}-\boldsymbol{\gamma}^\alpha)\cdot\boldsymbol{F}\right)\cdot$$

$$\boldsymbol{M}_\alpha - \frac{1}{2} m_{c\to w}[(\boldsymbol{V}^w - \boldsymbol{V}^s)^2 - (\boldsymbol{V}^c - \boldsymbol{V}^s)^2] - \frac{\boldsymbol{Q}}{T}\cdot\nabla_X T \geq 0. \quad \text{(III-20)}$$

Considering that $h_\alpha = g_\alpha + T\Theta_\alpha \ \ (\alpha = c, w)$, we have

$$T\sum_{\alpha=c,w}\nabla_X\cdot(\Theta_\alpha \boldsymbol{M}_\alpha) - \sum_{\alpha=c,w}\nabla_X\cdot h_\alpha \boldsymbol{M}_\alpha = T\sum_{\alpha=c,w}(\boldsymbol{M}_\alpha\cdot\nabla_X\Theta_\alpha) + T\sum_{\alpha=c,w}\Theta_\alpha\nabla_X\cdot\boldsymbol{M}_\alpha -$$

$$\sum_{\alpha=c,w}\nabla_X\cdot(g_\alpha + T\Theta_\alpha)M^\alpha = -\boldsymbol{M}_\alpha\cdot\sum_{\alpha=c,w}(\nabla_X g_\alpha + \Theta_\alpha\nabla_X T) - \sum_{\alpha=c,w} g_\alpha\nabla_X\cdot\boldsymbol{M}_\alpha \ . \quad \text{(III-21)}$$

Substituting Equation (III-21) into Equation (III-20), we can obtain

$$\boldsymbol{\pi}:\frac{d\Delta}{dt} + \sum_{\alpha=c,w}\big((\boldsymbol{g}-\boldsymbol{\gamma}^\alpha)\cdot\boldsymbol{F}\big)\cdot\boldsymbol{M}_\alpha + T\frac{d\Theta}{dt} - \frac{dE}{dt} - \boldsymbol{M}_\alpha\cdot\sum_{\alpha=c,w}(\nabla_X g_\alpha + \Theta_\alpha\nabla_X T) - \sum_{\alpha=c,w} g_\alpha\nabla_X\cdot$$

$$\boldsymbol{M}_\alpha - \frac{1}{2} m_{c\to w}[(\boldsymbol{V}^w - \boldsymbol{V}^s)^2 - (\boldsymbol{V}^c - \boldsymbol{V}^s)^2] - \frac{\boldsymbol{Q}}{T}\cdot\nabla_X T \geq 0. \quad \text{(III-22)}$$

Substituting $\mathrm{d}\Psi = dE - Td\Theta - \Theta dT$ into (III-22), and with the mass conservation (31) and (32), the Lagrangian formulation of the Clausius-Duhem inequality (III-22) can be written as follows,

$$\boldsymbol{\pi}:\frac{d\Delta}{dt} + \sum_\alpha g_\alpha\frac{dm_\alpha}{dt} - \Theta\frac{dT}{dt} - \frac{d\Psi}{dt} - (g_c - g_m)\varpi_{c\to w} - \frac{1}{2}\varpi_{c\to w}[(\boldsymbol{V}^w - \boldsymbol{V}^s)^2 - (\boldsymbol{V}^c - \boldsymbol{V}^s)^2] -$$

$$\sum_\alpha(\nabla_X g_\alpha + \Theta_\alpha\nabla_X T - (\boldsymbol{g}-\boldsymbol{\gamma}^\alpha)\cdot\boldsymbol{F})\cdot\boldsymbol{M}_\alpha - \frac{\boldsymbol{Q}}{T}\cdot\nabla_X T \geq 0 \quad \text{.(III-23) or (73)}$$

Appendix IV: Deriving the thermal balance equation.

Combining Equations (63) and (79), we can have

$$\frac{dE}{dt} = \frac{d\Psi}{dt} + T\frac{d\Theta}{dt} + \Theta\frac{dT}{dt} = \boldsymbol{\pi}:\frac{d\Delta}{dt} - \sum_\alpha\nabla_X\cdot(h_\alpha\boldsymbol{M}_\alpha) - \nabla_X\cdot\boldsymbol{Q} + \sum_\alpha\big((\boldsymbol{g}-\boldsymbol{\gamma}^\alpha)\cdot\boldsymbol{F}\big)\cdot\boldsymbol{M}_\alpha + \boldsymbol{R} -$$

$$\frac{1}{2}\varpi_{c\to w}[(\boldsymbol{V}^w - \boldsymbol{V}^s)^2 - (\boldsymbol{V}^c - \boldsymbol{V}^s)^2] \quad \text{.(IV-1)}$$

Considering that

$$-\sum_\alpha\nabla_X\cdot(h_\alpha\boldsymbol{M}_\alpha) = -\sum_\alpha\nabla_X\cdot(g_\alpha + T\Theta_\alpha)\boldsymbol{M}_\alpha = -\sum_\alpha\boldsymbol{M}_\alpha\cdot\nabla_X g_\alpha - \sum_\alpha g_\alpha\nabla_X\cdot\boldsymbol{M}_\alpha - \sum_\alpha\boldsymbol{M}_\alpha\cdot$$

$$\nabla_X(T\Theta_\alpha) - \sum_\alpha T\Theta_\alpha\nabla_X\cdot\boldsymbol{M}_\alpha \quad \text{.(IV-2)}$$

Substituting Equation (IV-2) into (IV-1), we can obtain

$$\frac{d\Psi}{dt} + T\frac{d\Theta}{dt} + \Theta\frac{dT}{dt} = \boldsymbol{\pi}:\frac{d\Delta}{dt} - \sum_\alpha\boldsymbol{M}_\alpha\cdot\nabla_X g_\alpha - \sum_\alpha g_\alpha\nabla_X\cdot\boldsymbol{M}_\alpha - \sum_\alpha\boldsymbol{M}_\alpha\cdot\nabla_X(T\Theta_\alpha) - \sum_\alpha T\Theta_\alpha\nabla_X\cdot\boldsymbol{M}_\alpha -$$

$$\nabla_X\cdot\boldsymbol{Q} + \sum_\alpha\big((\boldsymbol{g}-\boldsymbol{\gamma}^\alpha)\cdot\boldsymbol{F}\big)\cdot\boldsymbol{M}_\alpha + R_Q - \frac{1}{2}\varpi_{c\to w}[(\boldsymbol{V}^w - \boldsymbol{V}^s)^2 - (\boldsymbol{V}^c - \boldsymbol{V}^s)^2] \quad \text{,(IV-3)}$$

which can be written as follows,

$$\frac{d\Psi}{dt} + T\frac{d\Theta}{dt} + \Theta\frac{dT}{dt} = \boldsymbol{\pi}:\frac{d\Delta}{dt} - \sum_\alpha\boldsymbol{M}_\alpha\cdot\nabla_X g_\alpha - \sum_\alpha g_\alpha\nabla_X\cdot\boldsymbol{M}_\alpha - \sum_\alpha\boldsymbol{M}_\alpha\cdot\mathrm{T}\nabla_X(\Theta_\alpha) - \sum_\alpha\Theta_\alpha\boldsymbol{M}_\alpha\cdot\nabla_X T -$$

$$T\sum_\alpha\Theta_\alpha\nabla_X\cdot\boldsymbol{M}_\alpha - \nabla_X\cdot\boldsymbol{Q} + \sum_\alpha\big((\boldsymbol{g}-\boldsymbol{\gamma}^\alpha)\cdot\boldsymbol{F}\big)\cdot\boldsymbol{M}_\alpha + \boldsymbol{R} - \frac{1}{2}\varpi_{c\to w}[(\boldsymbol{V}^w - \boldsymbol{V}^s)^2 - (\boldsymbol{V}^c - \boldsymbol{V}^s)^2] \quad \text{.(IV-4)}$$

Considering that

$$T\frac{d\Theta}{dt} + \sum_\alpha\boldsymbol{M}_\alpha\cdot\mathrm{T}\nabla_X(\Theta_\alpha) + T\sum_\alpha\Theta_\alpha\nabla_X\cdot\boldsymbol{M}_\alpha = T\left[\frac{d\Theta}{dt} + \sum_\alpha(\boldsymbol{M}_\alpha\cdot\nabla_X\Theta_\alpha + \Theta_\alpha\nabla_X\cdot\boldsymbol{M}_\alpha)\right]$$

$= T\left[\frac{d\Theta}{dt} + \sum_\alpha \nabla_X \cdot (\Theta_\alpha \boldsymbol{M}_\alpha)\right]$,(IV-5)

and $\sum_\alpha g_\alpha \nabla_X \cdot \boldsymbol{M}_\alpha = g_c \nabla_X \cdot \boldsymbol{M}_c + g_w \nabla_X \cdot \boldsymbol{M}_w = g_c\left(-\varpi_{c\to w} - \frac{dm_c}{dt}\right) + g_w\left(\varpi_{c\to w} - \frac{dm_w}{dt}\right)$

$= (-g_c + g_w)\varpi_{c\to w} - \sum_\alpha g_\alpha \frac{dm_\alpha}{dt}$,(IV-6)

Equation (IV-4) can be rewritten as follows,

$T\left(\frac{d\Theta}{dt} + \sum_{\alpha=c,w} \nabla_X \cdot (\Theta_\alpha \boldsymbol{M}_\alpha)\right) = \boldsymbol{R}_Q - \nabla_X \cdot \boldsymbol{Q} + \Phi_1 + \Phi_3 + \Phi_\to = \boldsymbol{R}_Q - \nabla_X \cdot \boldsymbol{Q} + \Phi_M + \Phi_\to.$ (IV-7)or(80)

Combining the energy equation (40) and Equation (89), we can have

$\frac{\mathrm{d}e}{dt} + e\nabla_x \cdot \boldsymbol{V}^s = \frac{\mathrm{d}\psi}{dt} + T\frac{d\theta}{dt} + \theta\frac{dT}{dt} + e\nabla_x \cdot \boldsymbol{V}^s = \frac{\mathrm{d}\psi}{dt} + T\frac{d\theta}{dt} + \theta\frac{dT}{dt} + (\psi + T\theta)\nabla_x \cdot \boldsymbol{V}^s = \boldsymbol{\sigma}\colon \boldsymbol{d}^s - \sum_\alpha \nabla_x \cdot$

$(h_\alpha \boldsymbol{w}^\alpha) - \nabla_x \cdot \boldsymbol{q} + \sum_\alpha (\boldsymbol{g} - \boldsymbol{\gamma}^\alpha) \cdot (\boldsymbol{w}^\alpha) + \boldsymbol{r}_Q - \frac{1}{2}\Lambda_{c\to w}[(\boldsymbol{V}^w - \boldsymbol{V}^s)^2 - (\boldsymbol{V}^c - \boldsymbol{V}^s)^2]$. (IV-8)

Therefore, the above equation can be rewritten as follows,

$T\frac{d\theta}{dt} + T\theta\nabla_x \cdot \boldsymbol{V}^s = -\frac{\mathrm{d}\psi}{dt} - \theta\frac{dT}{dt} - \psi\nabla_x \cdot \boldsymbol{V}^s + \boldsymbol{\sigma}\colon \boldsymbol{d}^s - \sum_\alpha \nabla_x \cdot (h_\alpha \boldsymbol{w}^\alpha) - \nabla_x \cdot \boldsymbol{q} + \sum_\alpha (\boldsymbol{g} - \boldsymbol{\gamma}^\alpha) \cdot$

$(\boldsymbol{w}^\alpha) + \boldsymbol{r}_Q - \frac{1}{2}\Lambda_{c\to w}[(\boldsymbol{V}^w - \boldsymbol{V}^s)^2 - (\boldsymbol{V}^c - \boldsymbol{V}^s)^2]$. (IV-9)

Considering that $h_\alpha = g_\alpha + T\theta_\alpha$, we can have

$T\frac{d\theta}{dt} + T\theta\nabla_x \cdot \boldsymbol{V}^s = -\frac{\mathrm{d}\psi}{dt} - \theta\frac{dT}{dt} - \psi\nabla_x \cdot \boldsymbol{V}^s + \boldsymbol{\sigma}\colon \boldsymbol{d}^s - \sum_\alpha \nabla_x \cdot (g_\alpha \boldsymbol{w}^\alpha) - \sum_\alpha \nabla_x \cdot (T\theta_\alpha \boldsymbol{w}^\alpha) - \nabla_x \cdot \boldsymbol{q} +$

$\sum_\alpha (\boldsymbol{g} - \boldsymbol{\gamma}^{\boldsymbol{\alpha}}) \cdot (\boldsymbol{w}^\alpha) + \boldsymbol{r}_Q - \frac{1}{2}\Lambda_{c\to w}[(\boldsymbol{V}^w - \boldsymbol{V}^s)^2 - (\boldsymbol{V}^c - \boldsymbol{V}^s)^2]$. (IV-10)

Use of $\nabla \cdot (\zeta \boldsymbol{V}) = \zeta\nabla \cdot \boldsymbol{V} + \nabla\zeta \cdot \boldsymbol{V}$, we can have

$\nabla_x \cdot (g_\alpha \boldsymbol{w}^\alpha) = g_\alpha \nabla_x \cdot \boldsymbol{w}^\alpha + \boldsymbol{w}^\alpha \cdot \nabla_x g_\alpha$, and $\nabla_x \cdot (T\theta_\alpha \boldsymbol{w}^\alpha) = T\nabla_x \cdot (\theta_\alpha \boldsymbol{w}^\alpha) + (\theta_\alpha \boldsymbol{w}^\alpha) \cdot \nabla_x T$. (IV-11)

Substituting Equation (IV-11) into Equation (IV-10), we can obtain

$T\frac{d\theta}{dt} + T\theta\nabla_x \cdot \boldsymbol{V}^s + T\sum_\alpha \nabla_x \cdot (\theta_\alpha \boldsymbol{w}^\alpha) = \boldsymbol{r}_Q - \nabla_x \cdot \boldsymbol{q} + \boldsymbol{\sigma}\colon \boldsymbol{d}^s - \frac{\mathrm{d}\psi}{dt} - \theta\frac{dT}{dt} - \psi\nabla_x \cdot \boldsymbol{V}^s - \sum_\alpha g_\alpha \nabla_x \cdot \boldsymbol{w}^\alpha$

$-\sum_\alpha \boldsymbol{w}^\alpha \cdot \nabla_x g_\alpha - \sum_\alpha (\theta_\alpha \boldsymbol{w}^\alpha) \cdot \nabla_x T + \sum_\alpha (\boldsymbol{g} - \boldsymbol{\gamma}^\alpha) \cdot (\boldsymbol{w}^\alpha) - \frac{1}{2}\Lambda_{c\to w}[(\boldsymbol{V}^w - \boldsymbol{V}^s)^2 - (\boldsymbol{V}^c - \boldsymbol{V}^s)^2]$, (IV-12)

which can be rewritten as follows,

$T\frac{d\theta}{dt} + T\theta\nabla_x \cdot \boldsymbol{V}^s + T\sum_\alpha \nabla_x \cdot (\theta_\alpha w^\alpha) = \boldsymbol{r}_Q - \nabla_x \cdot \boldsymbol{q} + \varphi_1 + \varphi_3 + \varphi_\to.$ (IV-13) or (90)

Appendix V: Deriving Clausius-Duhem inequality related to soil skeleton.

From Equations (110) and (111), we have

$\theta = \theta_s + \sum_\alpha m_\alpha \theta_\alpha$, and $\Psi = \Psi_s + \sum_\alpha m_\alpha \Psi_\alpha = \Psi_s + \sum_\alpha m_\alpha \left(\mu_\alpha - \frac{p_\alpha}{\rho_\alpha}\right)$. (V-1)

Substituting Equations (V-1) into Equation (108), we can have

$$\boldsymbol{\sigma}:\frac{d\boldsymbol{\varepsilon}}{dt}+\sum\mu_\alpha\frac{dm_\alpha}{dt}-(\theta_s+\sum_\alpha m_\alpha\theta_\alpha)\frac{dT}{dt}-\frac{d\left(\Psi_s+\sum_\alpha m_\alpha\left(\mu_\alpha-\frac{p_\alpha}{\rho_\alpha}\right)\right)}{dt}\geq 0, \tag{V-2}$$

which can be rewritten as follows,

$$\boldsymbol{\sigma}:\frac{d\boldsymbol{\varepsilon}}{dt}-\theta_s\frac{dT}{dt}-\frac{d\Psi_s}{dt}+\sum\mu_\alpha\frac{dm_\alpha}{dt}-\sum_\alpha m_\alpha\theta_\alpha\frac{dT}{dt}-\sum_\alpha\left(\mu_\alpha-\frac{p_\alpha}{\rho_\alpha}\right)\frac{dm_\alpha}{dt}-\sum_\alpha m_\alpha\frac{d\left(\mu_\alpha-\frac{p_\alpha}{\rho_\alpha}\right)}{dt}\geq 0. \tag{V-3}$$

The last four items in (V-3) can be written as follows,

$$\sum\mu_\alpha\frac{dm_\alpha}{dt}-\sum_\alpha m_\alpha\theta_\alpha\frac{dT}{dt}-\sum_\alpha\left(\mu_\alpha-\frac{p_\alpha}{\rho_\alpha}\right)\frac{dm_\alpha}{dt}-\sum_\alpha m_\alpha\frac{d\left(\mu_\alpha-\frac{p_\alpha}{\rho_\alpha}\right)}{dt}=\sum_{\alpha=c,w}\left\{\mu_\alpha\frac{dm_\alpha}{dt}-\mu_\alpha\frac{dm_\alpha}{dt}+\right.$$

$$\left.\frac{p_\alpha}{\rho_\alpha}\frac{dm_\alpha}{dt}-m_\alpha\theta_\alpha\frac{dT}{dt}-m_\alpha\frac{d\mu_\alpha}{dt}+m_\alpha\frac{d\frac{p_\alpha}{\rho_\alpha}}{dt}\right\}. \tag{V-4}$$

Considering that $m_\alpha=\rho_\alpha\phi_\alpha$ and θ_α does not change with time, we can obtain

$$\mu_\alpha\frac{dm_\alpha}{dt}-\mu_\alpha\frac{dm_\alpha}{dt}+\frac{p_\alpha}{\rho_\alpha}\frac{dm_\alpha}{dt}-m_\alpha\theta_\alpha\frac{dT}{dt}-m_\alpha\frac{d\mu_\alpha}{dt}+m_\alpha\frac{d(\frac{p_\alpha}{\rho_\alpha})}{dt}=\frac{p_\alpha}{\rho_\alpha}\frac{dm_\alpha}{dt}-m_\alpha\theta_\alpha\frac{dT}{dt}-m_\alpha\frac{d(\frac{p_\alpha}{\rho_\alpha})}{dt}+$$

$$m_\alpha\frac{d(\theta_\alpha dT)}{dt}+m_\alpha\frac{d\left(\frac{p_\alpha}{\rho_\alpha}\right)}{dt}=\frac{p_\alpha}{\rho_\alpha}\frac{dm_\alpha}{dt}=p_\alpha\frac{d\phi_\alpha}{dt}. \tag{V-5}$$

Substituting Equations (V-4) and (V-5) into Inequality (V-3), we obtain the Clausius-Duhem inequality related to the skeleton as follows,

$$\boldsymbol{\sigma}:\frac{d\boldsymbol{\varepsilon}}{dt}-\theta_s\frac{dT}{dt}-\frac{d\Psi_s}{dt}+\sum_{\alpha=c,w}p_\alpha\frac{d\phi_\alpha}{dt}\geq 0. \tag{V-6) or (112).}$$

Appendix VI: Deriving some formula in Section 4.4 for constitutive model.

For plastic strain, we have $\varepsilon_v^p=\frac{1}{3}\left(\varepsilon_a^p+2\varepsilon_c^p\right)$, $\varepsilon_s^p=\frac{2}{3}\left(\varepsilon_a^p-\varepsilon_c^p\right)$, so $\sigma_{ij}d\varepsilon_{ij}^p$ in triaxial stress state can be expressed as $\sigma_a d\varepsilon_a^p+2\sigma_c d\varepsilon_c^p$. Considering $\sigma_m,\sigma_s,\varepsilon_v^p$, and ε_s^p, we have

$$\sigma_m d\varepsilon_v^p+\sigma_s d\varepsilon_s^p=\frac{1}{3}(\sigma_a+2\sigma_c)\left(d\varepsilon_a^p+2d\varepsilon_c^p\right)+\frac{2}{3}(\sigma_a-\sigma_c)\left(d\varepsilon_a^p-d\varepsilon_c^p\right)=\sigma_a d\varepsilon_a^p+2\sigma_c d\varepsilon_c^p. \tag{VI-1}$$

Therefore, the dissipation (148) can be expressed as follows,

$$\mathrm{D}=\sigma_m d\varepsilon_v^p+\sigma_s d\varepsilon_s^p+\bar{p}_c d\varphi_c^p+\bar{p}_w d\varphi_w^p+\xi_J d\chi_J. \tag{VI-2}$$

Substituting $d\varepsilon_v^p=-d\varphi_c^p-d\varphi_w^p$ into (VI-2), we can obtain

$$\mathrm{D}=-(\sigma_m-\bar{p}_c)d\varphi_c^p-(\sigma_m-\bar{p}_w)d\varphi_w^p+\sigma_s d\varepsilon_s^p+\xi_J d\chi_J\geq 0. \tag{VI-3) or (156)}$$

From the yield function (161), we have

$$\frac{\partial f}{\partial\xi_\alpha}=-\left[1-\left(\frac{\eta}{\xi_\alpha}\right)^n\right]^{-2}(-1)\eta^n(-n)(\xi_\alpha)^{-n-1}=-\frac{n}{\xi_\alpha\left[1-\left(\frac{\eta}{\xi_\alpha}\right)^n\right]^2}\left(\frac{\eta}{\xi_\alpha}\right)^n, \tag{VI-4}$$

$$\frac{\partial f}{\partial\xi_\beta}=-1, \tag{VI-5}$$

$$\frac{\partial f}{\partial\sigma_m^E}=\frac{1}{1-(\eta/\xi_\alpha)^n}+\frac{n}{\eta^2[1-(\eta/\xi_\alpha)^n]^2}\left(\frac{\eta}{\xi_\alpha}\right)^n, \tag{VI-6}$$

$$\frac{\partial f}{\partial\sigma_s}=-\frac{n}{\eta[1-(\eta/\xi_\alpha)^n]^2}\left(\frac{\eta}{\xi_\alpha}\right)^n. \tag{VI-7}$$

From (158), (162) and (163), we know that $\chi_\alpha = \varepsilon_s^p$ and $\chi_\beta = \varepsilon_v^p$, so we have

$$\frac{\partial \xi_\alpha}{\partial \chi_\alpha} = \frac{\partial \xi_\alpha}{\partial \varepsilon_s^p} = \frac{b}{c}\alpha_m exp\left(-\frac{\varepsilon_s^p}{c}\right), \quad \text{(VI-8)}$$

$$\frac{\partial \xi_\beta}{\partial \chi_\beta} = \frac{\partial \xi_\beta}{\partial \varepsilon_v^p} = \beta\sigma_{mr}^E \exp\left(\beta\varepsilon_v^p\right). \quad \text{(VI-9)}$$

From the plastic potential function h (164), we have

$$\frac{\partial h}{\partial \sigma_m^E} = \frac{1}{1-(\eta/\xi_{\alpha 1})^{n_1}} + \frac{n_1}{\eta^2[1-(\eta/\xi_{\alpha 1})^{n_1}]^2}\left(\frac{\eta}{\xi_{\alpha 1}}\right)^{n_1}, \quad \text{(VI-10)}$$

$$\frac{\partial h}{\partial \sigma_s} = -\frac{n_1}{\eta[1-(\eta/\xi_{\alpha 1})^{n_1}]^2}\left(\frac{\eta}{\xi_{\alpha 1}}\right)^{n_1} . \quad \text{(VI-11)}$$

Acknowledgments

This research was supported by the 100-Talent Program of the Chinese Academy of Sciences (Granted to Dr. Enlong Liu), the National Natural Science Foundation of China (Grant Nos. 41230630), Key Research Program of Frontier Sciences of Chinese Academy of Sciences (QYZDY-SSW-DQC015).

Nomenclature

$\mathbf{X}$	the position vector relative to a cartesian coordinate of reference configuration
$\boldsymbol{e}_i$	the base vectors
$\mathbf{x}$	the position vector relative to a cartesian coordinate of current configuration
$\mathbf{F}$	the deformation gradient
$\boldsymbol{\xi}$	the displacement vector
$\boldsymbol{V}^s$	the velocities of solid grains
$\boldsymbol{V}^\alpha$(α=c, w)	the velocities of in-pore phases (ice crystals and unfrozen water)
$\mathbf{M}_\alpha$	the Lagrangian flux attached to the initial configuration of phase α
$\boldsymbol{w}_\alpha$	the Eulerian mass flux
$\boldsymbol{n}$	the unit normal of current configuration
$\boldsymbol{N}$	the unit normal of initial configuration
$\boldsymbol{\vartheta}$	the filtration vector
$\boldsymbol{\gamma}^s$	the accelerations of soil skeleton
$\boldsymbol{\gamma}^\alpha(\alpha = c, w)$	the acceleration of phase α
$\boldsymbol{g}$	the gravitational acceleration
$\boldsymbol{\pi}$	the Piola-Kirchhoff stress tensor

1246	$\boldsymbol{\sigma}$	the Cauchy stress
1247	$\boldsymbol{\sigma}^{s}$	the separate existence of a partial volumetric stress related to the soil skeleton
1248	$\boldsymbol{\sigma}^{\alpha}(\alpha = c, w)$	the partial volumetric stress tensor related to the fluids
1249	$\boldsymbol{T}^{s}$	the traction vector of soil solid grain
1250	$\mathbf{T}^{\alpha}$	the traction vector of phase α
1251	$\mathbf{T}$	the total traction vector
1252	$\boldsymbol{\Delta}$	the Green-Lagrange strain tensor
1253	$\mathbf{d}^{\pi}(\pi = \mathrm{s}, c, w)$	the Eulerian strain rate tensor of phase π
1254	$\boldsymbol{J}_{Q}$	a surface rate of heat supply by conduction
1255	$\boldsymbol{r}_{Q}$	a volume density of the heat provided to REV by an external heat sources
1256	$\boldsymbol{q}$	an outgoing heat flow vector in current configuration
1257	$\boldsymbol{Q}$	the Lagrangian heat flow vector
1258	$\boldsymbol{R}_{\boldsymbol{Q}}$	the Lagrangian volume density of the heat provided to REV
1259	$\mathbf{k}_{\boldsymbol{\alpha}}$	the permeability tensor relative to the current configuration
1260	$\mathbf{K}_{\alpha}$	the permeability tensor relative to the initial configuration
1261	$\boldsymbol{\kappa}$	the thermal conductivity tensor relative to the current configuration
1262	$\boldsymbol{K}$	the thermal conductivity tensor relative to the initial configuration
1263	$\boldsymbol{\varepsilon}$	the strain tensor in infinitesimal transformation
1264	X_i	the components of a position vector of reference configuration
1265	x_{i}	the components of a position vector of current configuration
1266	F_{ij}	the components of the deformation gradient
1267	$\mathrm{d}\Omega_0$	the volume of the undeformed element at the reference configuration
1268	$\mathrm{d}\Omega$	the volume of the deformed element in the current configuration
1269	J	the Jacobian
1270	n	the Eulerian porosity
1271	ϕ	the Lagrangian porosity
1272	$\phi_{\alpha}(\alpha=c, w)$	the Lagrangian porosity of ice crystals or unfrozen water
1273	$S_{\alpha}(\alpha = c, w)$	the Lagrangian saturation degree of phase α
1274	φ_c et φ_w	the volume change due to deformation of the porous space
1275	$n_{\alpha}(\alpha = c, w)$	the Eulerian partial porosities of phase α

1276	$s_\alpha(\alpha = c, w)$	the Eulerian saturation degree of phase α
1277	ρ_s	the intrinsic mass densities of the solid matrix
1278	$\rho_\alpha(\alpha=c, w)$	the intrinsic mass densities of the in-pore component of phase α
1279	M_α	the Lagrangian flux attached to the initial configuration of fluid α
1280	m_α	the Lagrangian fluid mass content related to fluid α
1281	m_s	the mass of soil skeleton at current configuration
1282	w_α	the Eulerian mass flux of fluid α
1283	$m^0{}_s$	the mass of soil skeleton at initial configuration
1284	da	the current surface
1285	dA	the initial surface
1286	ρ_s^0	the initial matrix mass density
1287	$\Lambda_{\alpha\to\beta}$	the mass of phase α transforming into phase β per unit overall current volume and
1288		per unit time
1289	$\varpi_{\alpha\to\beta}$	the mass of phase α transforming into phase β per unit overall initial volume and
1290		per unit time
1291	ρ	the total apparent mass density
1292	p_α	the fluid pressure of phase α
1293	K_s	the kinetic energy associated with soil matrix in current configuration
1294	K_α	the kinetic energy associated with phase α in current configuration
1295	$\mathrm{P_{def}}$	the strain work rate of the RVE in Eulerian formulation
1296	$\mathcal{P}_{\mathrm{f,T}}$	the work rate of the RVE in Lagrangian formulation
1297	$\mathrm{P_{f,T}}$	the work rate of the RVE in Eulerian formulation
1298	$\mathcal{K}_s$	the kinetic energy associated with soil matrix in Lagrangian formulation
1299	$\mathcal{K}_\alpha$	the kinetic energy associated with phase α in Lagrangian formulation
1300	$\mathcal{P}_{\mathrm{def}}$	the strain work rate of the RVE
1301	Q^0	the external heat supply
1302	e_s	the specific (i.e. per unit mass) internal energy of the soil matrix
1303	$e_\alpha(\alpha = c, w)$	the specific (i.e. per unit mass) internal energy of the phase α
1304	e	the total internal energy per unit overall current volume
1305	$h_\alpha(\alpha = c, w)$	the fluid-specific enthalpy of phase α

1306	E	the overall Lagrangian densities of internal energy per unit of initial volume
1307	$\theta_\pi(\pi = \mathrm{s}, c, w)$	the specific entropy in current configuration of phase π
1308	θ	the total entropy per unit of overall current volume
1309	ψ	the Helmholtz free energy in Eulerian formulation
1310	Θ	the Lagrangian entropy density
1311	Ψ	the Lagrangian free energy density
1312	$g_\alpha(\alpha = c, w)$	the fluid-specific free enthalpy of phase α
1313	T	temperature
1314	$\Theta_\alpha(\alpha = c, w)$	the Lagrangian entropy density of phase α
1315	Φ	the total dissipation per unit of initial volume in Lagrangian formulation
1316	Φ_i	the dissipation per unit of initial volume with $i = 1,2,3$ in Lagrangian form
1317	$\Phi_\rightarrow$	the dissipation with phase change in Lagrangian formulation
1318	φ	the dissipations in Eulerian formulation
1319	φ_i	the Eulerian dissipation volume densities with $i = 1,2,3$ in Eulerian form
1320	$\varphi_\rightarrow$	the dissipation with phase change in Eulerian formulation
1321	$m_{c\rightarrow w}$	the mass of phase ice crystal transforming into unfrozen water per unit overall
1322		current volume and per unit time in infinitesimal transformation
1323	$\mu_\alpha(\alpha = c, w)$	the specific chemical potential of the saturating solution α
1324	Ψ_s	the skeleton free energy
1325	θ_s	the skeleton entropy density
1326	T_m	the melting temperature
1327	Σ_m	the melting entropy
1328	$\wp$	the function expression
1329	Γ	the Γ function
1330	U	the interfacial energy
1331	f	the yield function
1332	h	the plastic potential function

1333 References

1334 Andersland, O.B. and Ladanyi, B., 2004. Frozen ground engineering. John Wiley & Sons.

1335 Al-Rub, R.K.A., Darabi, M., 2012. A thermodynamic framework for constitutive modelling of time-
1336 and rate-dependent materials. Part I: Theory. International Journal of Plasticity 34, 61-92.
1337 Biot, M. A., 1941. General theory of three dimensional consolidation. Journal for Applied Physics 12,
1338 155-164.
1339 Biot, M. A., 1956. The theory of propagation of elastic waves in a fluid-saturated porous solid. I.
1340 low-frequency range. Journal of the Acoustic Society of America 28, 168-178.
1341 Boukpeti, N., 2008. One-dimensional analysis of a poroelastic medium during freezing. International
1342 Journal for Numerical and Analytical Methods in Geomechanics 32, 1661-1691.
1343 Collard, C., Favier, V., Berbenni, S., Berveiller, M., 2010. Role of discrete intra-granular slip bands on
1344 the strain-hardening of polycrystals. International Journal of Plasticity 26, 310-328.
1345 Coussy, O., 1989. A general theory of thermoporoelasticity for saturated porous materials. Transport in
1346 Media 4, 281-293.
1347 Coussy, O., 1995. Mechanics of porous continua. John Wiley & Sons Ltd.
1348 Coussy, O., 2004. Poromechanics. John Wiley & Sons Ltd.
1349 Coussy, O., 2005. Poromechanics of freezing materials. Journal of the Mechanics and Physics of Solids
1350 53, 1689-1718.
1351 Coussy, O., Monteir P. J.M., 2008. Poroelastic model for concrete exposed to freezing temperature.
1352 Cement and Concrete 38, 40-48.
1353 Darabi, M., Al-Rub, R.K.A., Masad, E. A., Huang, C.-W., 2012. A modified viscoplastic model to
1354 predict the permanent deformation of asphaltic materials under cyclic-compression loading at high
1355 temperatures. International Journal of Plasticity 35, 100-134.
1356 De Sciarra, F. M., 2012. Hardening plasticity with nonlocal strain damage. International Journal of
1357 Plasticity 34, 114-138.
1358 Halphen, B., Nguyen, Q. S., 1974. Plastic and visco-plastic materials with generalized potential. Mech.
1359 Res. Comm. 1, 43-47.
1360 Henann, D.L., Kamrin, K., 2014. Continuum thermomechanics of the nonlocal granular rheology.
1361 International Journal of Plasticity 60, 145-162.
1362 Hill, R., 1950. The mathematical theory of plasticity. Clarendon Press.
1363 Kamrin, K., 2010. Nonlinear elasto-plastic model for dense granular flow. International Journal of
1364 Plasticity 26, 167-188.

1365 Khan, A.S., Xiang, Y., Huang, S., 1991. Behaviour of Berea sandstone under confining pressure part I:
1366 Yield and failure surfaces, and nonlinear elastic response. International Journal of Plasticity 7(6):
1367 607-624.
1368 Krairi, A., Doghri, I., 2014. A thermodynamically-based constitutive model for thermoplastic polymers
1369 coupling viscoelasticity, viscoplasticity and ductile damage. International Journal of Plasticity 60,
1370 163-181.
1371 Lai, W. M., Rubin, D., Krempl, E., 2010. Introduction to continuum mechanics. Elsevier Inc..
1372 Lai Y., Jin, L., Chang, X., 2009. Yield criterion and elasto-plastic damage constitutive model for frozen
1373 sandy soil. International Journal of Plasticity 25, 1177-1205.
1374 Lai, Y., Yang, Y., Chang, X., Li, S., 2010. Strength criterion and elastoplastic constitutive model of
1375 frozen silt in generalized plastic mechanics. International Journal of Plasticity 26, 1461-1484.
1376 Lai, Y., Liao, M., Hu, K., 2016. A constitutive model of frozen saline sandy soil based on energy
1377 dissipation theory. International Journal of Plasticity 78, 84-113.
1378 Lai, Y., Xu, X., Dong, Y., Li, S., 2013. Present situation and prospect of mechanical research on frozen
1379 soils in China. Cold Regions Science and Technology 87, 6-18.
1380 Lai, Y. M., Wu, Z. W., Zhu, Y. L, Zhu, L. N., 1998. Nonlinear analysis for the coupled problem of
1381 temperature, seepage and stress fields in cold-region tunnels. Tunneling and Underground Space
1382 Technology 13(4), 434-440.
1383 Lee, M.Y., Fossum, A, Costin, L.S, Bronowski, D., 2002. Frozen soil material testing and constitutive
1384 modelling. Sandia report, Sand2002-0524, Sandia National Laboratories.
1385 Lei, X., Wong, H., Fabbri, A., Liman, A., Cheng, Y. M., 2014. A thermo-chemo-electro-mechanical
1386 framework of unsaturated expansive clays. Computers and Geotechnics 62, 175-192.
1387 Lemaitre, J., Chaboche, J. L., 1994. Mechanics of solid materials. Cambridge University Press.
1388 Li, N., Chen, B., Chen, F., Xu, X., 2000. The coupled heat-moisture-mechanic model of the frozen soil.
1389 Cold Regions Science and Technology 31, 199-205.
1390 Liu, E., Xing, H., 2009. A double hardening thermos-mechanical constitutive model for
1391 overconsolidated clays. Acta Geotechnica 4, 1-6.
1392 Liu, E., Yu, H.S., Zhou, C., Nie, Q., Luo, K., 2017. A binary-medium constitutive model for artificially
1393 structured soils based on the disturbed state concept and homogenization theory. International Journal
1394 of Geomechanics, 04016154.

1395 Loria, A. F. Loria, Frigo, B., Chiaia, B., 2017. A non-linear constitutive model for describing the
1396 mechanical behaviour of frozen ground and permafrost. Cold Regions Science and Technology 133,
1397 63-69.
1398 Lu, J. F., Tan, Y. P., Wang, J. H., 2011. A phase field model for the freezing saturated porous medium.
1399 International Journal of Engineering Science 49, 768-780.
1400 Muraleetharan, K.K., Liu, C., Wei, C., Kibbey, T.C.G., Chen, L., 2009. An elastoplastic framework for
1401 coupling hydraulic and mechanical behaviour of unsaturated soils. International Journal of Plasticity 25,
1402 473-490.
1403 Na, S. H., Sun, W. C., 2017. Computational thermo-hydro-mechanics for multiphase freezing and
1404 thawing porous media in the finite deformation range. Comput. Methods Appl. Meth. Engrg. 318,
1405 667-700.
1406 Neaupane, K.M., Yamabe, T., Yoshinaka, R., 1999. Simulation of a fully coupled
1407 thermo-hydro-mechanical system in freezing and thawing rock. International Journal of Rock
1408 Mechanics and Mining Science 36, 563-580.
1409 Neaupane, K.M., Yamabe, T., 2001. A fully coupled thermo-hydro-mechanical nonlinear model for a
1410 frozen medium. Computers and Geotechnics 28, 613-637.
1411 Nicot, F., Sibille, L., Darve, F., 2012. Failure in rate-independent granular materials as a bifurcation
1412 toward a dynamic regime. International Journal of Plasticity 2012, 136-154.
1413 Nishimura, S., Gens, A., Olivella, S., Jardine, R.J., 2009. THM-coupled finite element analysis of
1414 frozen soil: formulation and application. Geotechnique 59(3), 159-171.
1415 Sciarra, G., 2016. Phase field modeling of partially saturated deformable porous media. Journal of the
1416 Mechanics and Physics of Solids 94, 230-256.
1417 Shen, W.Q., Shao, J.F., 2016. An incremental micro-macro model for porous geomaterials with double
1418 porosity and inclusion. International Journal of Plasticity 83, 37-54.
1419 Sheng, D., Zhang, S., Niu, F., Cheng, G., 2014. A potential new frost heave mechanism in high-speed
1420 railway embankments. Geotechnique 64(2), 144-154.
1421 Steinhauser, M.O., Grass, K., Strassburger, E., Blumen, A., 2009. Impact failure of granular
1422 materials-Non-equilibrium multiscale simulations and high-speed experiments. International Journal of
1423 Plasticity 2009, 161-182.
1424 Thomas, H. R., Cleall, P., Li, Y.-C, Harris, C., Kern-Luetschg, M., 2009. Modelling of cryogenic

1425 processes in permafrost and seasonally frozen soils. Geotechnique 59, 173-184.
1426 Tsytovich, N. A., 1985. The mechanics of frozen ground. [Translated by Zhang, C. Q. and Zhu, Y.L.]
1427 Science Press.
1428 Xu, X., Wang, J., Zhang, L., 2010. Physics of frozen soils. Science Press.
1429 Xu, X., Wang, Y., Yin, Z., Zhang, H., 2017. Effect of temperature and strain rate on mechanical
1430 characteristics and constitutive model of frozen Helin loess. Cold Regions Science and Technology 136,
1431 44-51.
1432 Yang, P., Ke, J., Wang, J.G., Chow, Y.K., Zhu, F., 2006. Numerical simulation of frost heave with
1433 coupled water freezing, temperature and stress fields in tunnel excavation. Computers and Geotechnics
1434 33, 330-340.
1435 Yang, R., Lemarchand, E., Fen.-C., T., Azouni, A., 2015. A micromechanics model for partial freezing
1436 in porous media. International Journal of Solids and Structures 75-76, 109-121.
1437 Yao, Y. P., Hou, W., and Zhou, A. N., 2009. UH model: Three dimensional unified hardening model for
1438 overconsolidated clays. Geotechnique 59(5), 451–469.
1439 Yao, Y.P., Zhou, A. N., 2013. Non-isothermal unified hardening model: a thermo-elasto-plastic model
1440 for clays. Geotechnique 63(15), 1328-1345.
1441 Yao, Y. P., Kong, L. M., Zhou, A. N., and Yin, J. H., 2015. Timedependent unified hardening model:
1442 Three-dimensional elasto-viscoplastic constitutive model for clays. J. Eng. Mech.,
1443 10.1061/(ASCE)EM.1943-7889.0000885, 04014162.
1444 Zhang, S., Leng, W., Zhang, F., Xiong, Y., 2012. A simple thermo-elastoplastic model for geomaterials.
1445 International Journal of Plasticity 34, 93-113.
1446 Zhang, Y., 2014. Thermal-hydro-mechanical model for freezing and thawing of soils (Ph. D thesis), the
1447 University of Michigan.
1448 Zhang, Z., 2017. A thermodynamics-based theory for the thermos-poro-mechanical modeling of
1449 saturated clay. International Journal of Plasticity 92, 164-185.
1450 Zhou, J., Li, D., 2012. Numerical analysis of coupled water, heat and stress in saturated freezing soil.
1451 Cold Regions Science and Technology 72, 43-49.
1452 Zhou, M. M., Meschke, G., 2013. A three-phase thermo-hydro-mechanical finite element model for
1453 frezzing soils. International Journal for Numerical and Analytical Methods in Geomechanics 37,
1454 3173-3193.

Zhou, Y. W., Guo, D. X., Cheng, G. D., 2000. Frozen soil of China. Science Press.

Zhu, Q.Z., Shao, J.F., Mainguy, M., 2010. A micromechanics-based elastoplastic damage model for granular materials at low confining pressure. International Journal of Plasticity 26(4), 586-602.

Lists of Figures

Fig. 1 Macroscopic model of the REV of saturated frozen soils

Fig. 2 Comparisons of tested and simulated results of frozen sand soil at -1℃, -5℃ and -10℃ with 1MPa confining pressure: (a) Deviatoric stress-shear strain curves; (b) Volumetric strain-shear strain curves; (c) Predicted volumetric strain- pore pressure curves

Fig. 3 Comparisons of tested and simulated results of frozen saline sand soil at -6℃with 1MPa-10MPa confining pressures: (a) Deviatoric stress-shear strain curves; (b) Volumetric strain-shear strain curves; (c) Predicted volumetric strain- pore pressure curves

Fig. 4 Simulated results with varying $\alpha_m = \alpha_{m1}$ at 2.0MPa confining pressu(a) Deviatoric stress-shear strain curves; (b) Volumetric strain-shear strain curves; (c) Stress path of σ_m^E-σ_s

Fig. 5 Simulated results with varying κ at 2.0MPa confining pressures: (a) Deviatoric stress-shear strain curves; (b) Volumetric strain-shear strain curves; (c) Stress path of σ_m^E-σ_s

Fig. 6 Simulated results with varying γ_1 at 2.0MPa confining pressures: (a) Deviatoric stress-shear strain curves; (b) Volumetric strain-shear strain curves; (c) Stress path of σ_m^E-σ_s

Fig. 7 Simulated results with varying σ_{mr}^E at 2.0MPa confining pressures: (a) Deviatoric stress-shear strain curves; (b) Volumetric strain-shear strain curves; (c) Stress path of σ_m^E-σ_s

Fig. 8 Simulated results with varying $\beta = \beta_1$ at 2.0MPa confining pressures: (a) Deviatoric stress-shear strain curves; (b) Volumetric strain-shear strain curves; (c) Stress path of σ_m^E-σ_s

Fig. 9 Simulated results with varying $z = z_1$ at 2.0MPa confining pressures: (a) Deviatoric stress-shear strain curves; (b) Volumetric strain-shear strain curves; (c) Stress path of σ_m^E-σ_s

Fig. 10 Simulated results with varying κ_1 at 2.0MPa confining pressures: (a) Deviatoric stress-shear strain curves; (b) Volumetric strain-shear strain curves; (c) Stress path of σ_m^E-σ_s

Fig. 11 Simulated results with varying γ_2 at 2.0MPa confining pressures: (a) Deviatoric stress-shear strain curves; (b) Volumetric strain-shear strain curves; (c) Stress path of σ_m^E-σ_s